MULTIBEAM SURVEY OF WHEELER NORTH REEF
SAN CLEMENTE, CALIFORNIA

October 2020

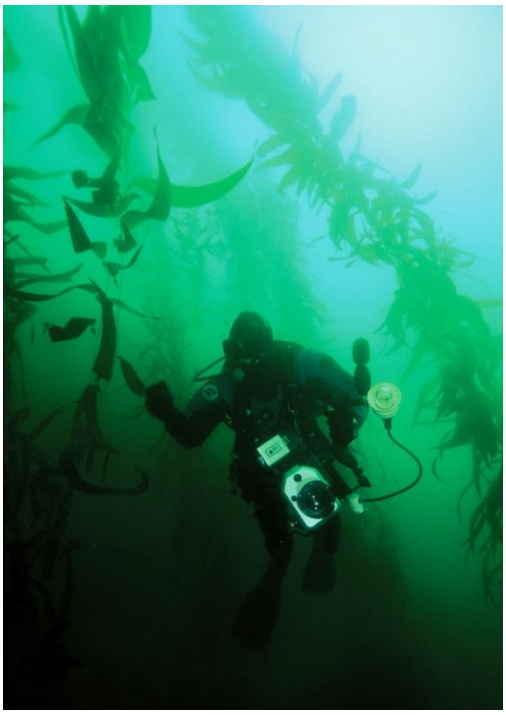

by

M. Hany S. Elwany, Ph.D.
Tim Norall, M.Sc.
Frederico Scarelli, Ph.D.
Cinquini & Passarino, Inc.

for

Southern California Edison Company
2244 Walnut Grove Avenue
Rosemead, CA 91770

COASTAL ENVIRONMENTS
2166 Avenida de la Playa, Suite E
La Jolla, CA 92037

14 December 2020
CE Reference No. 20-34

TABLE OF CONTENTS

LIST OF APPENDICES

LIST OF FIGURES

LIST OF TABLES

MULTIBEAM SURVEY OF WHEELER NORTH REEF, SAN CLEMENTE, CALIFORNIA

October 2020

1.0 INTRODUCTION

Wheeler North Reef (WNR) was constructed by Southern California Edison (SCE) as partial mitigation for impacts to marine resources that resulted from the San Onofre Nuclear Generating Station (SONGS). The reef was constructed in three phases. Phase 1, the experimental reef, with an area of 22.4 acres, consists of seven blocks of eight modules, each of which is 40 m x 40 m (for a total of 56 modules), and was completed on 29 September 1999 (Coastal Environments [CE], 1999). The final Phase 2 reef consisted of 17 polygons with a total area of 152 acres (CE 2008a, b), and was completed on 11 September 2008. Phase 3 consists of 20 polygons covering an area of about 200 acres and was completed on 20 July 2020 (CE, 2020a, b). The total area of WNR as of 20 July 2020 is 373.1 acres (Table 5-4).

WNR is located offshore of San Clemente between the San Clemente Pier and San Mateo Point (Figure 1-1) in approximately 11 to 15 m water depth. Periodic surveys, every five years, are required by the California Coastal Commission (CCC), according to Special Condition #12 of SCE's CCC construction permit (CDP #E-07-010, dated 2 February 2008), to ensure that the reef's footprint is maintaining its areal coverage.

This multibeam survey assessed the boundaries of the reef approximately five years after the most recent survey, which was in 2014. The survey included 100% coverage of the area occupied by the WNR, encompassing the 20 (Phase 3) and 17 (Phase 2) final constructed polygons, as well as the 56 experimental modules (Figures 1-2 and 1-3). This report compares the module and polygon boundaries obtained during this 2020 survey with those obtained during the 2009 and 2014 surveys (CE, 2014).

Multibeam survey operations were carried out from 7 October 2020 through 10 October 2020. Multibeam bathymetry data were collected throughout the defined project area and were used to estimate the module and polygon boundaries. The survey was carried out during high tides to avoid kelp (Figures 1-3 and 1-4). All of the data presented in this report are presented as WGS84, UTM Zone 11 (meters). Vertical sounding reference is Mean Lower Low Water (MLLW). Tide corrections are based upon actual NOAA-verified data from Station 9410230 (La Jolla). Figure 1-3 presents the vessel tracks used for this survey.

This survey found the total estimated area for Phases 1, 2 and 3 to be, respectively, 24.79, 150.74, and 197.52 acres. Table 5-4 compares the area of WNR in the 2008, 2009, 2014, and 2020 surveys.

This report consists of 7 chapters and 7 appendices. Chapter 1 is the introduction, Chapter 2 describes the data acquisition, survey methods and instrumentation, Chapters 3 and 4 present the data processing effort. The multibeam survey results are summarized in Chapters 5 and 6 and graphically in Appendices A-G.

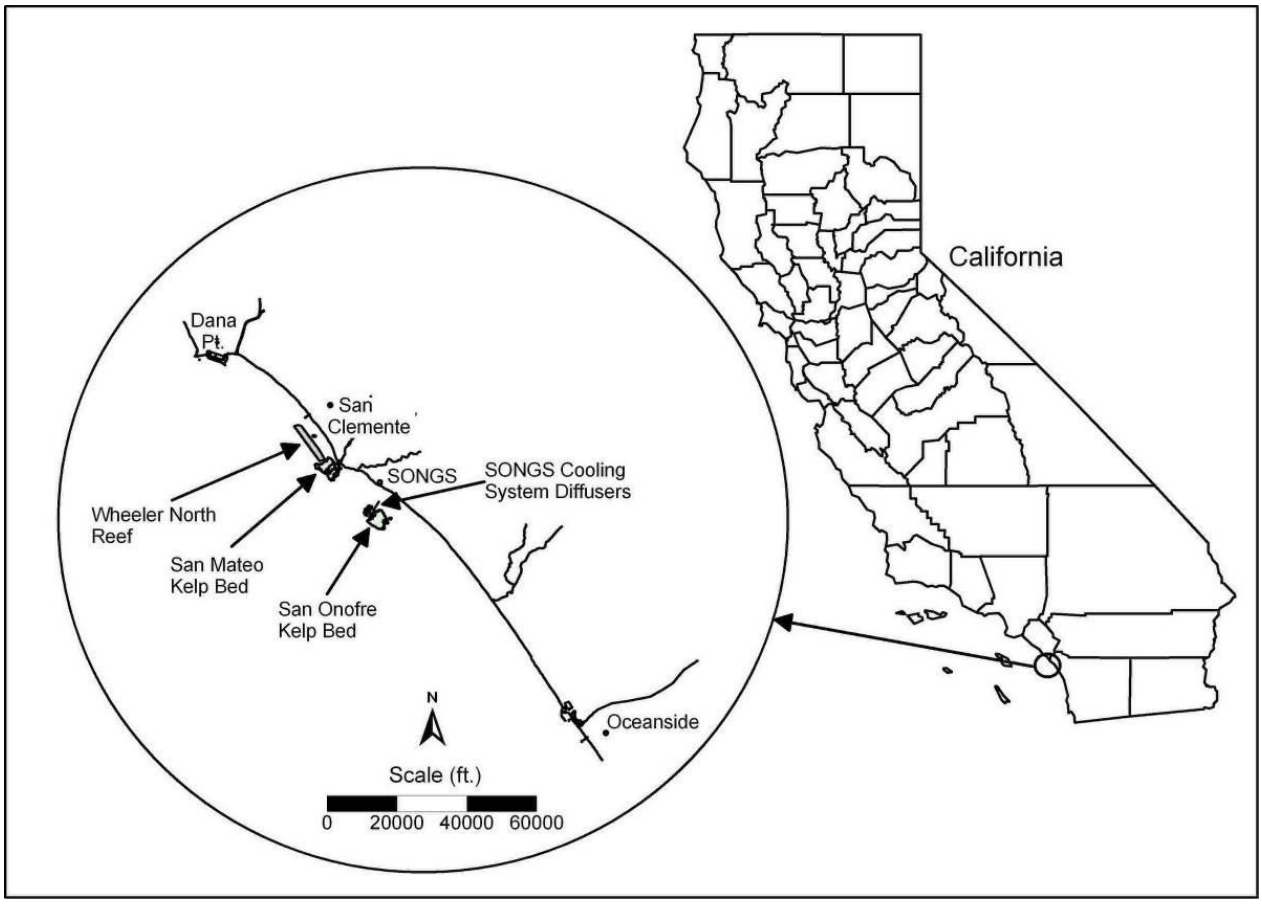

Figure 1-1. Location of Wheeler North Reef at San Clemente, California.

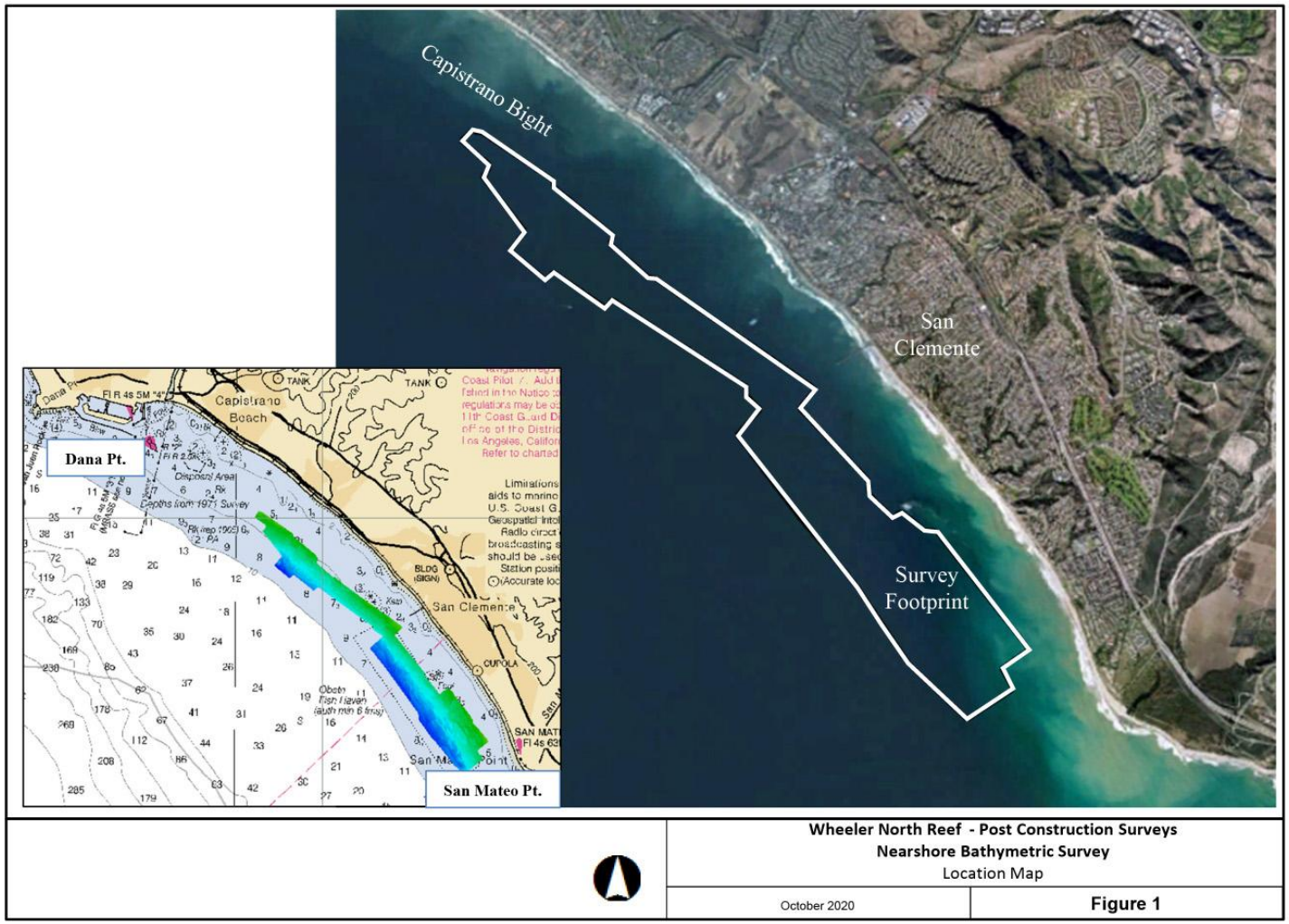

Figure 1-2. Wheeler North Reef, October 2020 Bathymetric Survey Area.

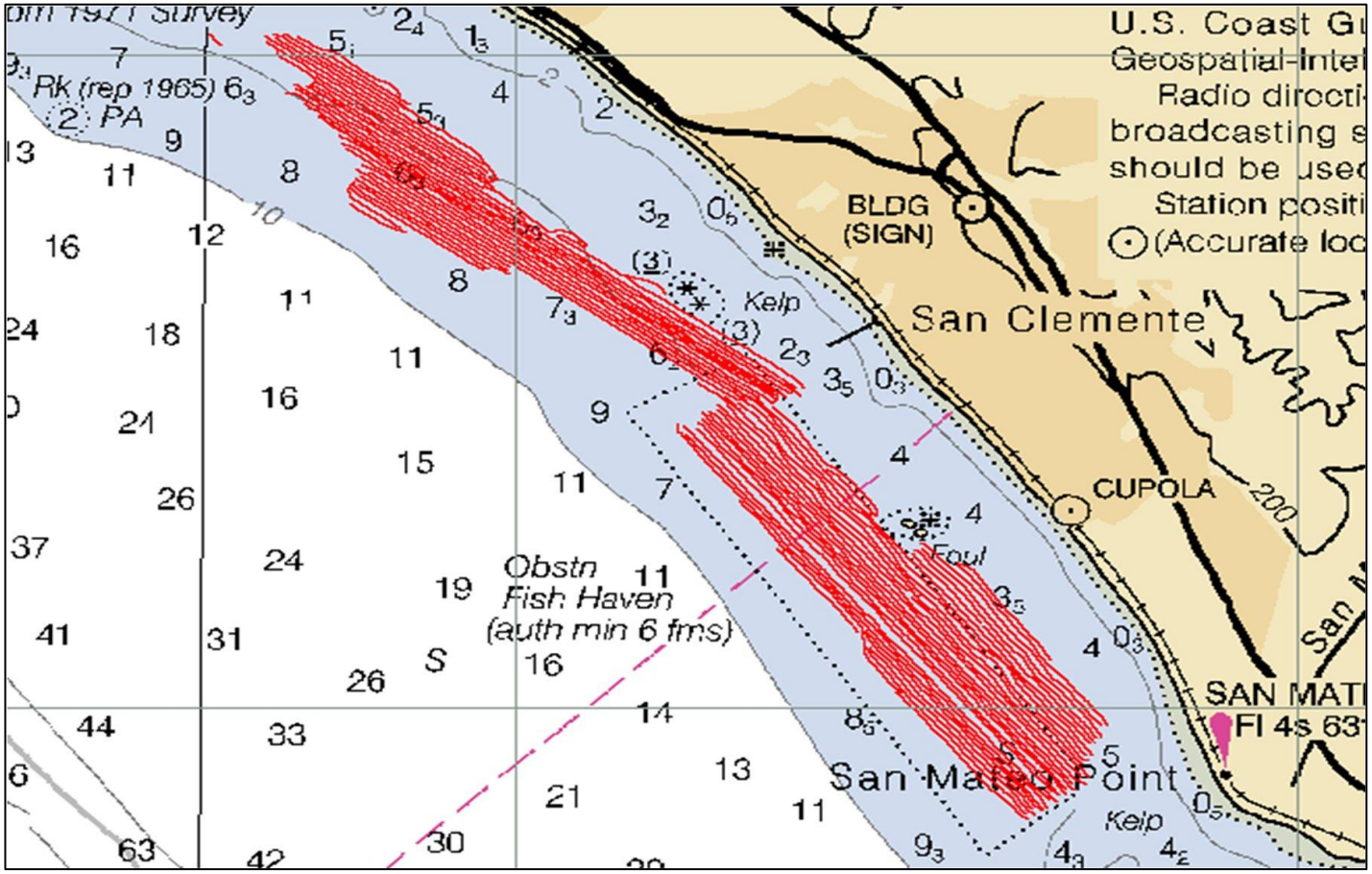

Figure 1-3. Vessel track lines for October 2020 survey.

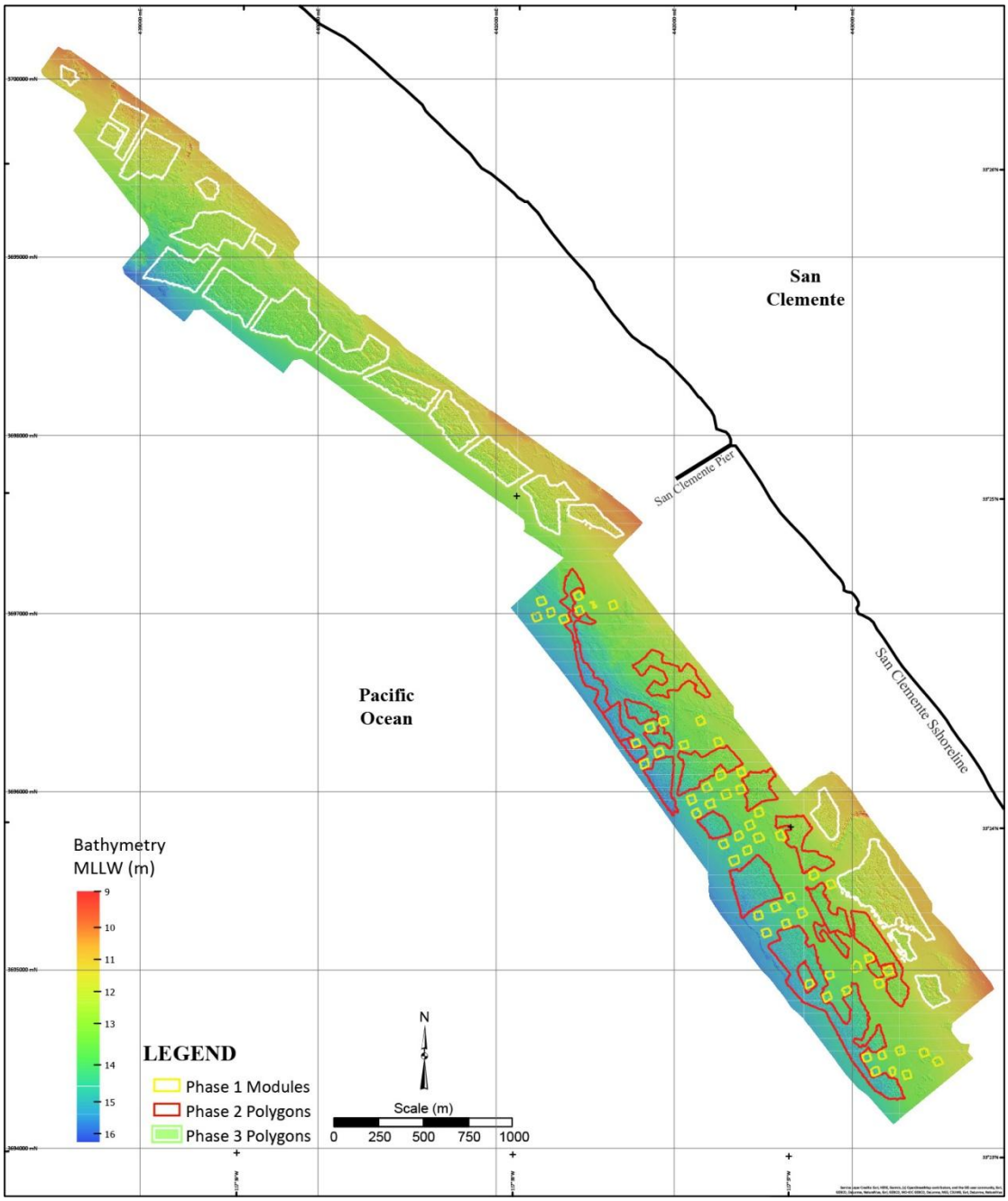

Figure 1-4. Boundaries of Wheeler North Reef, consisting of 56 modules – each module is 40 m x 40 m (7 blocks constructed in 1999), 17 polygons (constructed in 2008), and 20 polygons (constructed in 2020) overlaid on multibeam bathymetric data (October 2020).

2.0 DATA ACQUISITION AND SURVEY METHOD

2.1 VESSEL

The *R/V North River*, a 34-foot survey vessel, was used for the project. The vessel was equipped with the following primary equipment for execution of the survey:

- *Reson SeaBat T50-R* Multibeam Echosounder (MBES), over-the-side mounted
- *Applanix POS MV Wavemaster* (type 42) Motion Reference Unit, Heading, & Positioning System
- *Applied Microsystems Limited* (AML) Sound Velocity Probe for Sound Velocity Profiles through the water column (SVP)
- *Hypack / Hysweep* navigation software

2.2 GLOBAL POSITIONING SYSTEM (GPS) VESSEL POSITIONING

The vessel was equipped with an Applanix Position and Orientation System for Marine Vessels (POS MV) to measure and calculate vessel position and navigation data. Position and heading were determined in real time using two Trimble Zephyr L1/L2 GPS antennas as primary and secondary units, which were connected to a Trimble BD982 L1/L2 GPS card residing in the POS MV. The POS MV was configured to accept differential GPS (DGPS) corrections from Leica's SmartNet subscription. The inertial navigation system, implemented by the POS MV, computes a position through integration with GPS position, heading, and motion of the Inertial Measurement Unit (IMU).

The differential corrections were output at 50 Hz to achieve a real-time vessel position accuracy of 0.10 m to 0.20 m, which was sent to the acquisition systems and *Hypack* software.

Hypack navigation software, running on a *Windows 7*-based PC, was used for vessel navigation. *Hypack* presented vessel position data in graphical and tabular format for quality control (QC) purposes. The following display windows were used:

- Coverage – the Coverage window showed navigation information in plan view. This included vessel position and orientation, survey lines, background plots, charts, and features.
- Data – the Data window was configured to show tabular navigation information. Typically, this window was set to display position, time and date, line name, distance to start and end of line, distance off-line, heading, course over ground, speed, and status of data logging and events.
- Time-Series – the Time-Series window was used to look at specific data items in graphical format, such as the plot of the sound speed at the sonar head.

After acquisition, position and navigation data were post-processed to achieve position accuracy of < 0.10 m. A post-processed Kinematic GPS (KGPS) solution was used for final positioning and refinement of the inertial solution. Therefore, it was necessary to acquire dual-frequency GPS data at known locations in the San Clemente area to act as ground control stations for the survey. KGPS processing was carried out in *Applanix POSPac v8.1* software using an *Applanix Smart Base* (ASB) network and the vessel's GPS data.

The ASB is a routine within POSPac processing software that uses multiple Continually Operating Reference Stations (CORS) and International GPS Service (IGS) stations. Dual-frequency GPS data from these stations are acquired and used to compute a virtual reference station for each point along the remote track line. This method prefers the survey area to be completely within a triangular network, and it typically yields results with RMS error values less than 10 centimeters (cm).

2.3 HORIZONTAL AND VERTICAL DATUM

2.3.1 Horizontal Datum

All data are delivered in North American Datum 1983 (NAD83) 2011 (epoch 2017.750), projected in Universal Transverse Mercator (Z11N), in meters.

2.3.2 Vertical Datum

All depth data were reduced to the local tidal datum (MLLW) based on a chart datum separation between the NAVD88 geodetic datum and local MLLW.

The distance between the NAVD88 datum and the MLLW datum was calculated using NOAA's VDatum software (http://vdatum.noaa.gov). For the survey area, VDatum calculated the NAVD88 datum to be an average of 0.0.3 meters (0.003 feet standard deviation) above MLLW, based on the Geoid12B model. Final chart sets are presented in meters MLLW for mapping purposes.

2.4 MOTION SENSOR AND VESSEL HEADING

A *POS/MV* (version 5) *Wavemaster* motion sensor system measured vessel dynamic motion and orientation (heave, pitch, roll, and heading). The system consists of an IMU, two GPS receivers, and a processing unit.

The IMU uses a series of linear accelerometers and angular rate sensors that work in tandem to determine vessel attitude solutions. The combined GPS solution of each antenna is used to estimate the orientation and heading of the vessel. Offsets for the IMU and GPS antenna were determined and included as input to the software.

Motion, heading, and position data were sent to the Hypack navigation system for real-time navigation and data QC. These data were also logged directly to the acquisition system CPU in the *POS MV* proprietary format.

2.5 SOUND-VELOCITY PROFILES

Sound-velocity profiles (SVP) were acquired using an *AML* sound velocity probe. The *AML* probe measures velocity and pressure observations at a rate of approximately eight times per second. For each cast, the probe was held at the surface for two minutes to reach temperature equilibrium. The probes were then manually lowered at the rate of about 1 meter per second (m/s) to the seafloor and raised to the surface at the same rate. Sound-velocity casts were conducted regularly so that MBES data could be corrected for refraction.

2.6 MULTIBEAM ECHOSOUNDER

The survey boat was equipped with an over-the-side, pole-mounted *Reson SeaBat T50-R* (400 kHz) MBES system, designed to operate nominally between water depths of 0 to 325 feet. The MBES was used to collect bathymetry and backscatter data from about -3 m to -17 m water depth during the survey. Survey speed was kept between 2 to 4 knots to insure low turbulence around the multibeam transducer pole.

Data received by the *SeaBat* sonar-processing unit were viewed directly in the *Reson* user interface monitor, where bathymetry quality was continually monitored during acquisition operations. The information was also monitored through the *Hypack* acquisition software, through which various windows displayed a 3D bathymetry profile, and swath coverage so that adjustments to sonar settings or vessel speed could be made, if appropriate, to improve data quality. A data window also displayed position, speed, heading, and attitude data received from the *POS MV*, and data logging status.

Hypack software was used to start and stop backscatter data logging in *Reson's* S7K file format and to name lines. Power, gain, and range settings were controlled directly through the *Reson* user interface monitor and varied according to water depth and data quality.

2.7 CALIBRATIONS AND QUALITY CONTROL

In addition to the online QC tools and displays available in *POS MV*, *Reson* User Interface monitor, and *Hypack*, as described in previous sections, the following calibrations and checks were also conducted.

2.7.1 Vessel Offset Survey

Dimensions of the vessel were taken after all equipment was mobilized, and offsets between the various sonar systems and sensors were measured utilizing a robotic total station with an error band of ± 2 mm.

2.7.2 MBES Patch Test Calibration

A multibeam patch test was run, so that the MBES data could be corrected for the timing, pitch, yaw, and roll errors that exist between the MBES head and the IMU unit. Data collected during the mobilization patch tests were processed using CARIS Calibration Editor. Table 2-1 presents the final patch test results. Final offsets were entered into SIS before the survey commenced.

2.7.3 Bar Check

A bar check calibration of the sonar system was performed to relate observed (recorded) depths to the true depth of water, and thus calculate any error in the system's raw depth readings (as well as verify the accuracy of the vessel offset survey and vessel draft measurement).

A bar check calibration is performed by lowering a horizontal metal plate to a known depth below the waterline. Then, data at that depth are acquired using the sonar system and processed in real time in the *Hypack* software's Bar Check routine. Thus, the vessel's equipment offsets measured during the offset survey, the sound-velocity profile taken at the time of acquisition, and the survey's static draft measurement are all applied to the data to calculate the difference between the sonar's measurement of the horizontal bar and the actual, known depth below the waterline. Any difference in the measured depth versus the known depth can be attributed to error in the sound-velocity profile, the static draft measurement procedure, the vessel offset survey, and/or the sonar system's internal capabilities.

The bar check results indicate that the system was calibrated vertically to within 0.03 feet – 0.09 feet uncertainty. Thus, no adjustment to the vessel draft was required in post processing.

2.7.4 Multibeam Sonar Performance Test

A performance test was performed on the multibeam survey vessel sonar system, the *Reson Seabat T50-R*. For this "beam angle test," a reference surface is generated from high density data with a swath width reduced to 45 degrees to minimize any outer beams being used in the reference surface. The reference surface is then compared to multibeam data run with a full swath to approximate the performance of the vessel. A reference site was selected that had a relatively flat bottom at a reasonable survey depth. The results of the test indicate the system is functioning within IHO Special Order standards. The results also help the survey team analyze the amount of overlap required for the survey and the best swath width to use during multibeam acquisition.

In 9.5 meters of water (31 feet), the test calculated a mean difference of 0.01 feet when using a swath width of 135 degrees, with a standard deviation of 0.10 feet. Further analysis showed that the outer beams, from 140 degrees to 150 degrees (i.e., 70 degrees to 75 degrees on each side of the swath), exhibited a standard deviation of approximately 0.19 feet. Thus, it was concluded that the multibeam data should be limited to a swath width of 135 degrees to minimize uncertainty in the outer beams. This testing helped determine the best swath width to use during acquisition to ensure that accuracy specifications were met.

2.7.5 Total Propagated Uncertainty (TPU)

Error estimates for all survey sensors were entered in the *Hypack Vessel File* (HVF). These error estimates were used in *Hypack* to calculate the Total Propagated Uncertainty (TPU) at the 95% confidence interval for the horizontal and vertical components for each individual sounding. The values that were entered in the *Hypack* HVF for the survey sensors are the specified manufacturer accuracy values and were downloaded from the Hypack website **http://www.hypack.com/tpu/**. The following is a breakdown and explanation of the manufacturer and survey-derived values used in the error model:

- Navigation – A value of 0.10 m was entered for the positional accuracy. This value was selected based on a review of the DGPS solution accuracies.
- Gyro/Heading – All vessels were equipped with a (*POS MV*) version 5 *Wavemaster*, so a value of 0.02 degrees was entered in the HVF as per manufacturer specs.
- Heave – The heave percentage of amplitude was set to 5%, and the Heave was set to 0.05 m, as per manufacturer specs. However, the actual heave uncertainty that was used in the total vertical uncertainty calculation was derived from the *Applanix POS MV* error calculations for the delayed heave component of the POS MV navigation file (i.e., the *.pos* file).
- Pitch and Roll – As per the manufacturer accuracy values, both were set to 0.02 degrees.
- Timing – All data was time stamped when created (not when logged) using a single timing source. Position, attitude (including True Heave), and heading were all time stamped in the POS MV on the UTC epoch. This UTC string was also sent to the Reson processor via a serial string, yielding timing accuracies on the order of one millisecond. Therefore, a timing error of 0.001 seconds was entered for all sensors on all vessels.
- All vessel and sensor offsets were derived via conventional surveying techniques while the vessel was dry-docked. The results yielded errors of 0.01 m.
- Vessel speed – set to 0.10 m/s for the vessel file since a *POS MV* with a 50 Hz measurement rate was in use.
- Loading – Estimated vessel loading error set to 0.01 m. This was the best estimate of how the measured static draft changed through the survey day.
- Draft – It was estimated that draft could be measured to within 0.01 m; therefore, values in this range were entered.
- IMU alignment Standard Deviation for the Gyro and Roll/Pitch were set to 0.10 degrees since this is the estimated misalignment between the IMU and the vessel reference frame.
- Tide error estimates were set to 0.063 m, based on the observed tidal data from NOAA station 9410170.
- Sound-velocity profile errors were set to 0.05 m/s based on published specifications from the manufacturer, and sound velocity measurements at the surface were estimated to have an error of 0.25 m/s based on the sound-velocity probe attached at the *Reson T50-R* head (this sound-velocity probe is used for beam steering in the multibeam system).

The calculated vertical and horizontal errors, or TPU values, were then used to create finalized CUBE (Combined Uncertainty Bathymetry Estimator) surfaces that used only soundings meeting or exceeding project accuracy specifications. CUBE surfaces were created at a 30 cm (1-foot) resolution for the entire survey area. Based on these TPU values, the overall vertical error of the soundings for the project ranged from 0.41 feet to 0.77 feet. For areas with water depths shallower than 15 feet, the total vertical uncertainty ranged from 0.41 feet to 0.50 feet. Only in areas with water deeper than 15 feet did the vertical uncertainty increase to a maximum of 0.77 feet. The total horizontal uncertainty for the soundings ranged from 0.36 feet to 0.69 feet, exhibiting the greatest uncertainty in the deepest water, as expected.

Table 2-1. Patch test results.

Calibration	Navigation Timing Error	Pitch Offset	Azimuth Offset	Roll Offset
10/7/2020 10/9/2020	0.00 sec	0.050°	-0.400°	-0.155°

3.0 DATA PROCESSING

Data were initially reviewed aboard the survey vessel to assure that data quality and anticipated coverage were achieved. Final processing was carried out utilizing *QPS QIMERA* multibeam processing software (Version 2.2.5).

3.1 GEODETIC CONTROL

A network of GPS base stations within the San Clemente area was used to calculate a virtual reference station for the project.

For this survey, three ground control stations were included in the ASB network, with station San OnofreCA2 CS2007 (SONG) designated as the primary station in the network.

3.2 SOUND-VELOCITY PROFILE PROCESSING

Processed sound-velocity profiles were used to correct the bathymetry for sound refraction, or ray bending. *Qimera's* Sound Velocity Editor routine was used to process each sound-velocity profile, removing duplicated points and noise from the cast.

3.3 PATCH TEST PROCESSING

A patch test was completed for the MBES using reservoir topology to bring swaths run at varying speeds, headings, and overlaps into coincidence. Patch tests are employed every time the sonar mounting or beam configuration is changed so that data can be corrected for navigation timing, pitch, azimuth, and roll offsets, which may exist between the MBES transducer and the IMU.

The *POS MV* system was used as the single timing source for all data (Navigation, Multibeam, Attitude, and Heading). The Attitude, Heading, and Navigation are all time stamped by the same system (*POS MV*), and as a result, the Navigation Time Error is the same as the Roll Time Error, Pitch Time Error, or Azimuth Time Error. Since the Roll Time Error is the easiest to determine, it was used to compute the Navigation Time Error. A single line was run over an area of flat seabed. The line has to be surveyed in seas where the vessel is experiencing some amount of roll. In the Hypack Subset Editor, data from the outer beams of the line on an along track orientation is reviewed. The error was estimated by adjusting the Roll Time Error until the seabed appeared flat. This procedure was repeated over additional subsets to verify the results.

The pitch error adjustment was performed on sets of two coincident lines, run at the same velocity, over sloping terrain or a conspicuous object, in opposite directions. The navigation timing error was already identified. The nadir beams from each line were compared and brought into alignment by adjusting the pitch error value.

The azimuth error adjustment was performed on sets of two lines run over a conspicuous topographic feature. Lines were run in opposite directions, at the same velocity with the same outer beams crossing the feature. The navigation timing error and pitch error were already identified. Data from the same outer beams for each line were compared and brought into alignment, by adjusting the azimuth error value.

The roll error adjustment was performed on sets of two coincident lines, run over flat terrain, at the same velocity, in the opposite direction. The navigation timing error, pitch error, and azimuth error were already identified. Data across a swath were compared for each line and brought into agreement, by adjusting the roll error value.

Patch test data were then corrected using the identified values, and the process was repeated to check their validity.

Calculated values were then entered in to the *Hysweep Editor* in *Hypack* so that data could be corrected during the processing procedure.

3.4 BATHYMETRY PROCESSING

The multibeam data were processed in *QPS Qimera* software. The raw S7K files were imported into *Qimera*. The data were reduced to NAVD88 elevations based on corrections from the vessel offsets entered into the vessel configuration settings, the PPK tide calculations relative to the aforementioned CORS station, and the sound velocity profiles processed in the sound velocity editor routine.

The sound velocity profiles were applied to the survey lines based on their temporal and geographic spacing. The *Qimera* software was used to apply the sound velocity corrections based on whichever sound velocity cast was geographically closest to the survey data, as long as the cast was taken within two hours of time of acquisition of the bathymetry.

Once the data were reduced to NAVD88, each line was manually inspected in *Qimera's Swath Editor* routine.

The *Swath Editor* was used only to reject obvious noise from the dataset, as the majority of the data cleaning was performed in *Qimera's Slice Editor* routine, which allowed for area-based editing, viewing the overlap of multiple survey lines to better aid the decision process about which soundings should be rejected from the final dataset. Figure 3-1 illustrates *Qimera's Slice Editor*, displaying multiple survey lines overlapping with one another.

Once all multibeam bathymetry were cleaned, a final digital terrain model was generated at a 0.25 m by 0.25 m (≈ 1-foot x1-foot) grid spacing. This model was then exported to XYZ format and geo-Tiff format as a sun-illuminated image.

Each survey line was exported to Generic Sensor Format (GSF) from the *Qimera* software. This GSF format contained the processed bathymetry records, as well as the raw

backscatter imagery to allow for generation of a multibeam sidescan mosaic in the QPS FMGT software.

3.5 BACKSCATTER SIDESCAN PROCESSING

To generate a mosaic of the sonar imagery, each GSF file was imported into *QPS FMGT* (version 7.8.5) software. The mosaic process within the software corrects the sonar beam intensity for each sonar ping's power, gain, and pulse length settings. It also accounts for the estimated absorption (decibels per kilometer) of the sonar energy through the water column.

The overlap between adjacent survey lines was blended to create as seamless a mosaic as possible. The mosaic was then exported to geo-tiff format. The resulting mosaic provides a map of the relative changes in intensity of the seafloor across the survey area. When viewed in conjunction with the bathymetric digital terrain model, the combination of the topography and reflectance of the seafloor enable the viewer to better understand the conditions of the seabed at the time of data acquisition.

3.6 DIGITIZATION OF POLYGON AND MODULE BOUNDARIES

Efforts made to filter out the presence of kelp from the multibeam bathymetry data were successful, leading to a high-quality data set. The quality of the backscatter data was reduced due to the presence of kelp plants in the water column, leading to increased noise in the data set. Therefore, the multibeam bathymetry data was the preferred data set for the delineation of the boundaries of the reef. A boundary is defined as the interface between the sand and the hard substrate. A boundary may change as the result of the erosion or accretion of the modules or polygons. The backscatter data were utilized to aid in the delineation of any areas that were difficult to interpret. These areas were small and carefully delineated.

Any newly exposed hard substrate areas included within the boundary of the reef have met the following criteria: (1) the texture of the relief had to be visible; (2) kelp plants were already present in the area; and (3) the boundaries could not be expanded into areas with natural hard substrate.

Figure 3-2 shows an example of the integration of the collected data (bathymetry, and backscatter data) in determining the boundary of Polygon 18. The majority of the modules and polygons had good correlation between the bathymetrically determined boundaries and the backscatter data.

The southern and eastern sides of Module 8 were surveyed three times, and each boundary line was processed independently. The boundary lines of each side were overlaid on top of each other for the southern and eastern boundaries of the module, and the results are presented in Figures 3-3 and 3-4, respectively. The results indicate that the errors which may be induced by the survey method are small.

Polygons 4 and 21 were digitized independently by two surveyors based on the criteria stated above. The results are shown in Figures 3-5 and 3-6. The difference in computed area from the two surveyors was very small, about 0.4%.

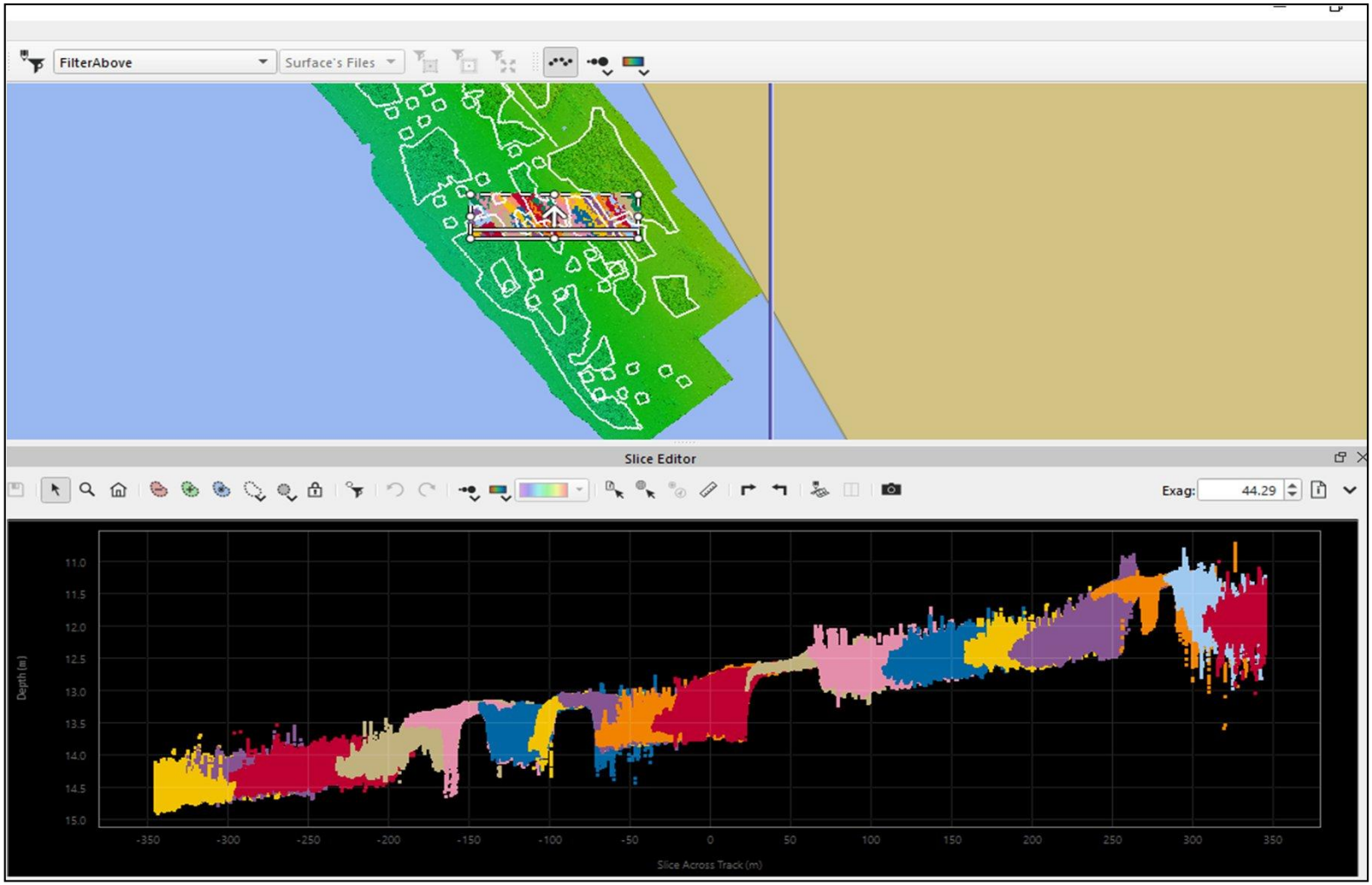

Figure 3-1. Record of bathymetric raw data for a stack of transact running from east to west showing the raw data prior to editing.

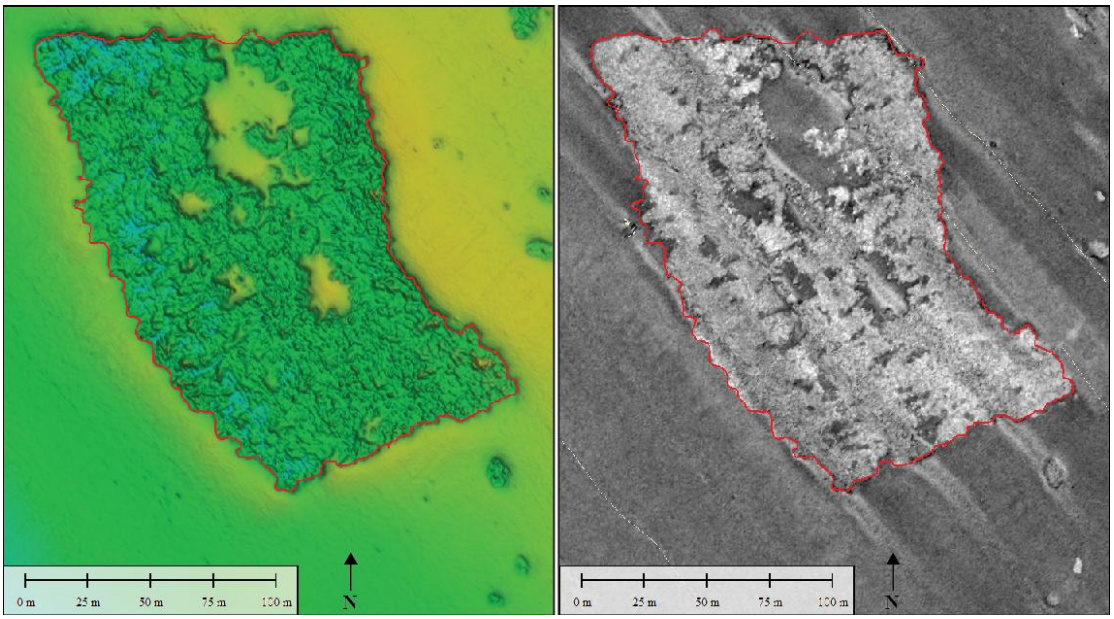

Figure A **Figure B**

Figure 3-2. Figure A shows the module boundary as estimated from bathymetry data. Figure B shows the boundary of Polygon 18 as estimated in Figure A overlaid on Polygon 18 backscatter image.

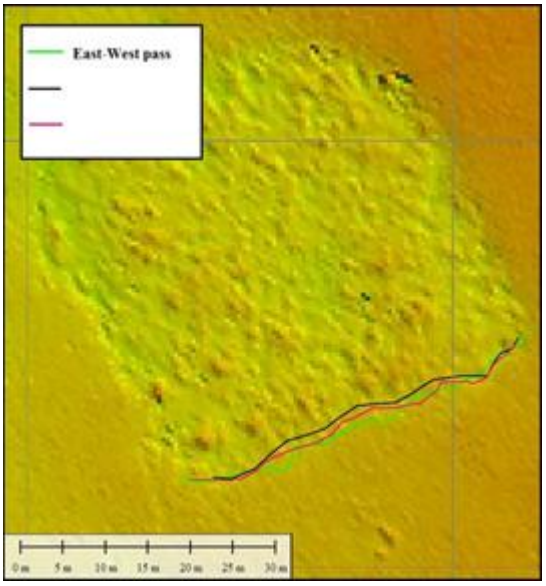

Figure A

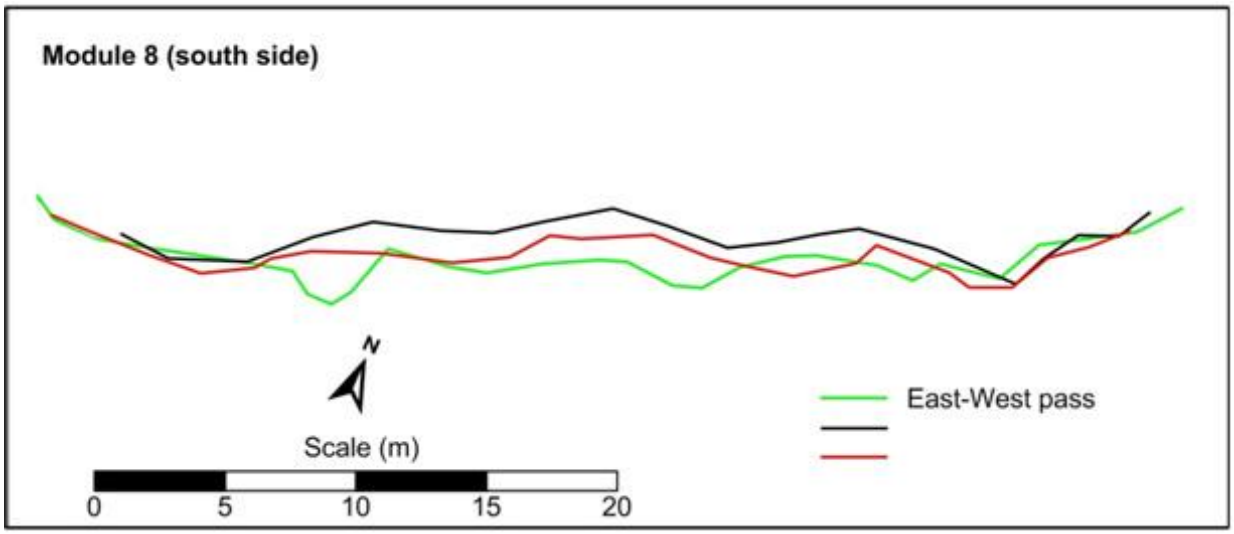

Figure B

Figure 3-3. Survey repeatability of the southern boundary of Module 8 for three survey passes. Figure A shows the southern boundary of Module 8 as estimated from three survey passes overlaid on multibeam bathymetry. Figure B is an enlargement of the southern boundary estimates from the three passes.

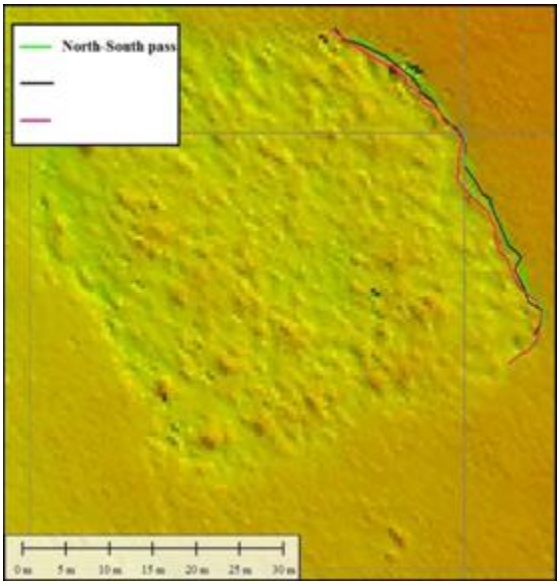

Figure A

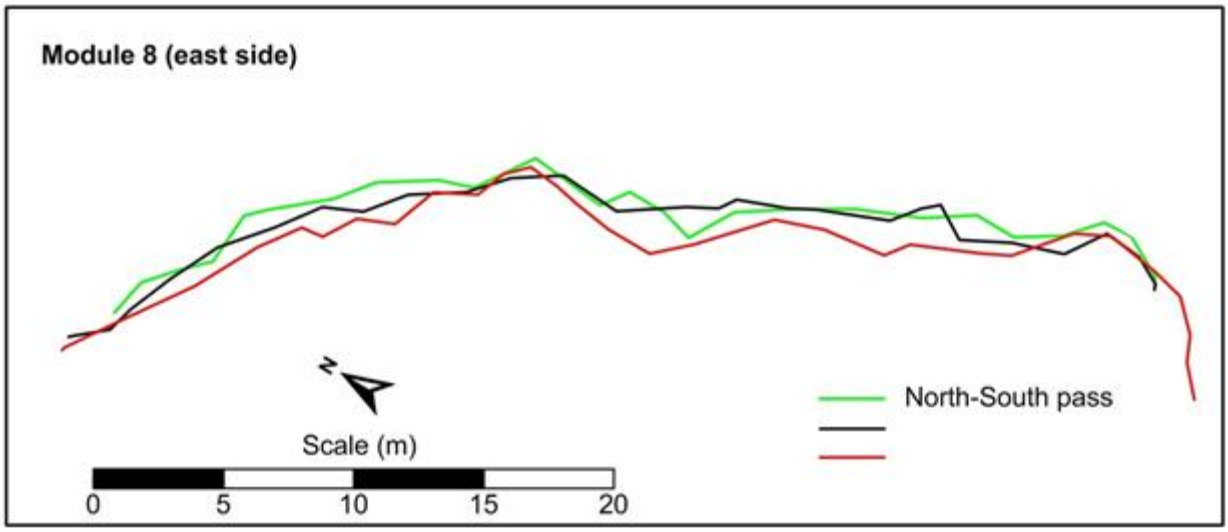

Figure B

Figure 3-4. Survey repeatability of the eastern boundary of Module 8 for three survey passes. Figure A shows the eastern boundary of Module 8 as estimated from three survey passes overlaid on multibeam bathymetry. Figure B is an enlargement of the eastern boundary as estimated from the three passes.

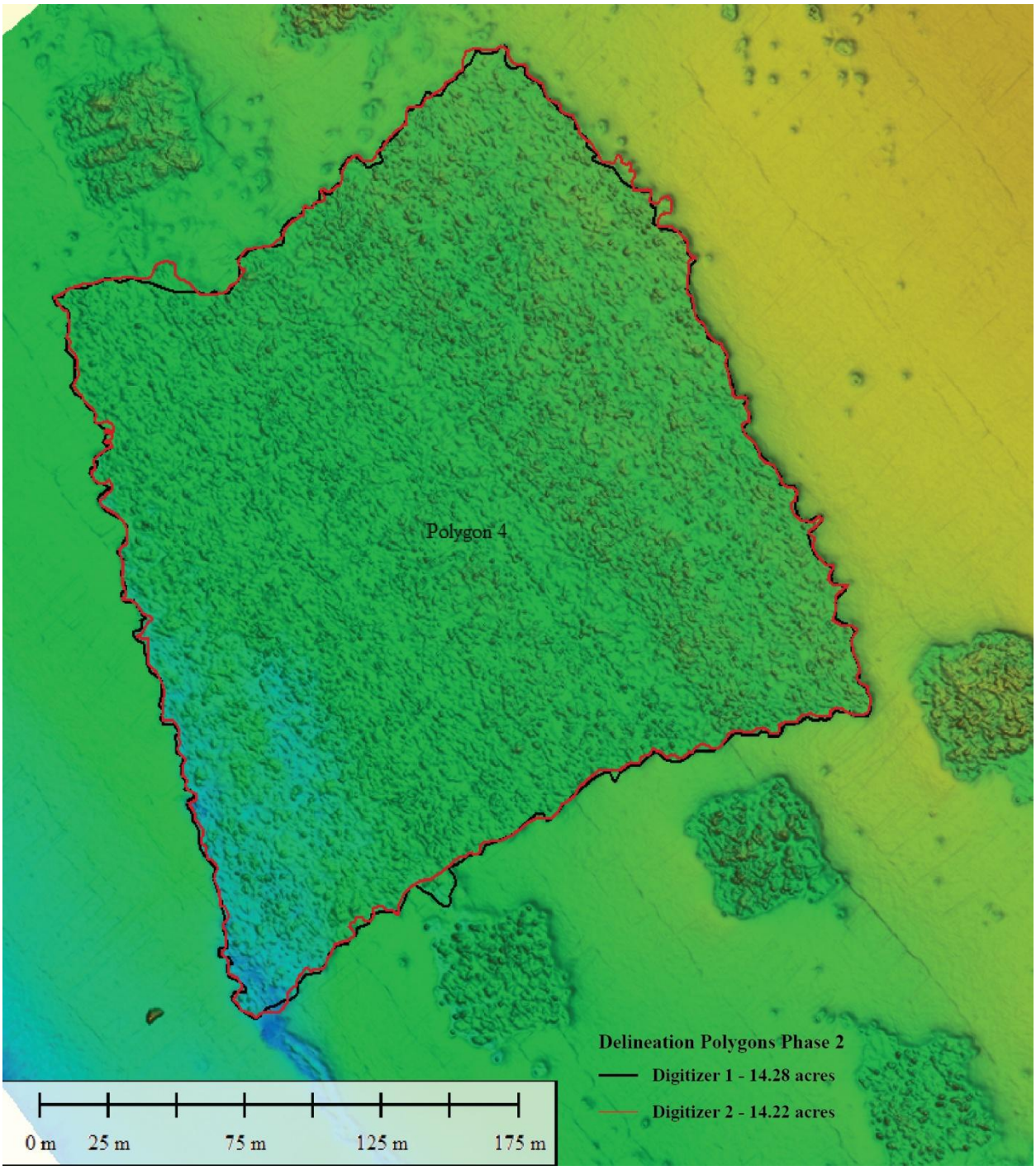

Figure 3-5. Boundary digitization results for Polygon 4 based on bathymetry data, as obtained by two independent surveyors. The difference in calculating the area between the two surveyors was 0.4%.

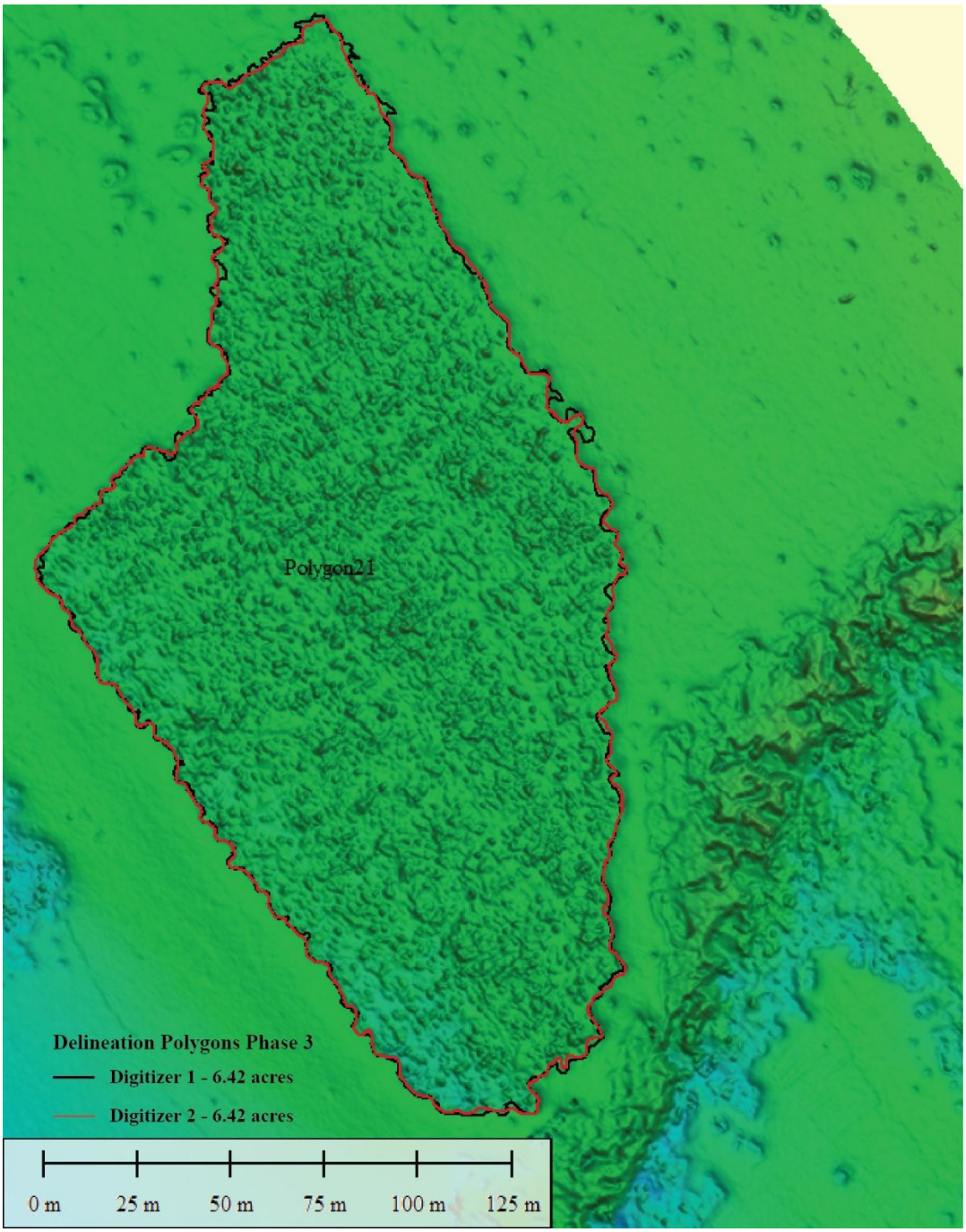

Figure 3-6. Boundary digitization results for Polygon 21 based on bathymetry data, as obtained by two independent surveyors. The difference in calculating the area between the two surveyors was 0.05%.

4.0 CHARTING AND DELIVERABLES

4.1 XYZ FILES

XYZ files of the bathymetry were exported from the *QPS* processing software. These XYZ files are simple ASCII text files. The multibeam data is provided at a 0.30-meter grid spacing and a 0.45-meter grid spacing.

4.2 BATHYMETRY AND IMAGERY CHARTS

Upon completion of data processing and all QC checks, the digital terrain model of the bathymetry was exported to geo-tiff format for charting in *Esri ARC GIS*. The charts were then published in PDF format. Likewise, the imagery mosaic from *QPS' FMGT* software was exported to geo-tiff for charting, which was also exported to PDF.

Deliverables are summarized as follows:

- Chart 1: Polygon and Module Overview on Color-Shaded Multibeam Bathymetry
  This map shows the modules and polygons colored by phase; polygons are labeled with their number, overlaid onto color-shaded illuminated relief (at 0.45 m resolution).
- Chart 2: Backscatter Mosaic
  This map shows the mosaicked backscatter imagery (at 0.2 m resolution).
- Chart 3: Greyscale Multibeam Bathymetry with 1-meter Contours
  Shows greyscale shaded illuminated relief (at 0.45 m resolution) with contours at 1-meter intervals.
- Chart 4: Color-Shaded Multibeam Bathymetry with 1-meter Contours
  Shows color-shaded illuminated relief (at 0.45 m resolution) with contours at 1-meter intervals.
- Chart 5: Bathymetry (0.5-meter Contours) with Polygons and Modules
  Shows bathymetry as 0.5-meter contours without illuminated relief, overlaid on the polygons and modules.

5.0 MULTIBEAM SONAR SURVEY RESULTS

Plots for the digitized boundaries for the 2020 survey are found in Appendices A (Modules) and B and C (Polygons), overlaid onto the boundary results from the September 2009 and October 2014 surveys for comparison. The areas of the modules (Phase 1), based on the digitized bathymetric data, are shown in Table 5-1, while the areas of the polygons (Phase 2) are shown in Table 5-2. The results of the 2020 survey are presented in Table 5-3. Table 5-4 compares the area of WNR in the 2008, 2009, 2014, and 2020 surveys. An increase of less than 1% in the total area of hard substrate occurred from October 2014 through October 2020. The digitized 2020 boundaries for the reef modules and polygons are overlaid onto the bathymetric, color-coded, sun-illuminated images in Appendices D, E, and F. A summary of the survey data is presented in Appendix G in the form of large-scale drawings. Selected examples of the footprints of the modules and polygons are shown in Figures 5-1 through 5-3.

The shallow, nearshore coastal environment is a dynamic habitat with sediment transport varying over the area of the WNR. Some polygons/modules lost areas of hard substrate due to a combination of subsidence of the placed rock material and sand movement, while others gained area due to the re-exposure of areas that had previously been buried, or to the exposure of new hard substrate caused by scouring at the edges of the existing artificial reef. Even so, the footprints of the polygons/modules have remained remarkably similar to those delineated during the 2009 survey, as shown in Figure 5-4 for Polygons 1, 2, 3, 12, and 13.

Table 5-1. Experimental reef module areas from multibeam surveys conducted in September 2009 and October 2014 and 2020.

Module ID	Module area, in acres (from bathymetry)			Module ID	Module area, in acres (from bathymetry)		
	Sep 2009[a]	Oct 2014[a]	Oct 2020		Sep 2009[a]	Oct 2014[a]	Oct 2020
1	0.48	0.43	0.43	29	0.48	0.48	0.48
2	0.45	0.44	0.43	30	0.49	0.47	0.52
3	0.49	0.44	0.36	31	0.48	0.45	0.46
4	0.36	0.31	0.28	32	0.44	0.49	0.46
5	0.42	0.44	0.44	33	0.45	0.48	0.49
6	0.44	0.46	0.44	34	0.48	0.46	0.51
7	0.47	0.45	0.43	35	0.46	0.46	0.45
8	0.45	0.45	0.45	36	0.45	0.46	0.46
9	0.39	0.41	0.39	37	0.51	0.48	0.52
10	0.42	0.46	0.45	38	0.49	0.49	0.52
11	0.38	0.42	0.40	39	0.43	0.43	0.46
12	0.39	0.40	0.38	40	0.44	0.42	0.46
13	0.60	0.60	0.56	41	0.40	0.44	0.40
14	0.48	0.47	0.49	42	0.45	0.46	0.47
15	0.39	0.40	0.40	43	0.44	0.47	0.48
16	0.51	0.50	0.51	44	0.44	0.46	0.45
17	0.43	0.45	0.45	45	0.49	0.46	0.49
18	0.44	0.42	0.45	46	0.42	0.42	0.42
19	0.41	0.43	0.43	47	0.44	0.44	0.46
20	0.40	0.40	0.40	48	0.40	0.43	0.44
21	0.48	0.48	0.47	49	0.45	0.45	0.46
22	0.46	0.47	0.48	50	0.46	0.40	0.46
23	0.46	0.44	0.48	51	0.39	0.40	0.41
24	0.47	0.42	0.44	52	0.43	0.44	0.45
25	0.46	0.47	0.46	53	0.37	0.35	0.39
26	0.53	0.50	0.54	54	0.38	0.37	0.39
27	0.45	0.45	0.44	55	0.29	0.21	0.09
28	0.45	0.43	0.43	56	0.39	0.43	0.40
	TOTAL AREA (PHASE 1 MODULES)				**24.79**	**24.67**	**24.79**

[a] From Coastal Environments (2009 and 2014).

Table 5-2. Polygon areas from 2008, 2009, 2014, and 2020 multibeam data.

Sequential Polygon ID	As-built (2008[a]) area (acres)	Sep 2009[b] area (acres)	Oct 2014[c] area (acres)	Oct 2020 area (acres)
1	13.83	13.48	13.20	13.07
2	38.88	37.75	37.69	38.15
3	6.61	6.19	6.09	6.80
4	14.05	13.99	13.61	14.22
5	9.48	9.60	9.53	9.64
6	4.26	4.29	4.22	4.34
7	6.8	6.69	6.71	6.79
7a	12.2	12.24	12.09	12.06
8	7.64	7.50	7.49	7.56
9	2.52	2.62	2.58	2.54
10	3.89	3.88	3.79	3.71
11	3.48	3.69	3.69	3.67
12	1.35	1.34	1.33	1.35
13	2.85	2.92	2.89	2.78
14	2.12	2.18	2.10	2.06
15	5.54	5.47	5.55	5.51
16	11.19	11.22	11.00	11.09
17	5.32	5.41	5.56	5.41
TOTAL AREA (PHASE 2 POLYGONS)	**152.02**	**150.46**	**149.13**	**150.74**

[a] From Coastal Environments (2008a,b).
[b] From Coastal Environments (2009).
[c] From Coastal Environments (2014).

Table 5-3. Polygon areas from 2020 multibeam data.

Sequential Polygon ID	As-built (2020) area (acres)
18	4.92
19	2.70
20	28.13
21	6.42
23	5.87
24	11.79
25	11.44
26	11.29
27	10.76
28	12.50
29	18.83
30	14.35
31	14.09
32	2.00
33	14.85
34	2.42
37	13.37
38	2.82
39	7.46
40	1.51
TOTAL AREA (PHASE 3 POLYGONS)	**197.52**

Table 5-4. Summary of Wheeler North Reef Area for 2008, 2009, 2014, and 2020 surveys.

Wheeler North Reef	As-built (2008) area (acres)	Sep 2009 area (acres)	Oct 2014 area (acres)	Oct 2020 area (acres)
As-built				
Phase 1 Modules	24.79[a]	24.79	24.67	24.79
Phase 2 Polygons	152.02	150.46	149.13	150.74
Phase 3 Polygons	—	—	—	197.52
TOTAL (ACRES)	**176.81**	**175.25**	**173.80**	**373.05**
Modules plus Polygons except #5 and 7a				
Phase 1 Modules	24.79	24.79	24.67	24.79
Phase 2 Polygons	130.34	128.62	127.51	129.04
Phase 3 Polygons	—	—	—	197.52
TOTAL (ACRES)	**155.13**	**153.41**	**152.18**	**351.35**

[a] From Coastal Environments (2008a,b).
[b] From Coastal Environments (2009).
[c] From Coastal Environments (2014).

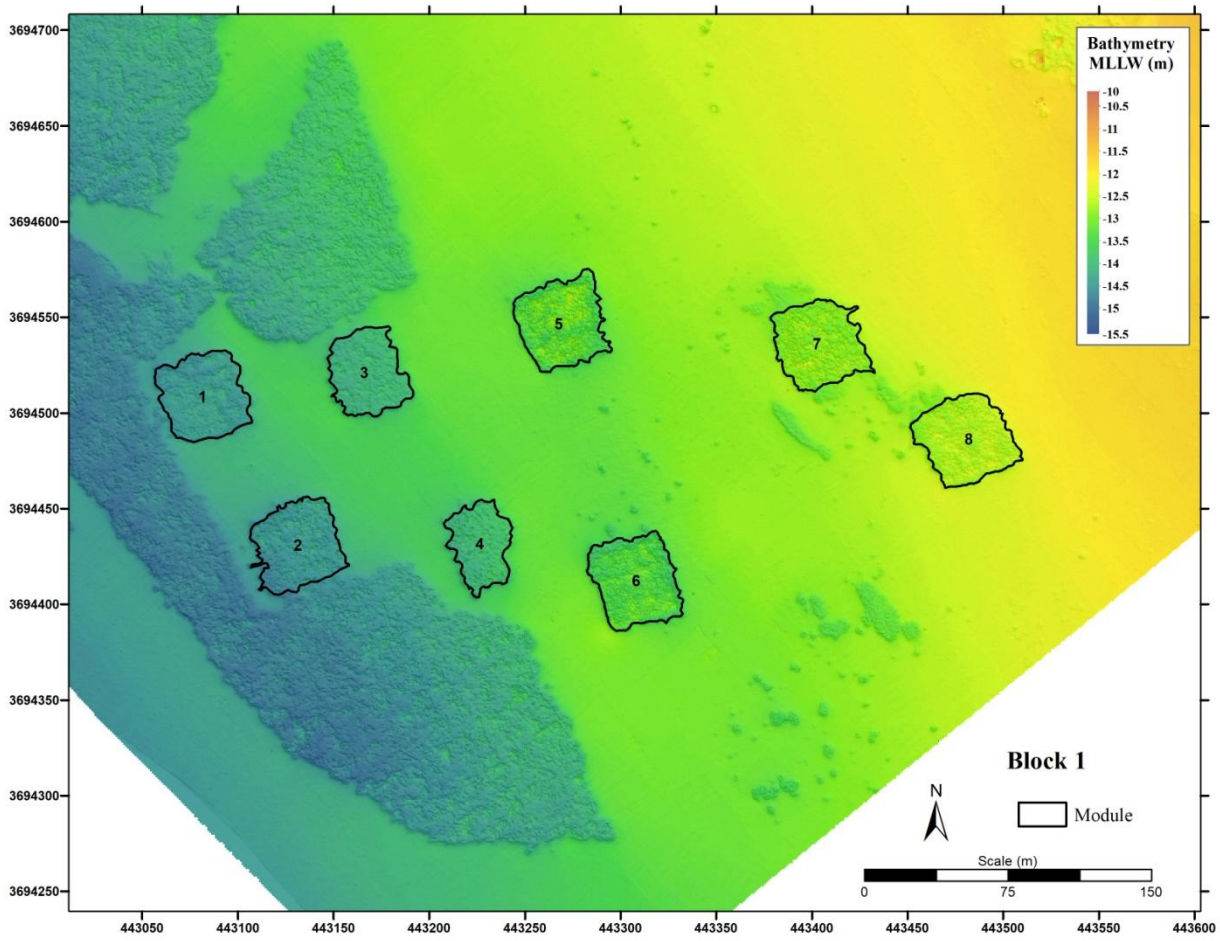

Figure 5-1. Footprint of the modules for Block 1 from October 2020 survey.

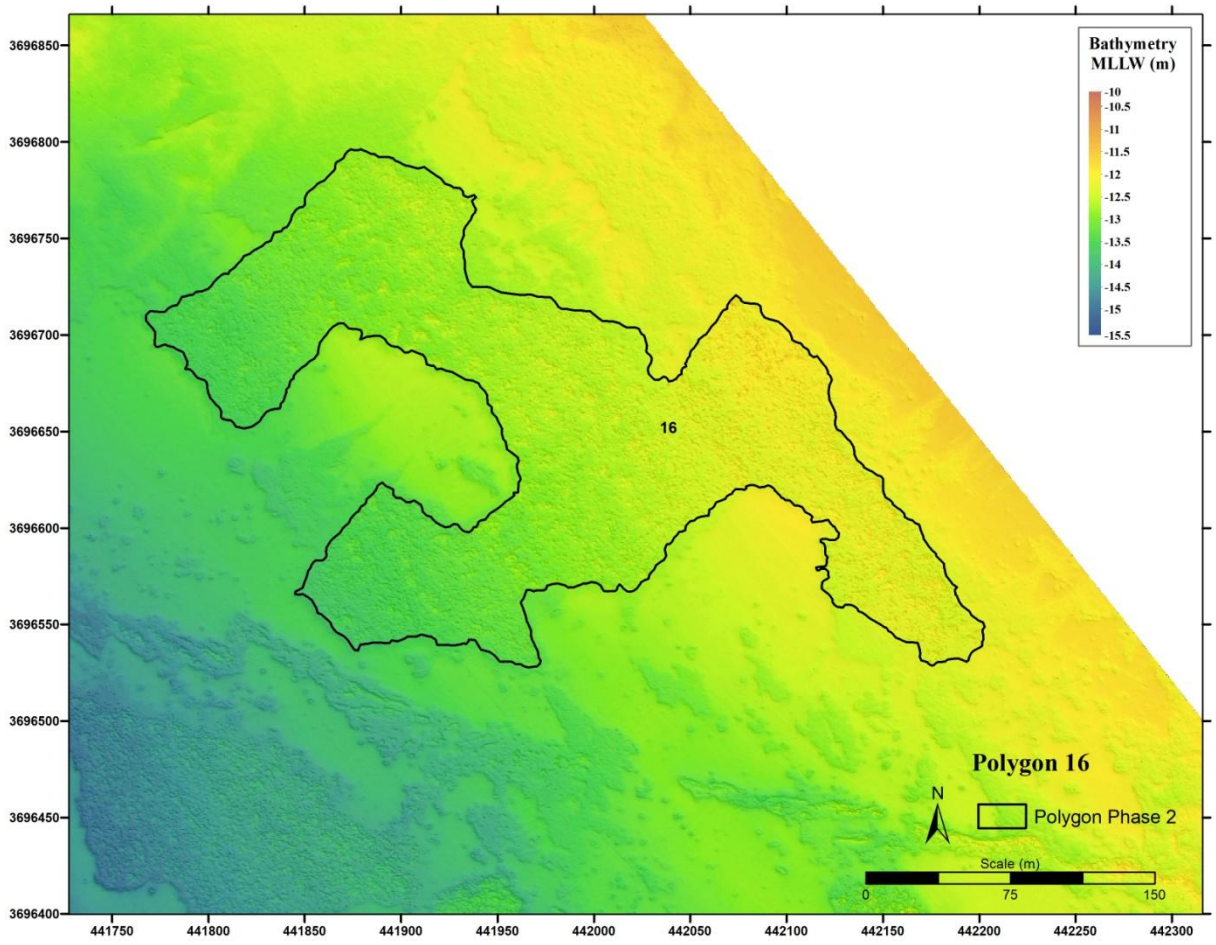

Figure 5-2. Footprint of Polygon 16 from October 2020 survey.

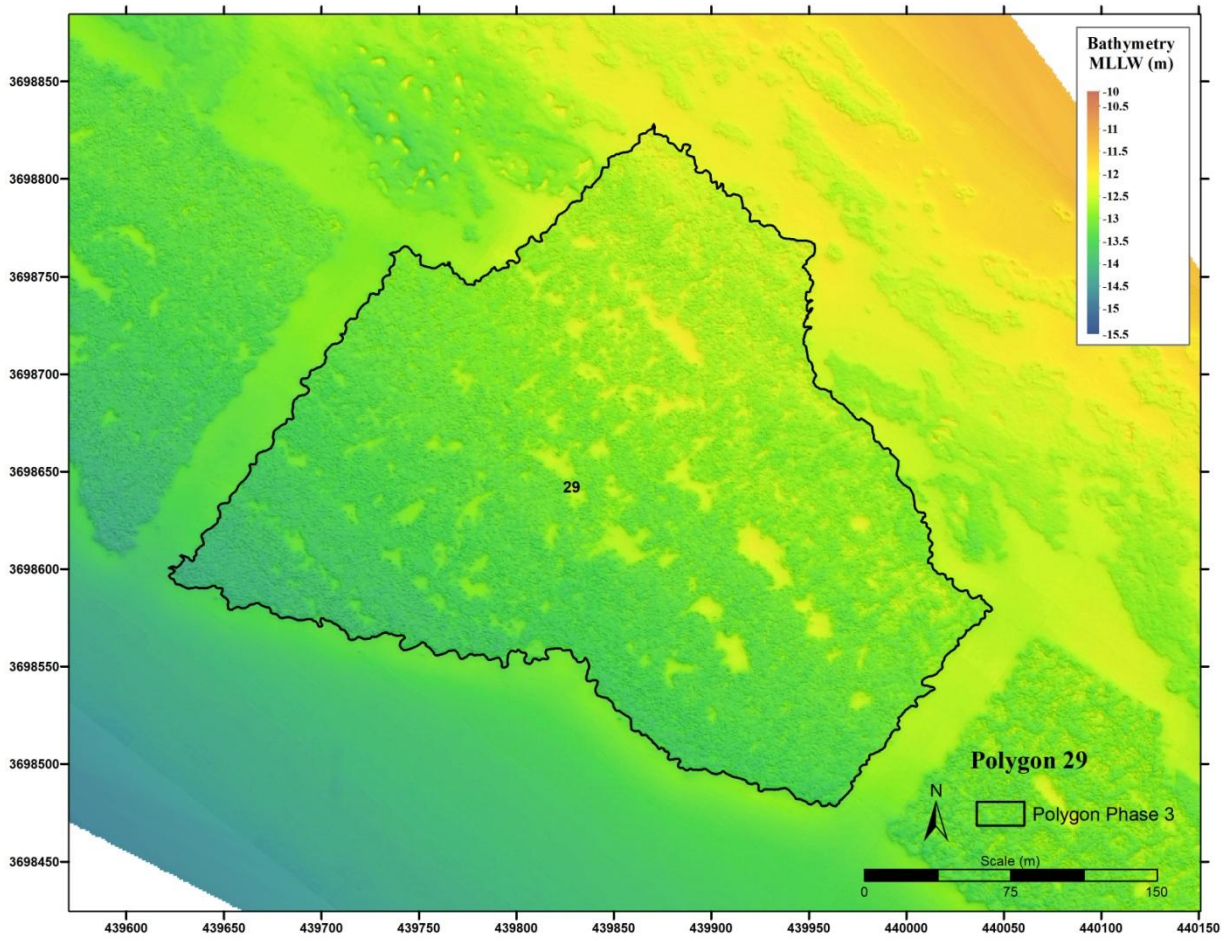

Figure 5-3. Footprint of Polygon 29 from October 2020 survey.

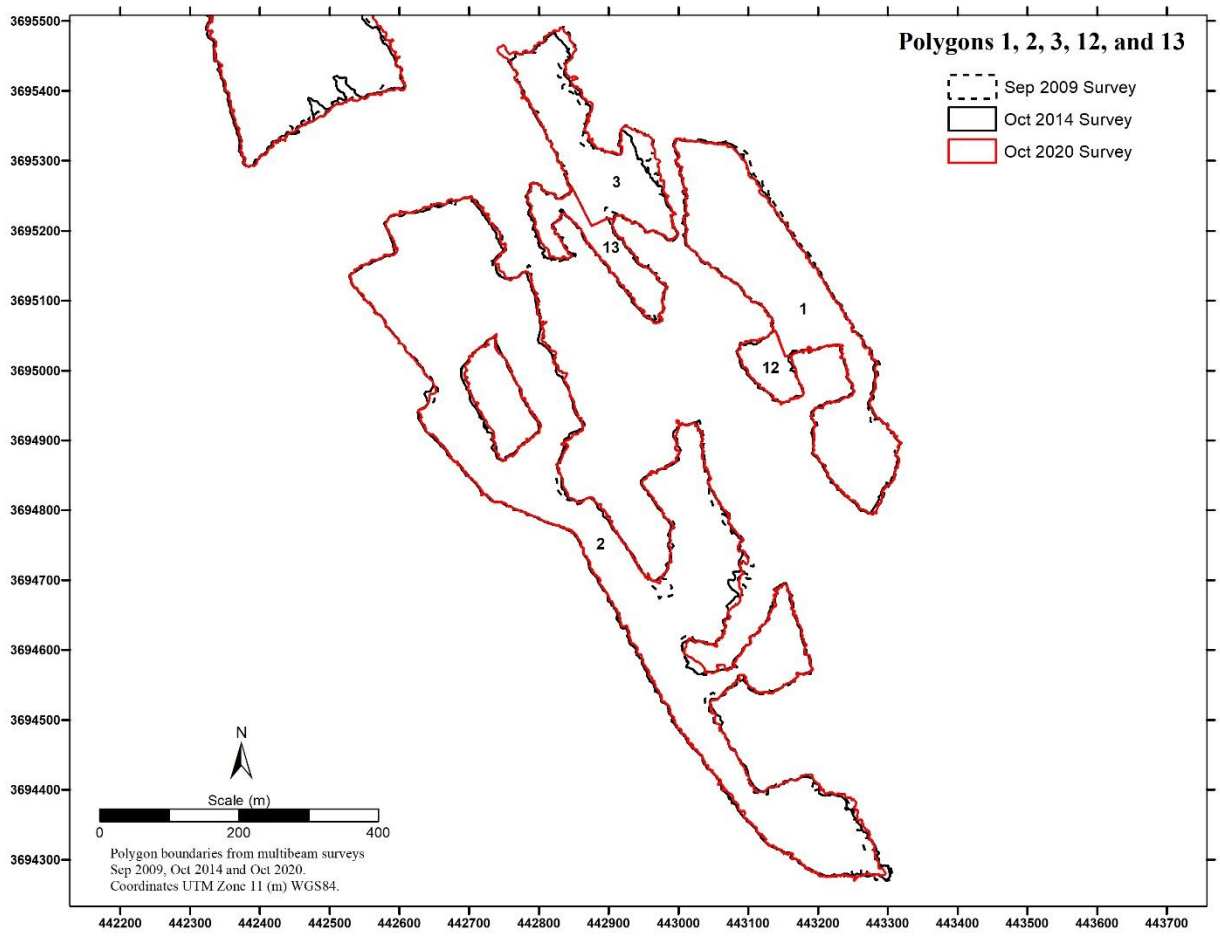

Figure 5-4. Comparison of footprints for Polygons 1, 2, 3, 12, and 13 from multibeam surveys during September 2009, October 2014, and October 2020.

6.0 SUMMARY AND CONCLUSIONS

A multibeam survey was carried out from 7 October 2020 through 10 October 2020 to determine the area of hard substrate of WNR. The reef consists of 56 (40 m x 40 m) modules and 37 polygons, ranging in size from 1.35 to 38.88 acres.

The bathymetric survey was conducted using high frequency (400 kHz) multibeam sonar with a small beam width (0.5 degrees) to maximize feature detection capabilities for the water depths of the survey area. Depths within the survey footprint range from -8 m to approximately -17 m, MLLW. A total of 193 track lines were surveyed. The survey covered 100% of the reef areas (Figures 1-2 and 1-3).

The survey performed during October 2020, in order to assess the hard substrate coverage of the WNR, obtained high-quality multibeam data in spite of the presence of kelp. The survey was carried out during high tides as the water overtopped the kelp canopy to minimize kelp entanglement in the MBES.

The bathymetric data was the primary data source in delineating the boundaries of the modules and polygons. Backscatter data were utilized to aid in delineation of the areas that were difficult to interpret based on bathymetric data alone (Figure 3-2).

The repeatability of the survey was tested with two methods. The first method involved surveying the southern and eastern edge of Module 8 three times from different directions (Figures 3-3 and 3-4). The second method consisted of digitizing the edges of the polygon using two independent surveyors (Figures 3-5 and 3-6). The results show that the survey accuracy and digitizing deviation is within 1-2 m, and that the deviation from one point to another fluctuates, such that the survey error in estimating the total area is likely to be 1% or less.

From reviewing the results from 2009, 2014 and 2020 surveys, one can notice that some of the natural reef features inshore of WNR have become buried by sand movement, a phenomenon that has also been observed on the easternmost boundary of WNR. However, although some small, inshore areas have become buried, the reef's boundaries have remained remarkably similar to those seen in the 2009 and 2014 surveys. The results of the survey are presented graphically in Appendices A-G.

The changes in area among all modules between October 2014 and October 2020 were small. The results of the 2014 and 2020 surveys show that the total area of the modules was 24.67 acres in 2014 and 24.79 acres in 2020 (Table 5-4). This equates to an increase of 0.5% in total module areas. While for Phase 1 and Phase 2 combined, the October 2014 survey (Table 5-4) showed a total WNR area (excluding Polygons 5 and 7a) of 152.18 acres, vs. the October 2020 survey, which showed a total area 153.83 acres, accounting for an increase of 1%. After the construction of Phase 3, the total acres of the reef based on October 2020 survey is 373.1 acres.

7.0 REFERENCES

California Coastal Commission (CCC), 2008. Coastal Development Permit #E-07-010 (Southern California Edison Company). Adopted on 2 February 2008, California Coastal Commission, 45 Fremont Street, Suite 2009, San Francisco, CA 94105-2219. 35 pp.

Coastal Environments, 1999. Construction of Southern California Edison Experimental Artificial Kelp Reef, San Clemente, California, Volume I. Report submitted to Southern California Edison, 2244 Walnut Grove Avenue, Rosemead, CA 91770. CE Ref. No. 99-14, 24 November 1999. 35 pp. and 4 appendices.

Coastal Environments, 2008a. Final Construction Report for Wheeler North Reef at San Clemente, California (SONGS Artificial Reef Mitigation Project, Phase 2 Mitigation Reef), Volume I. Report submitted to Southern California Edison Company, 2244 Walnut Grove Avenue, Rosemead, CA 91770. CE Reference No. 08-33, 4 November 2008. 43 pp. and 4 appendices.

Coastal Environments, 2008b. Final Construction Report for Wheeler North Reef at San Clemente, California (formerly the SONGS Artificial Reef Mitigation Project, Phase 2 Mitigation Reef), Volume II: Data Report. Prepared for Southern California Edison Company, 2244 Walnut Grove Avenue, Rosemead, CA 91770. CE Reference No. 08-34, 5 November 2008 (revised 12 December 2008). 8 pp. and 7 appendices.

Coastal Environments, 2009. Multibeam Survey of Wheeler North Reef, San Clemente, California. Prepared for Southern California Edison Company, 2244 Walnut Grove Avenue, Rosemead, CA 91770. CE Reference No. 09-23, 9 November 2009. 21 pp. and 9 appendices.

Coastal Environments, 2014. Multibeam Survey of Wheeler North Reef, San Clemente, California. Prepared for Southern California Edison Company, 2244 Walnut Grove Avenue, Rosemead, CA 91770. CE Reference No. 14-25, 19 December 2014. 27 pp. and 5 appendices.

Coastal Environments, 2020a. Construction of Wheeler North Reef at San Clemente, California (SONGS Artificial Reef, Mitigation Project, Phase 3 Expansion Project), Final Report Volume I, Technical Report. Report submitted to Southern California Edison Company, 2244 Walnut Grove Avenue, Rosemead, CA 91770. CE Ref. No. 20-32, 30 November 2020. 44 pp. + 2 appendices.

Coastal Environments, 2020b. Construction of Wheeler North Reef at San Clemente, California (SONGS Artificial Reef, Mitigation Project, Phase 3 Expansion Project), Final Report Volume II, Data Report. Report submitted to Southern California Edison Company, 2244 Walnut Grove Avenue, Rosemead, CA 91770. CE Ref. No. 20-33, 30 November 2020. 11 pp. + 8 appendices.

U.S. Army Corps of Engineers, 2013. Hydrographic Survey Manual, Engineering and Design Manual No. EM-1110-2-1003, Washington D.C.

APPENDIX A

COMPARISON OF MODULE BOUNDARIES FROM 2009 (BATHYMETRY), OCTOBER 2014 (BATHYMETRY), AND OCTOBER 2020 (BATHYMETRY) FOR BLOCKS 1-7

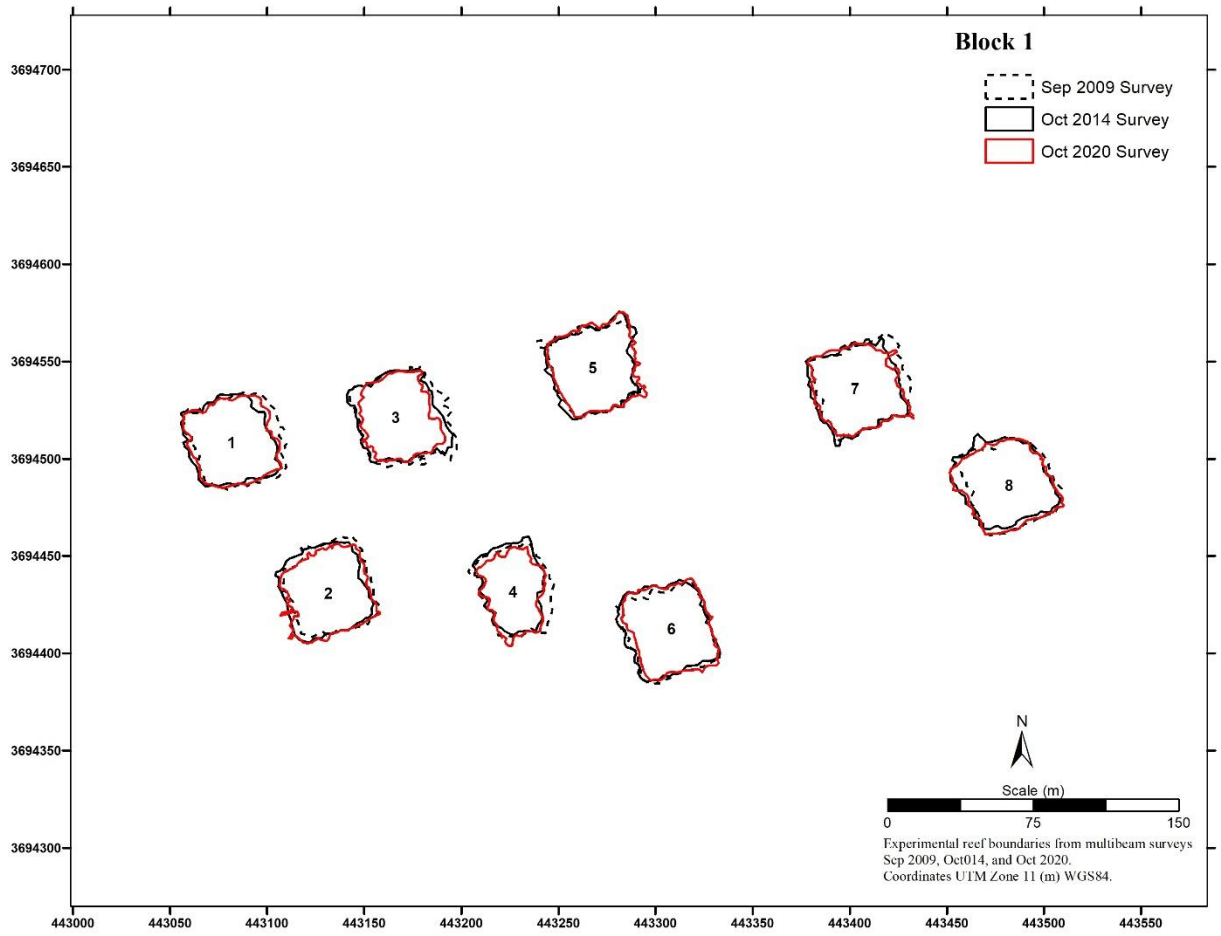

Figure A-1. Comparison of module boundaries from 2009 (bathymetry), October 2014 (bathymetry), and October 2020 (bathymetry) for Block 1.

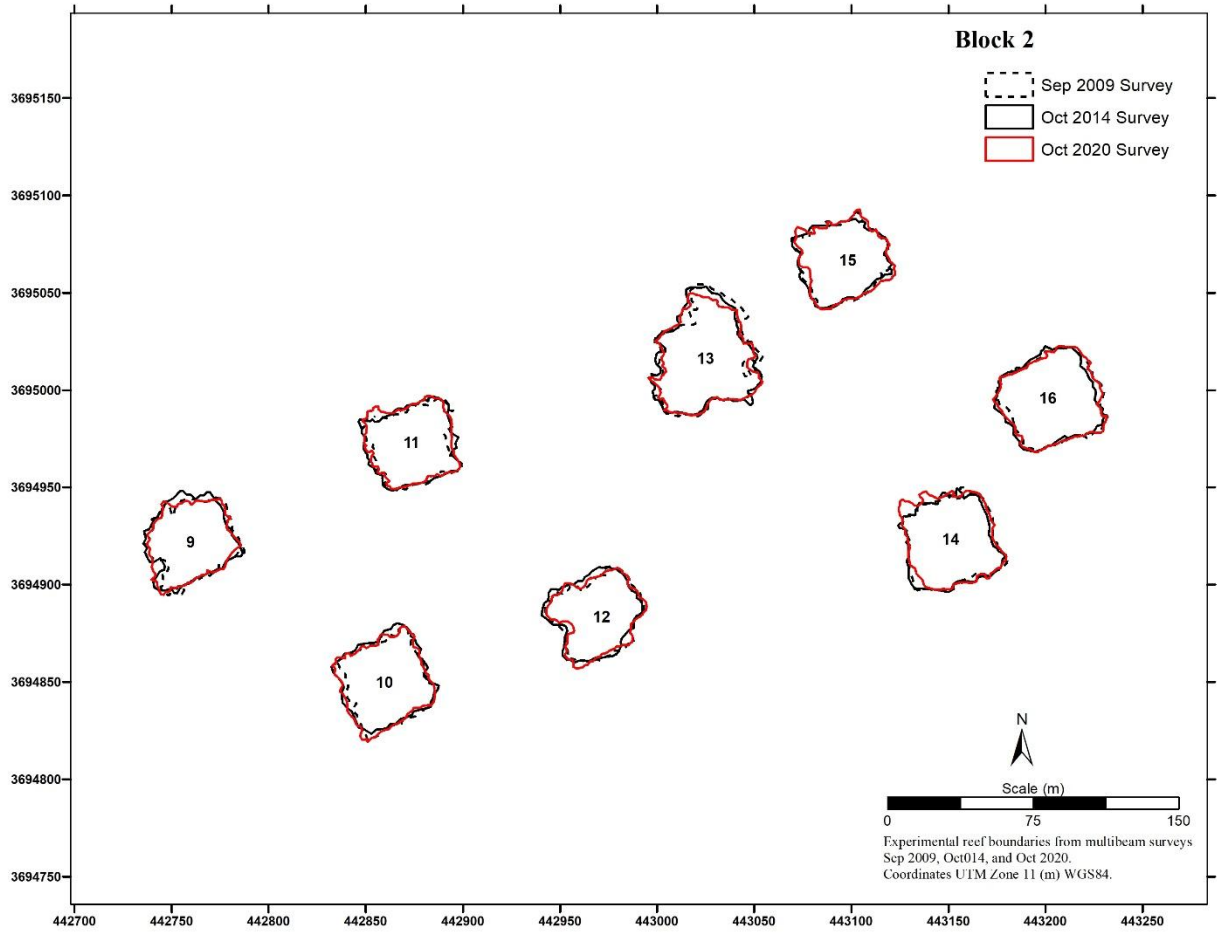

Figure A-2. Comparison of module boundaries from 2009 (bathymetry), October 2014 (bathymetry), and October 2020 (bathymetry) for Block 2.

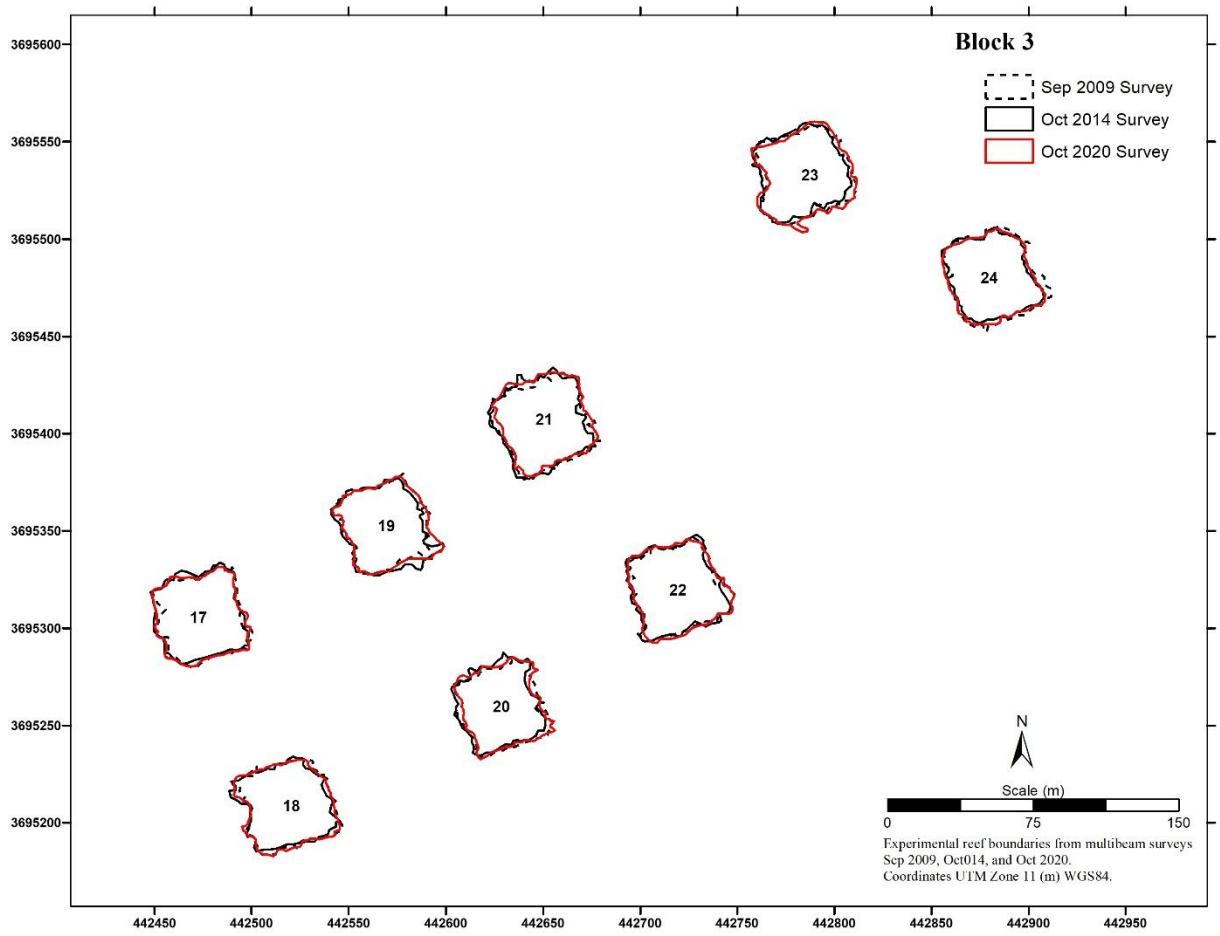

Figure A-3. Comparison of module boundaries from 2009 (bathymetry), October 2014 (bathymetry), and October 2020 (bathymetry) for Block 3.

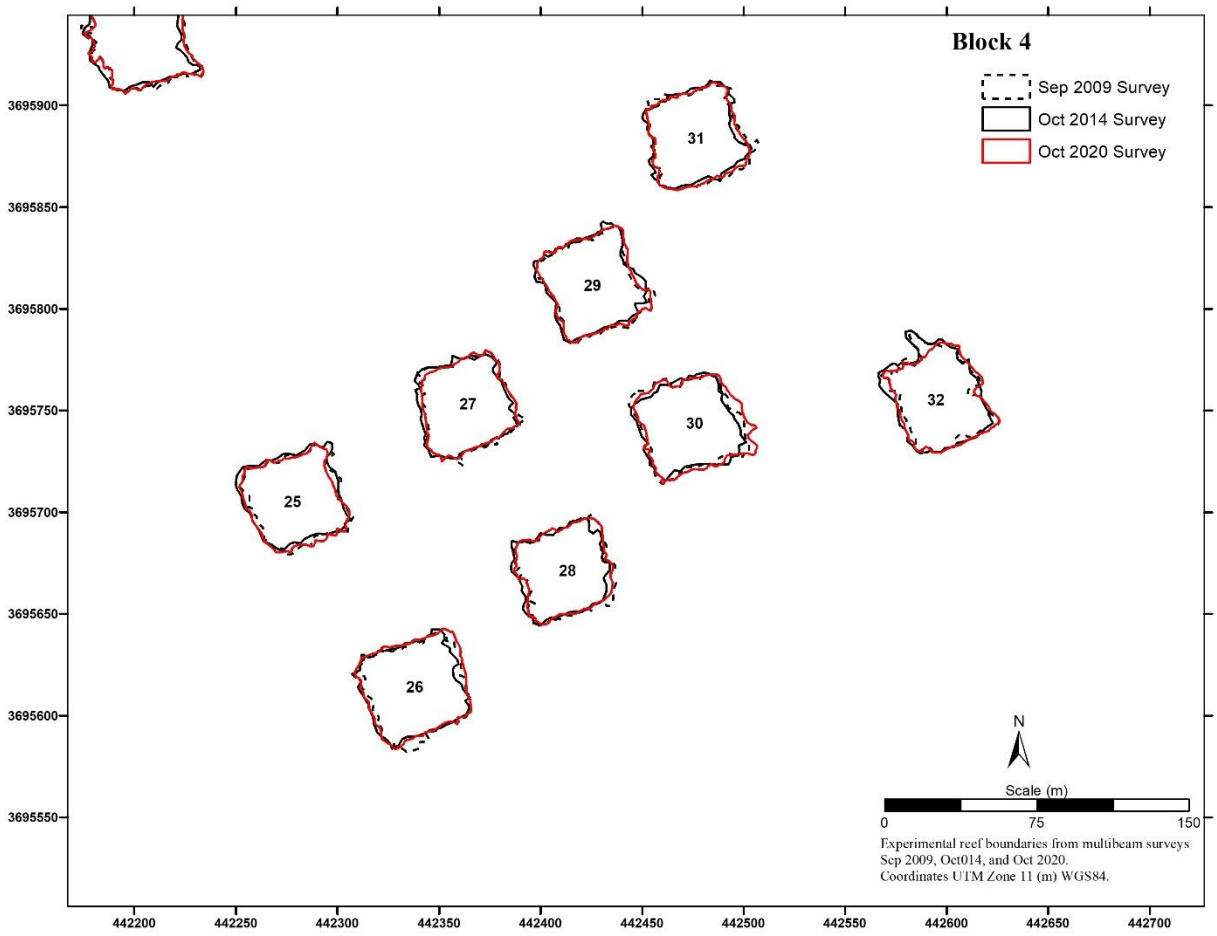

Figure A-4. Comparison of module boundaries from 2009 (bathymetry), October 2014 (bathymetry), and October 2020 (bathymetry) for Block 4.

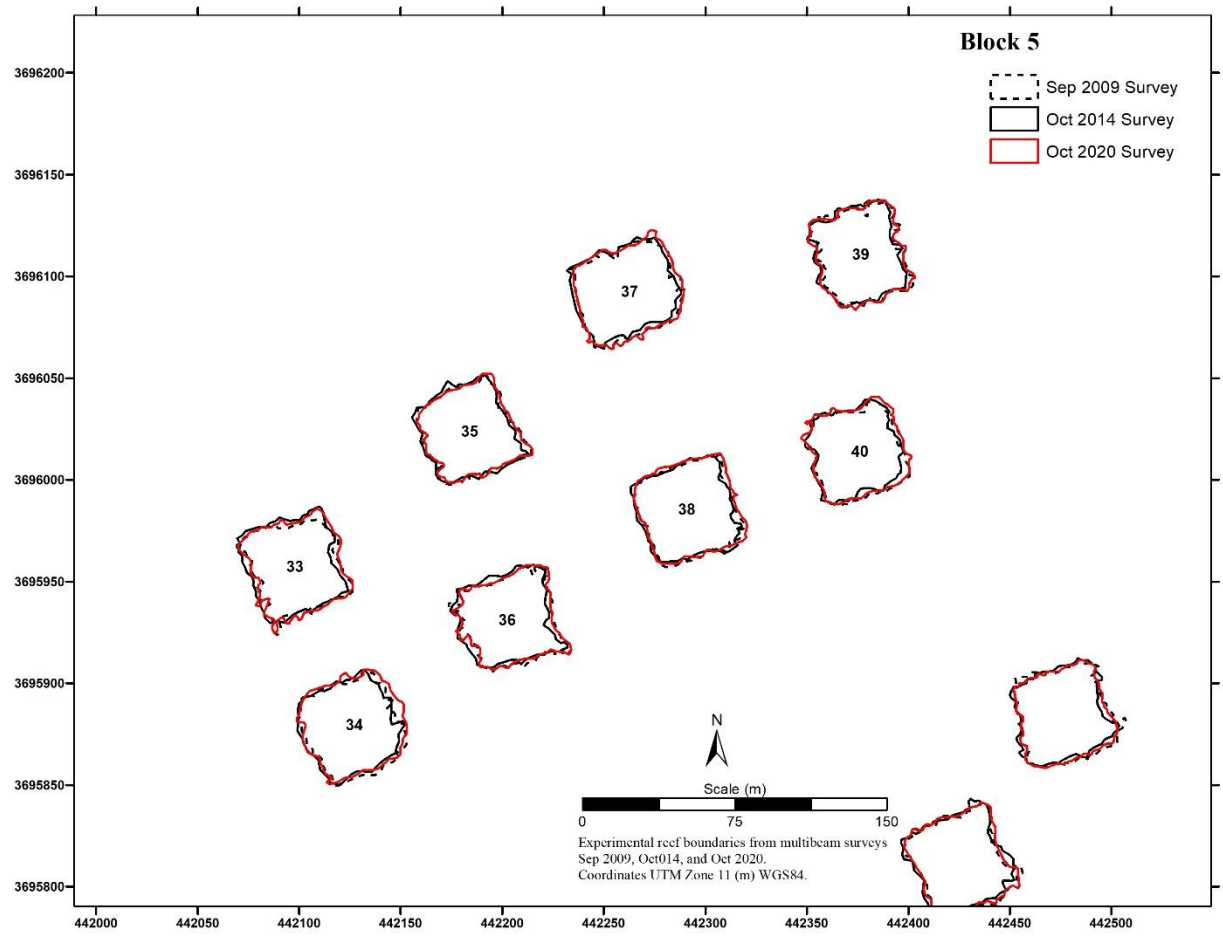

Figure A-5. Comparison of module boundaries from 2009 (bathymetry), October 2014 (bathymetry), and October 2020 (bathymetry) for Block 5.

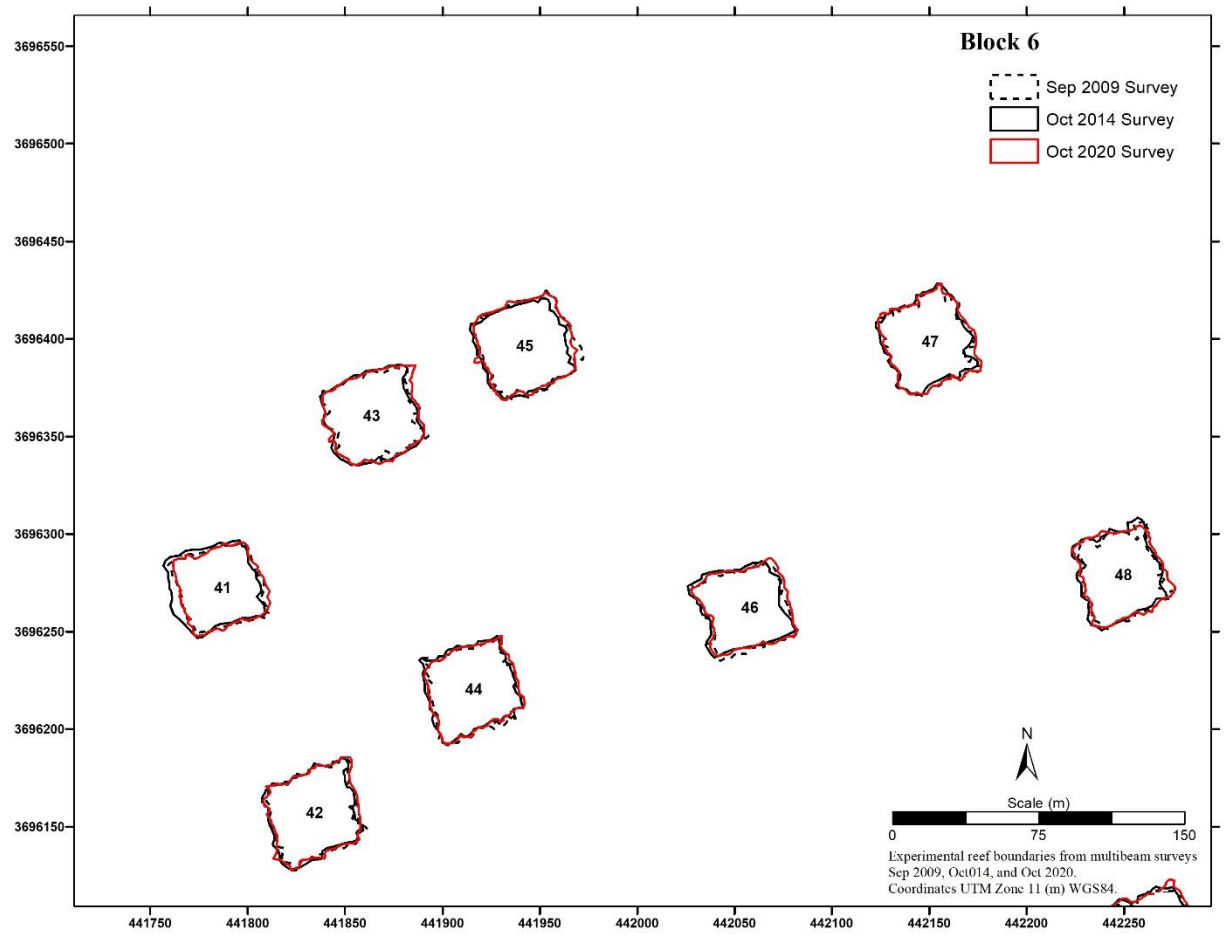

Figure A-6. Comparison of module boundaries from 2009 (bathymetry), October 2014 (bathymetry), and October 2020 (bathymetry) for Block 6.

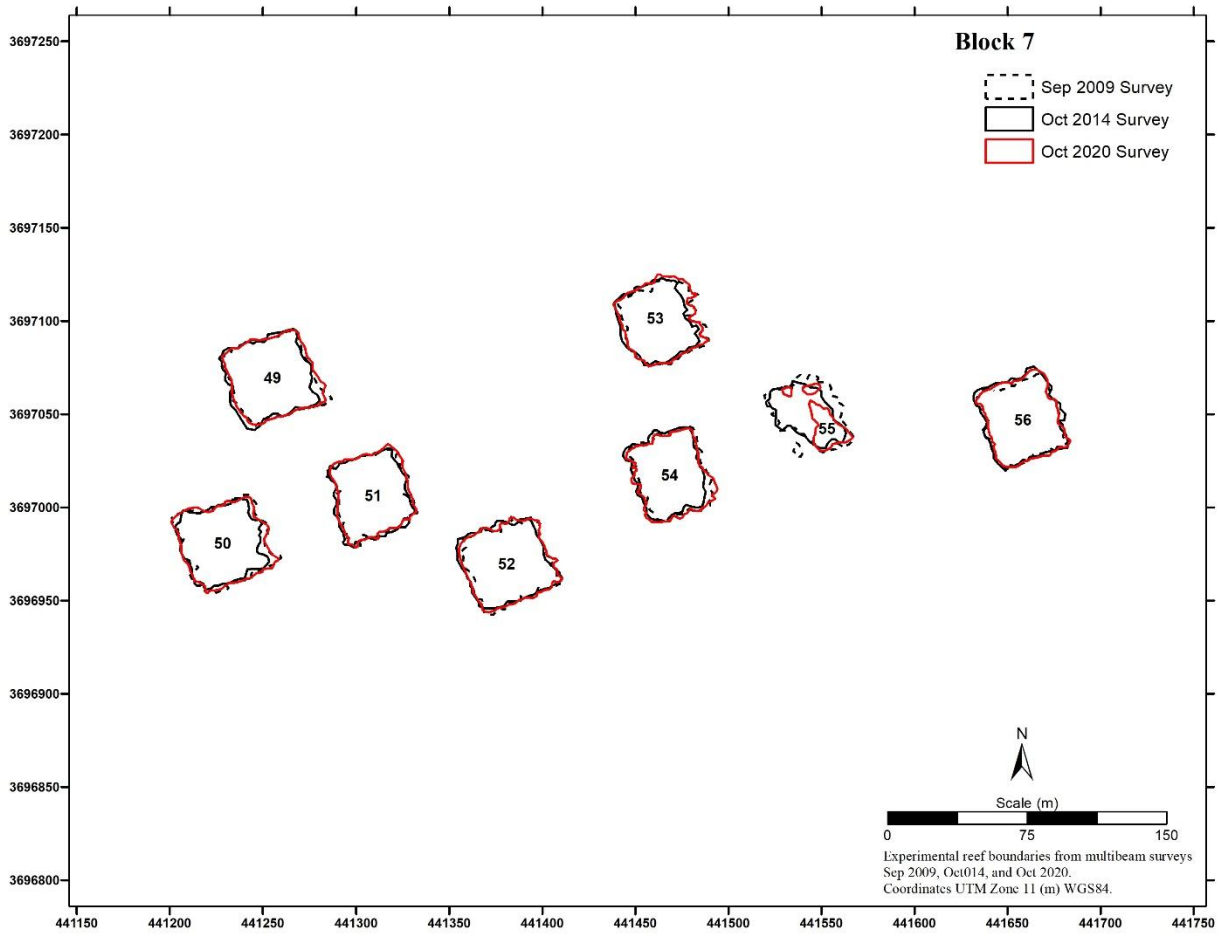

Figure A-7. Comparison of module boundaries from 2009 (bathymetry), October 2014 (bathymetry), and October 2020 (bathymetry)for Block 7.

APPENDIX B

COMPARISON OF POST-CONSTRUCTION (2009), OCTOBER 2014, AND OCTOBER 2020 BOUNDARIES FROM BATHYMETRY DATA FOR POLYGONS 1-17

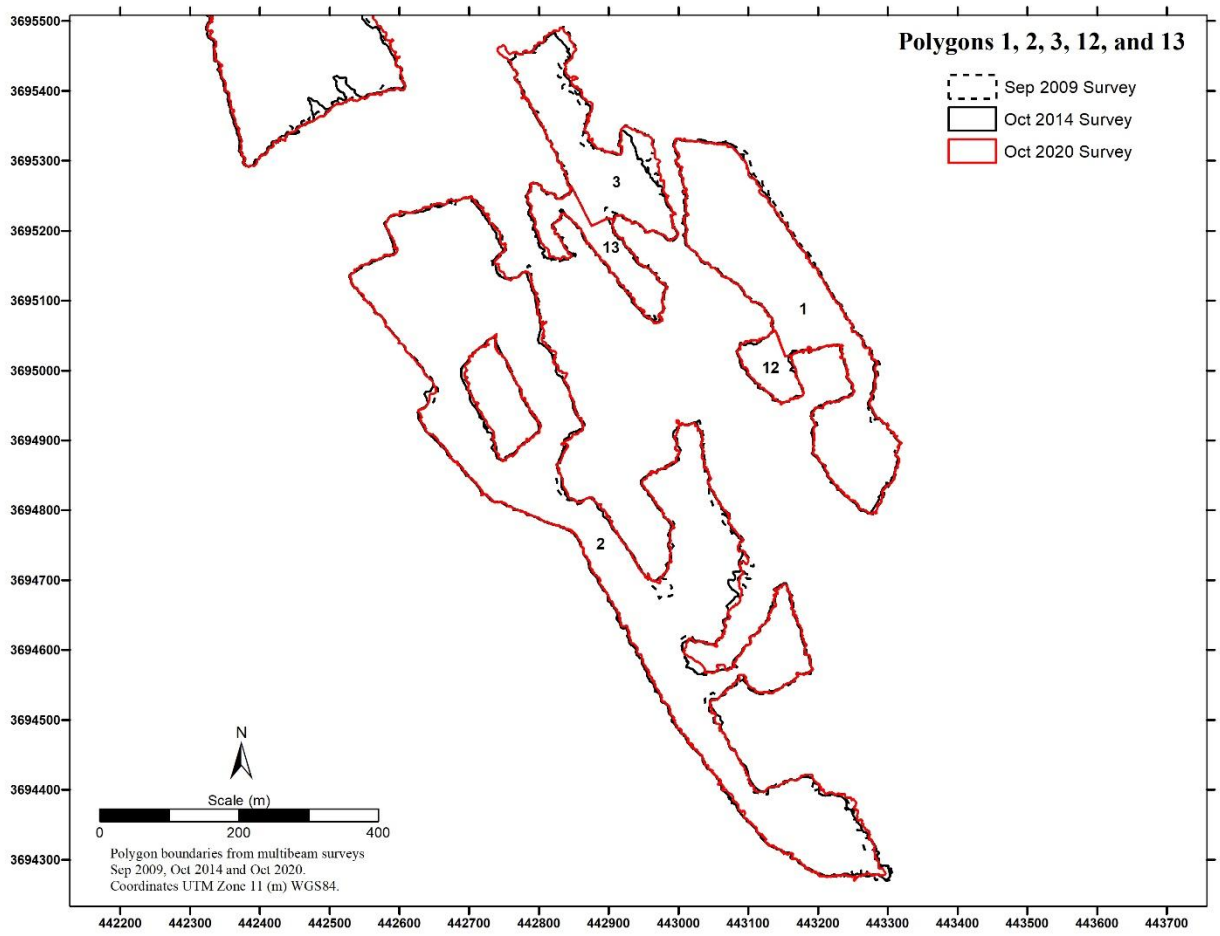

Figure B-1. Comparison of post-construction (2009), October 2014, and October 2020 boundaries from bathymetry data for Polygons 1, 2, 3, 12, and 13.

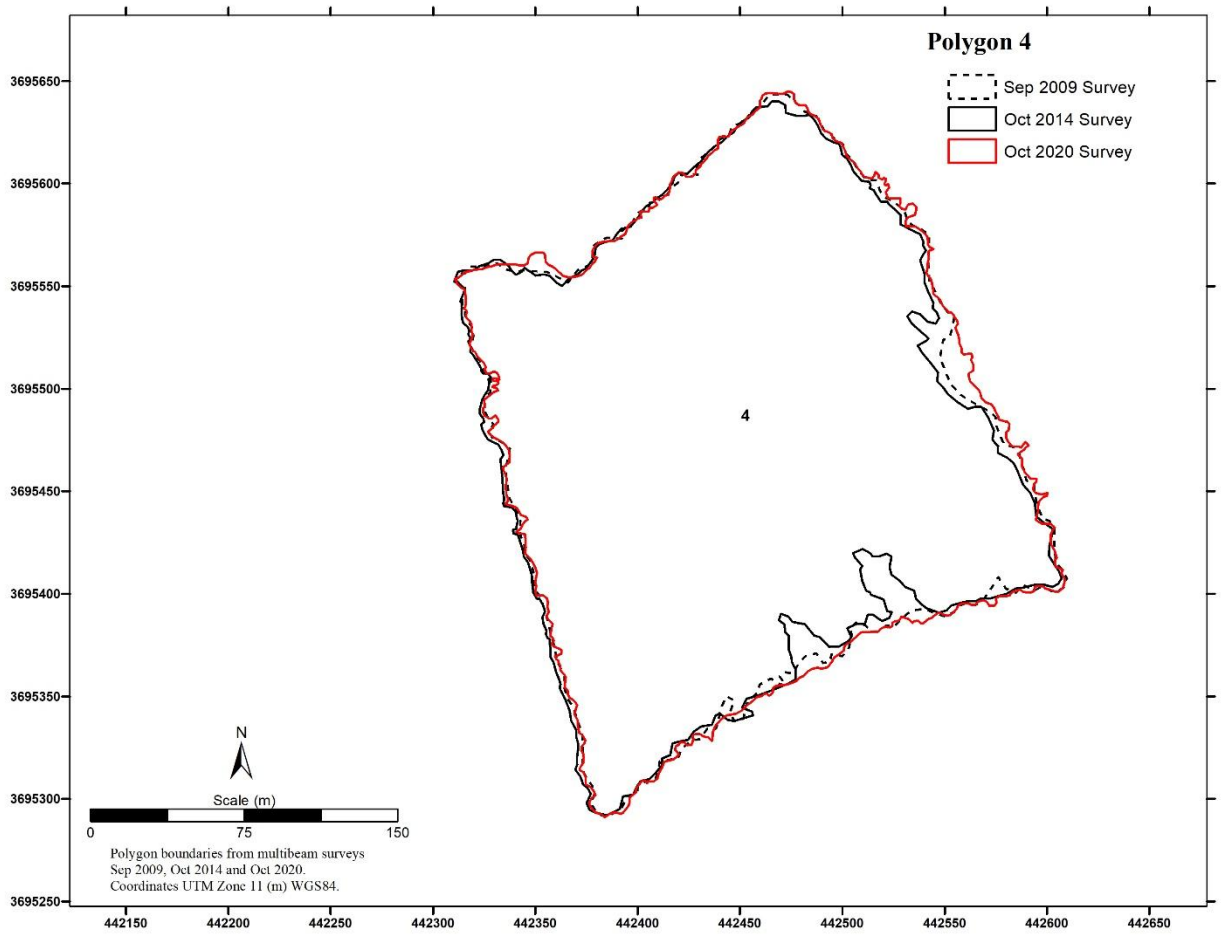

Figure B-2. Comparison of post-construction (2009), October 2014, and October 2020 boundaries from bathymetry data for Polygon 4.

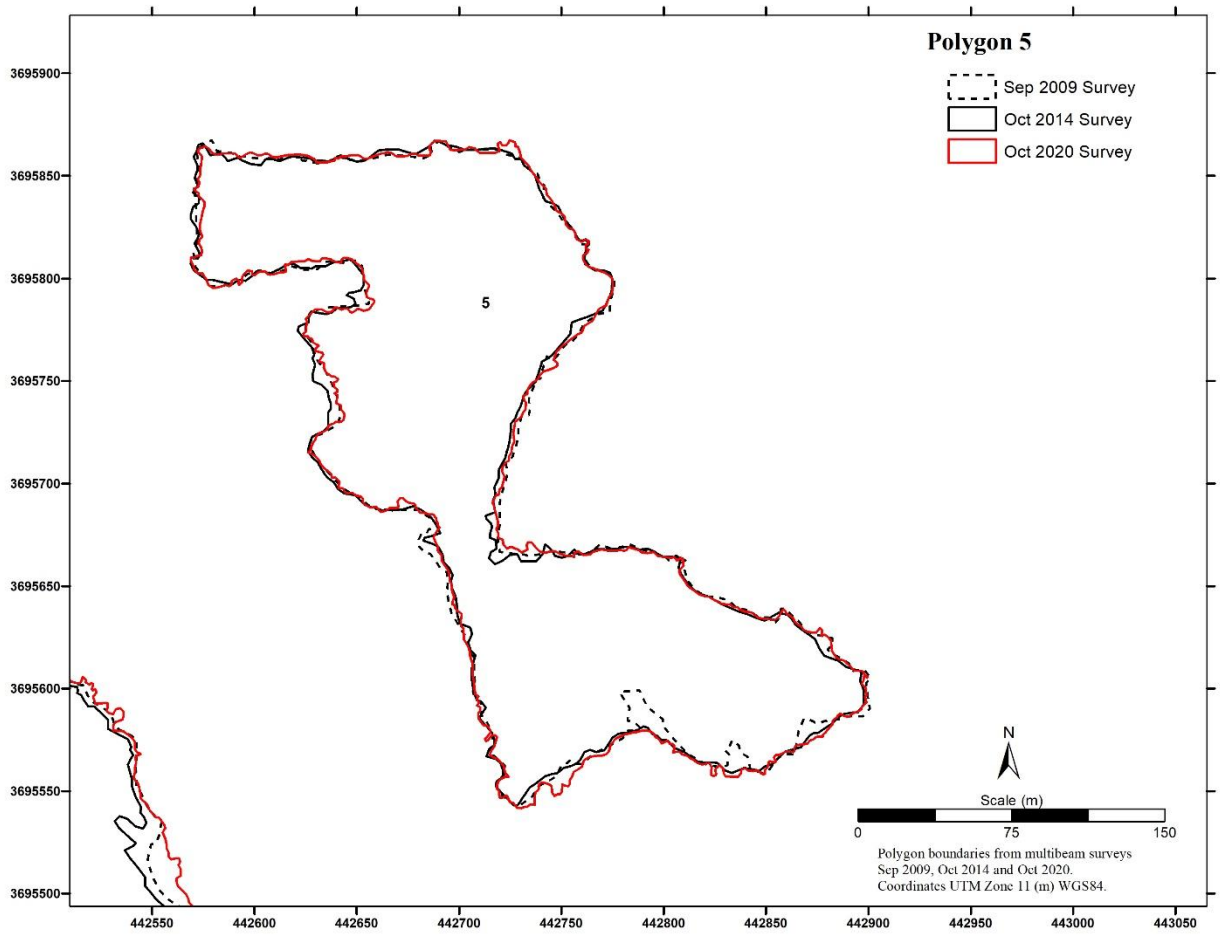

Figure B-3. Comparison of post-construction (2009), October 2014, and October 2020 boundaries from bathymetry data for Polygon 5.

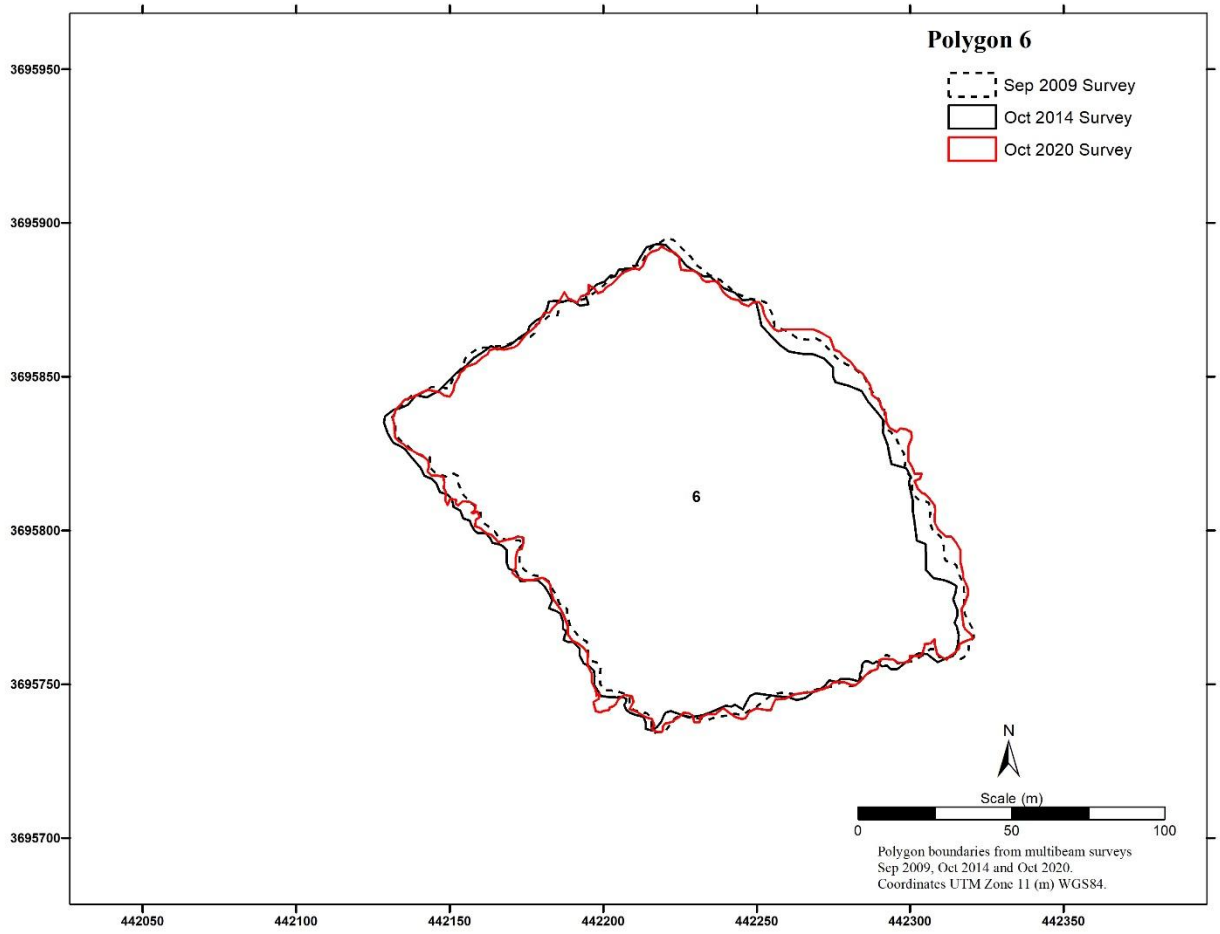

Figure B-4. Comparison of post-construction (2009), October 2014, and October 2020 boundaries from bathymetry data for Polygon 6.

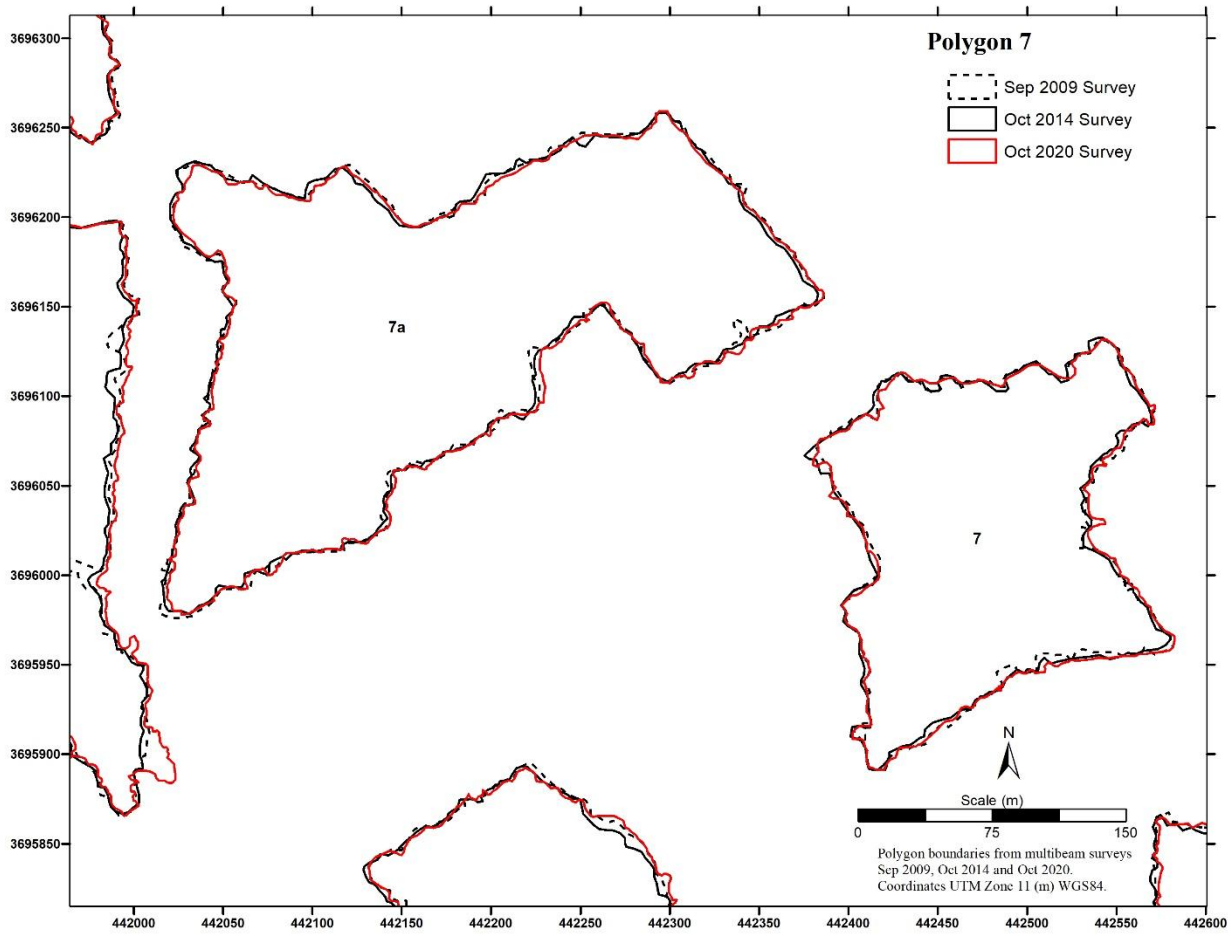

Figure B-5. Comparison of post-construction (2009), October 2014, and October 2020 boundaries from bathymetry data for Polygon 7.

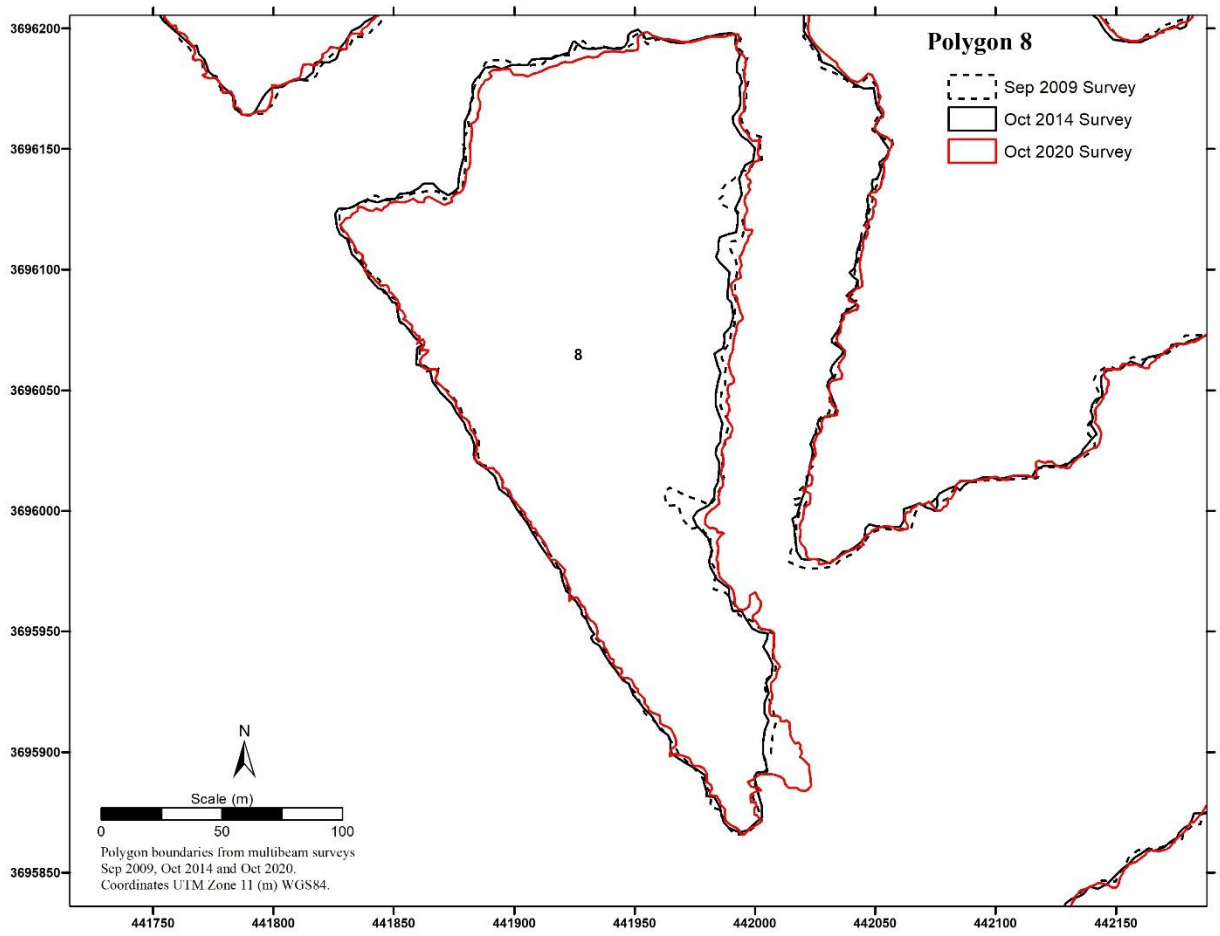

Figure B-6. Comparison of post-construction (2009), October 2014, and October 2020 boundaries from bathymetry data for Polygon 8.

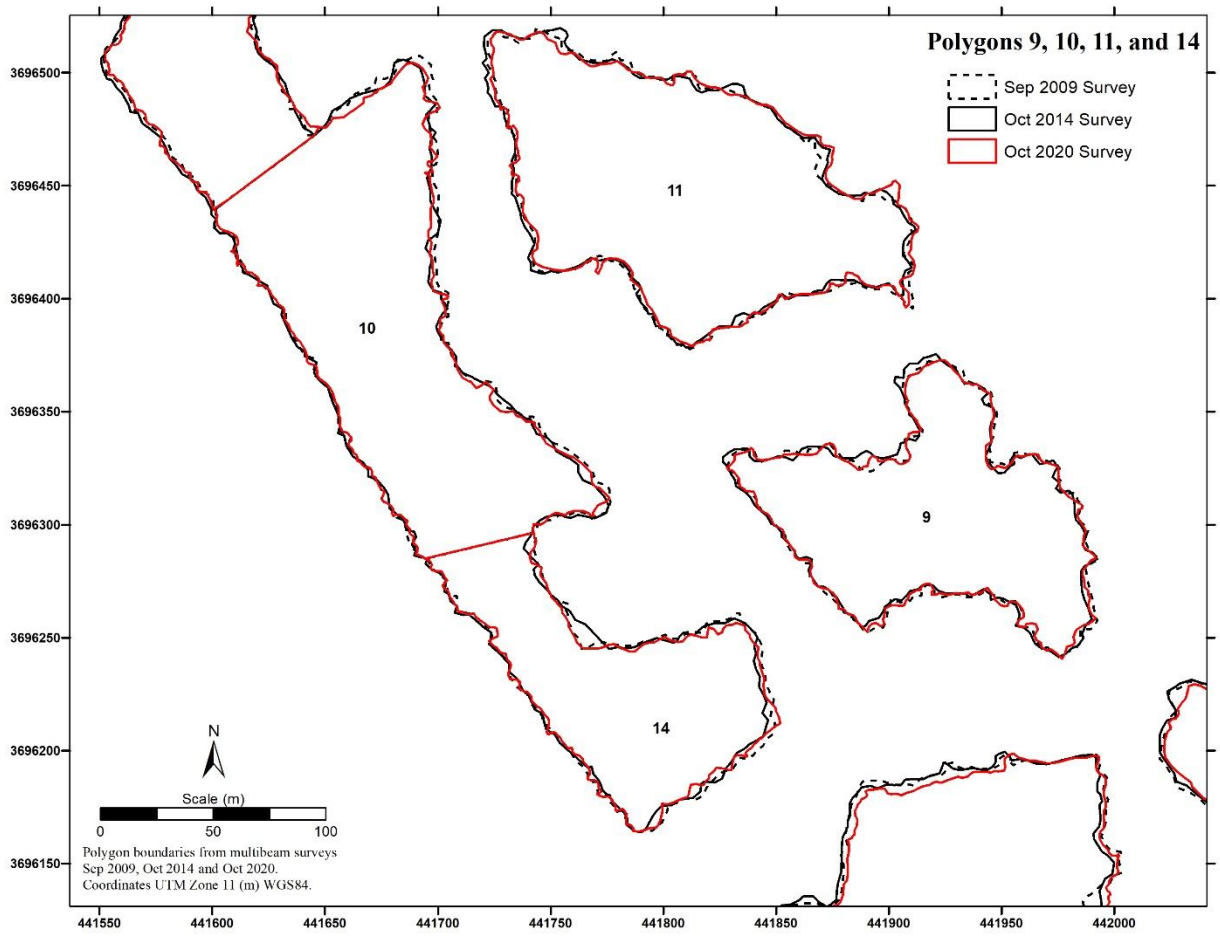

Figure B-7. Comparison of post-construction (2009), October 2014, and October 2020 boundaries from bathymetry data for Polygons 9, 10, 11, and 14.

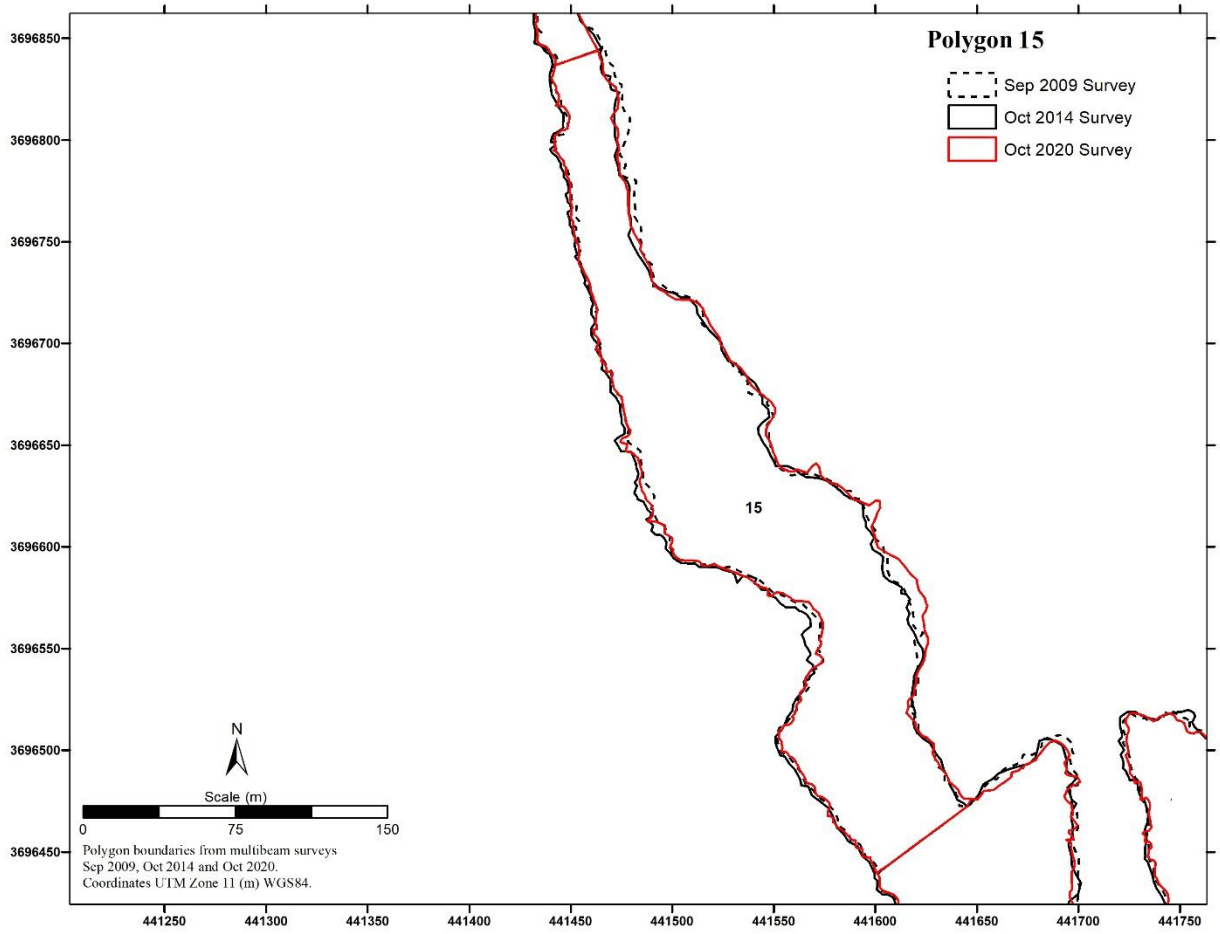

Figure B-8. Comparison of post-construction (2009), October 2014, and October 2020 boundaries from bathymetry data for Polygon 15.

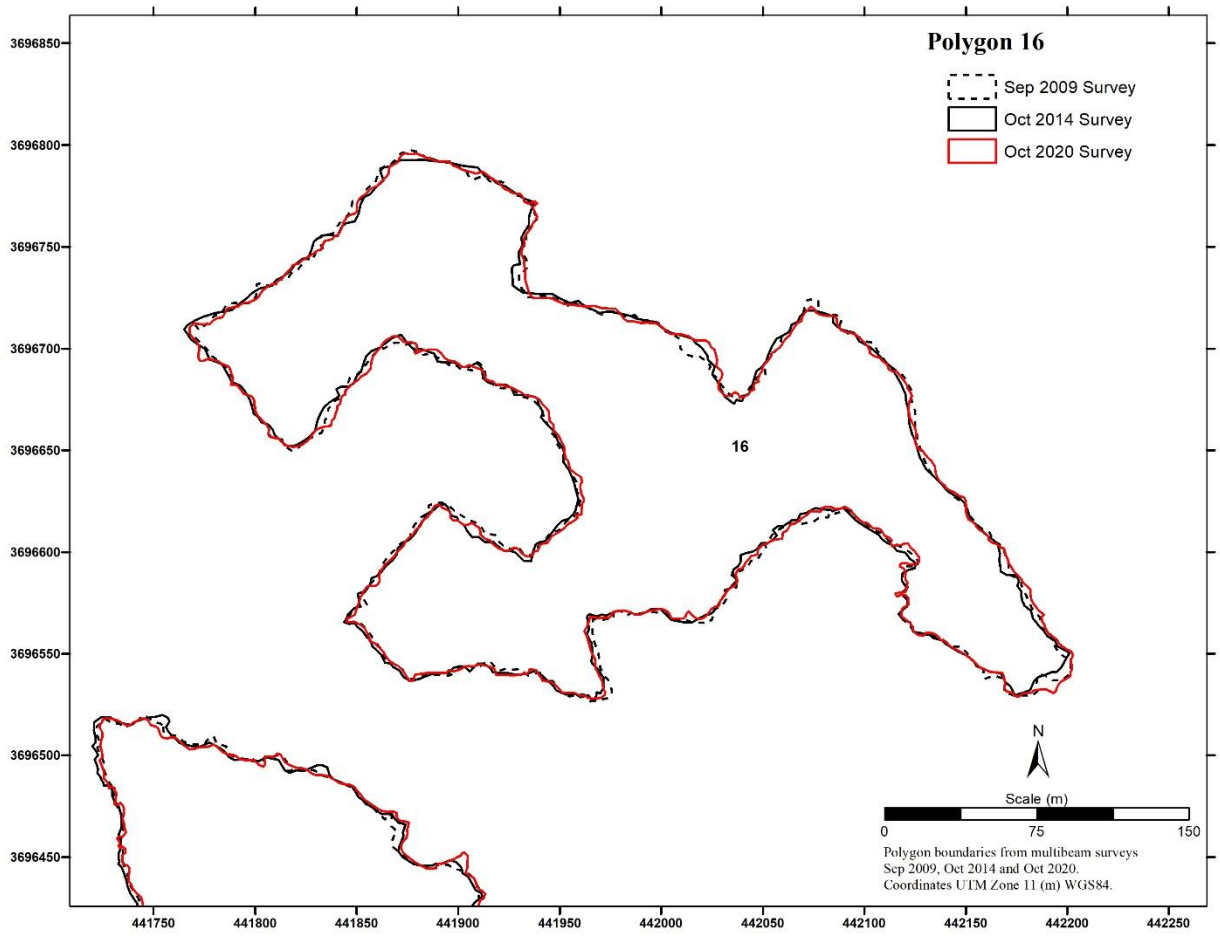

Figure B-9. Comparison of post-construction (2009), October 2014, and October 2020 boundaries from bathymetry data for Polygon 16.

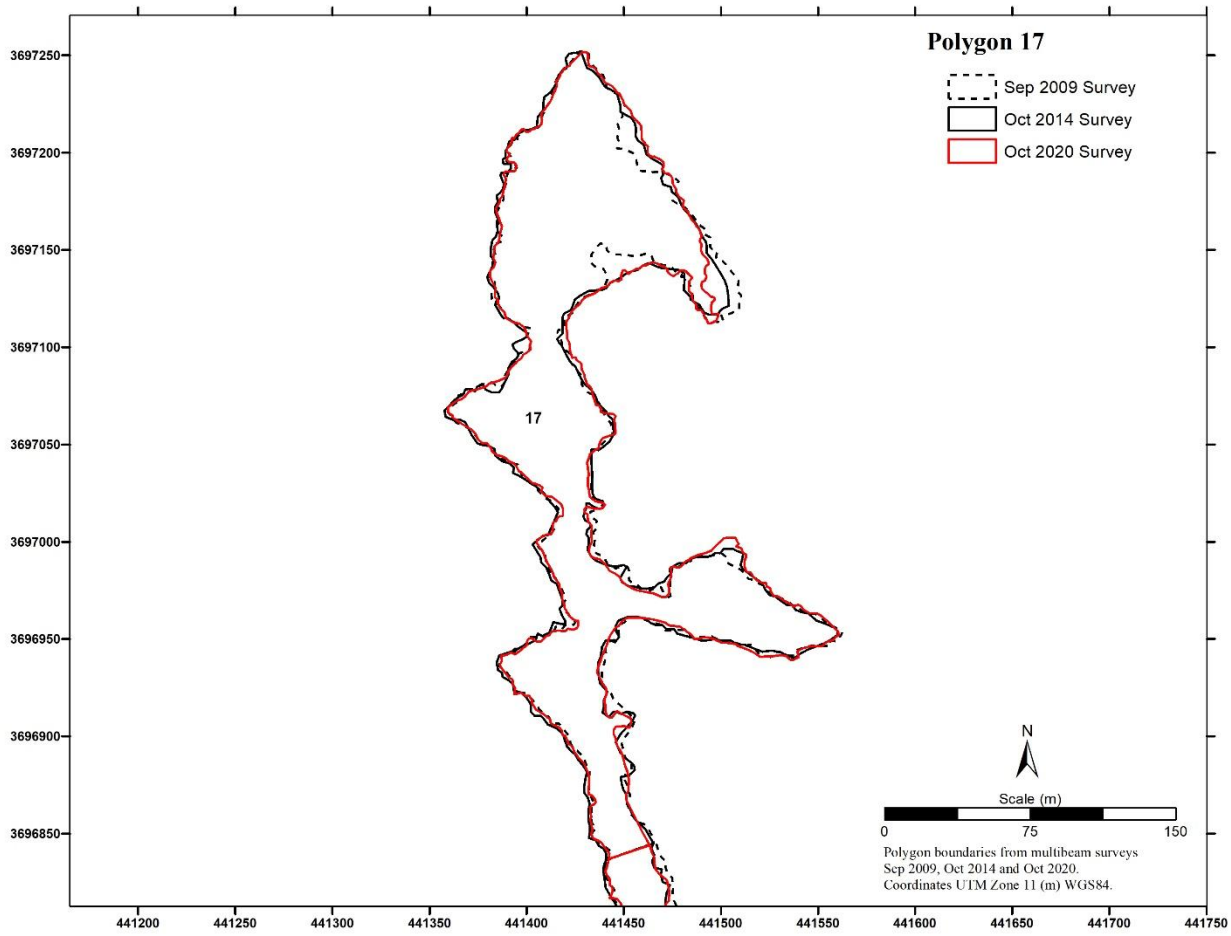

Figure B-10. Comparison of post-construction (2009), October 2014, and October 2020 boundaries from bathymetry data for Polygon 17.

APPENDIX C

POST-CONSTRUCTION BOUNDARIES FROM OCTOBER 2020 BATHYMETRY DATA FOR POLYGONS 18-40

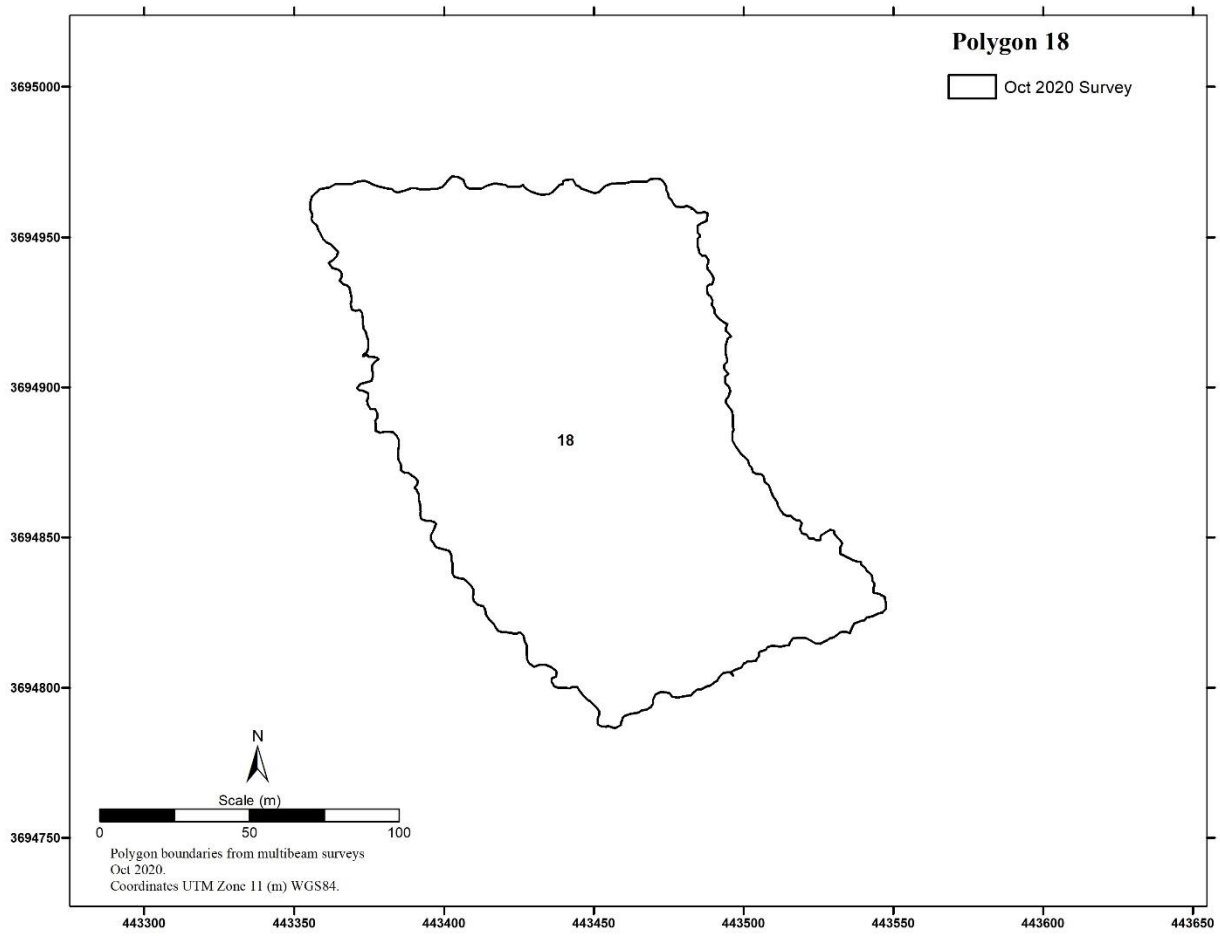

Figure C-1. Post-construction boundaries from October 2020 bathymetry data for Polygon 18.

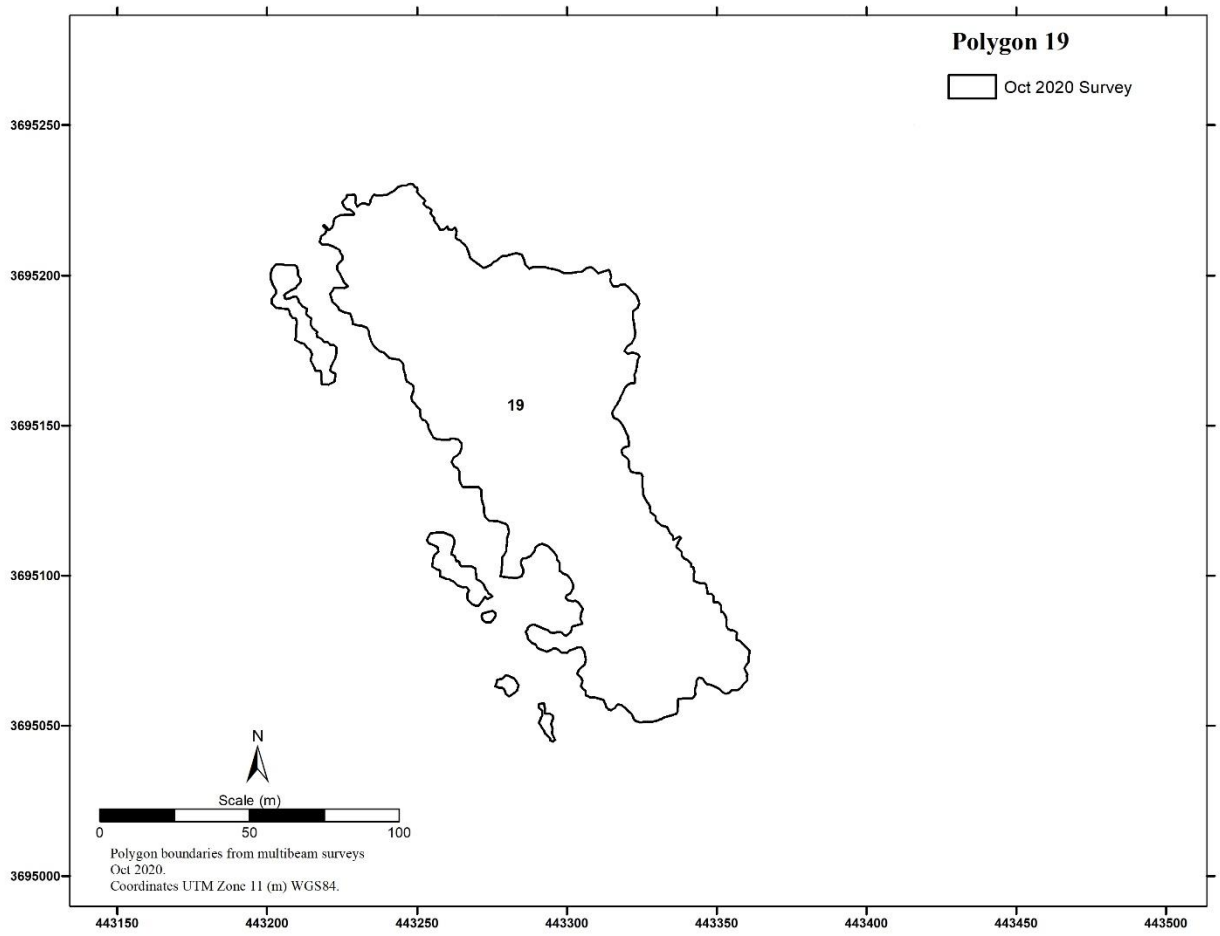

Figure C-2. Post-construction boundaries from October 2020 bathymetry data for Polygon 19.

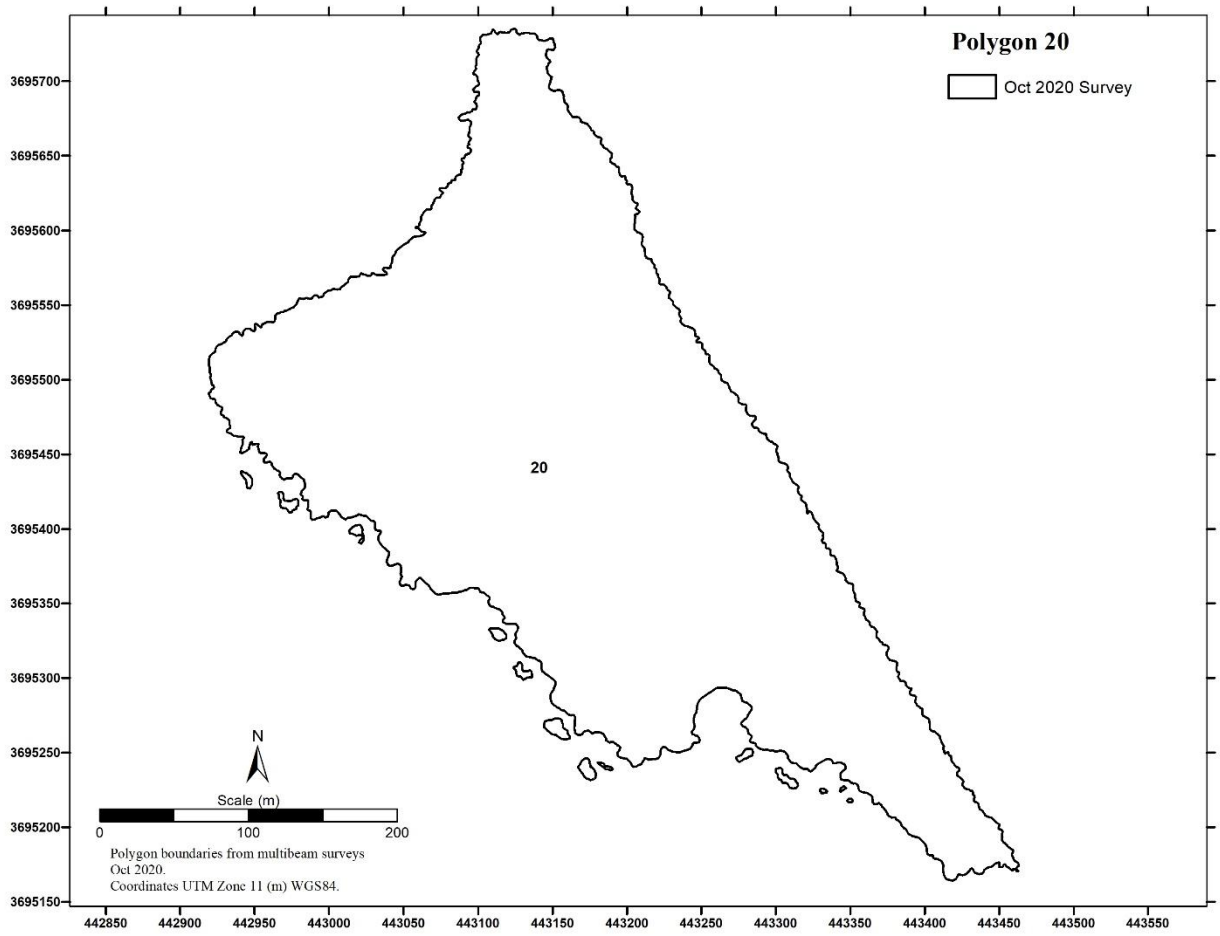

Figure C-3. Post-construction boundaries from October 2020 bathymetry data for Polygon 20.

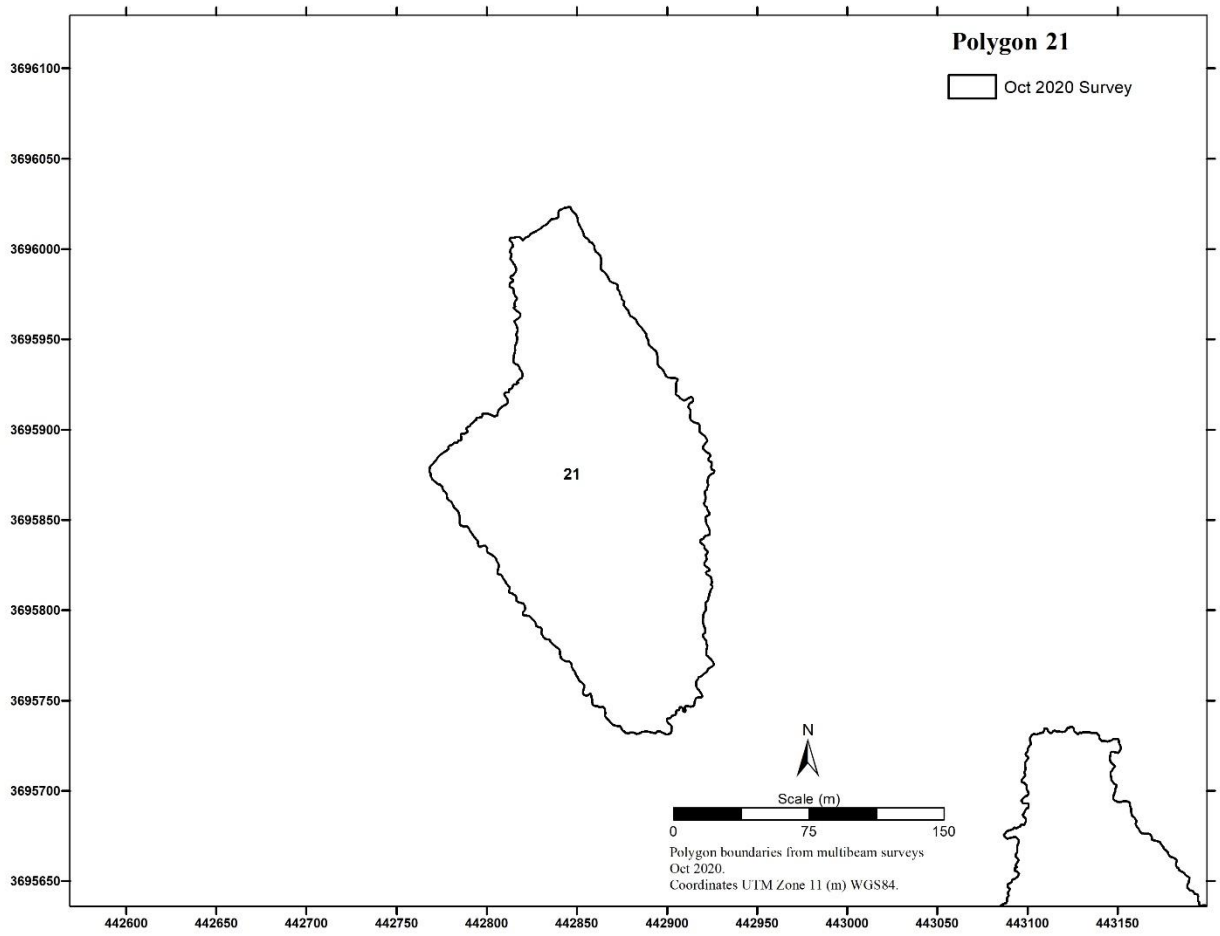

Figure C-4. Post-construction boundaries from October 2020 bathymetry data for Polygon 21.

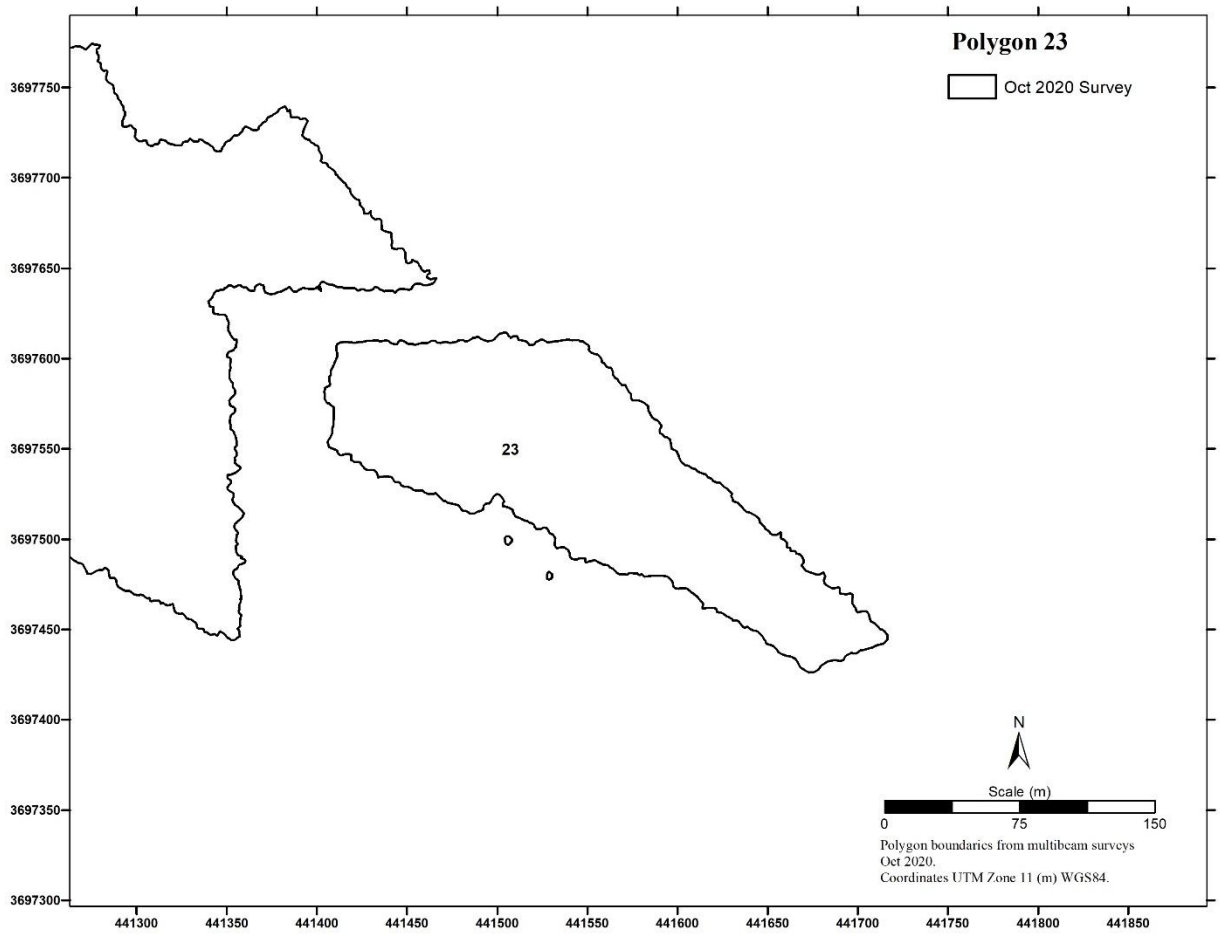

Figure C-5. Post-construction boundaries from October 2020 bathymetry data for Polygon 23.

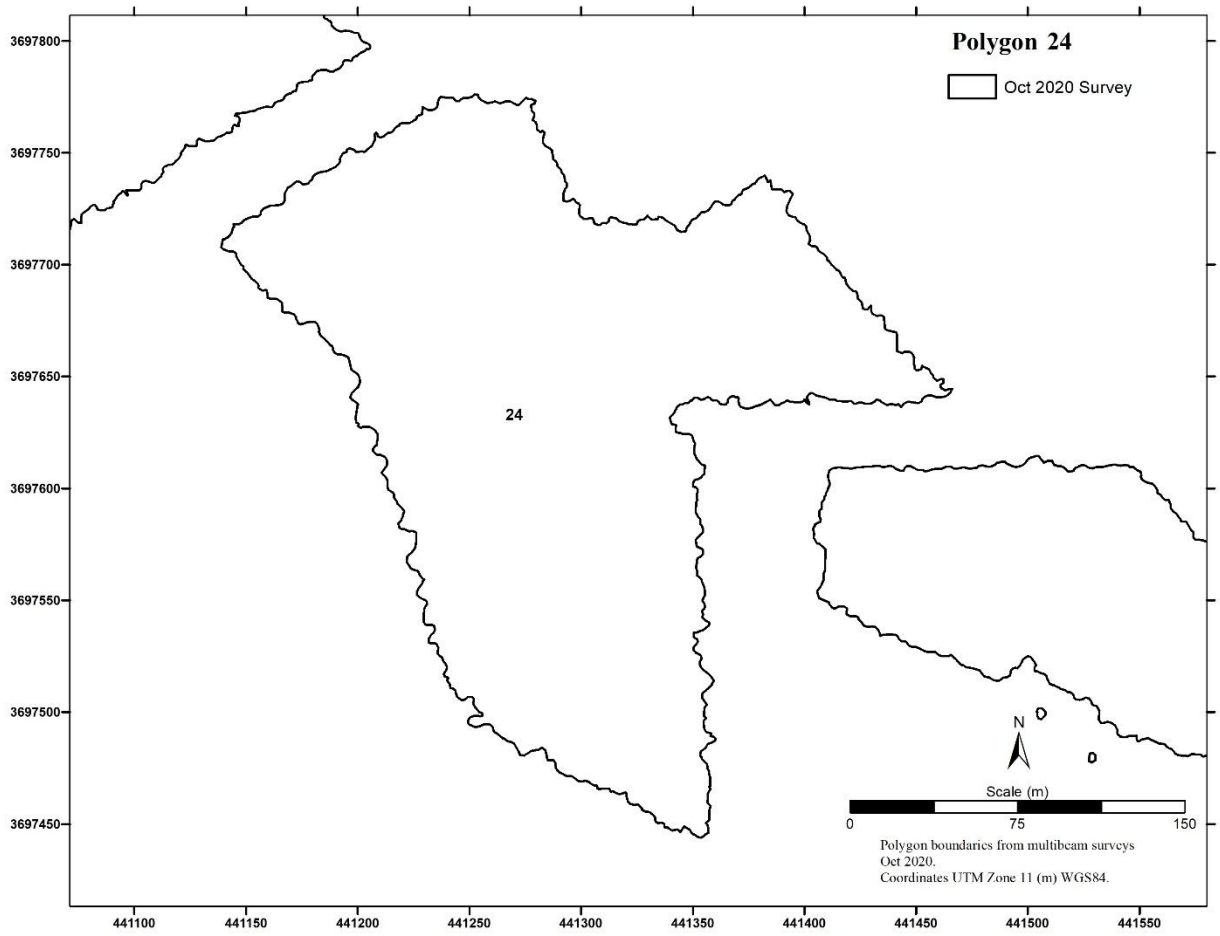

Figure C-6. Post-construction boundaries from October 2020 bathymetry data for Polygon 24.

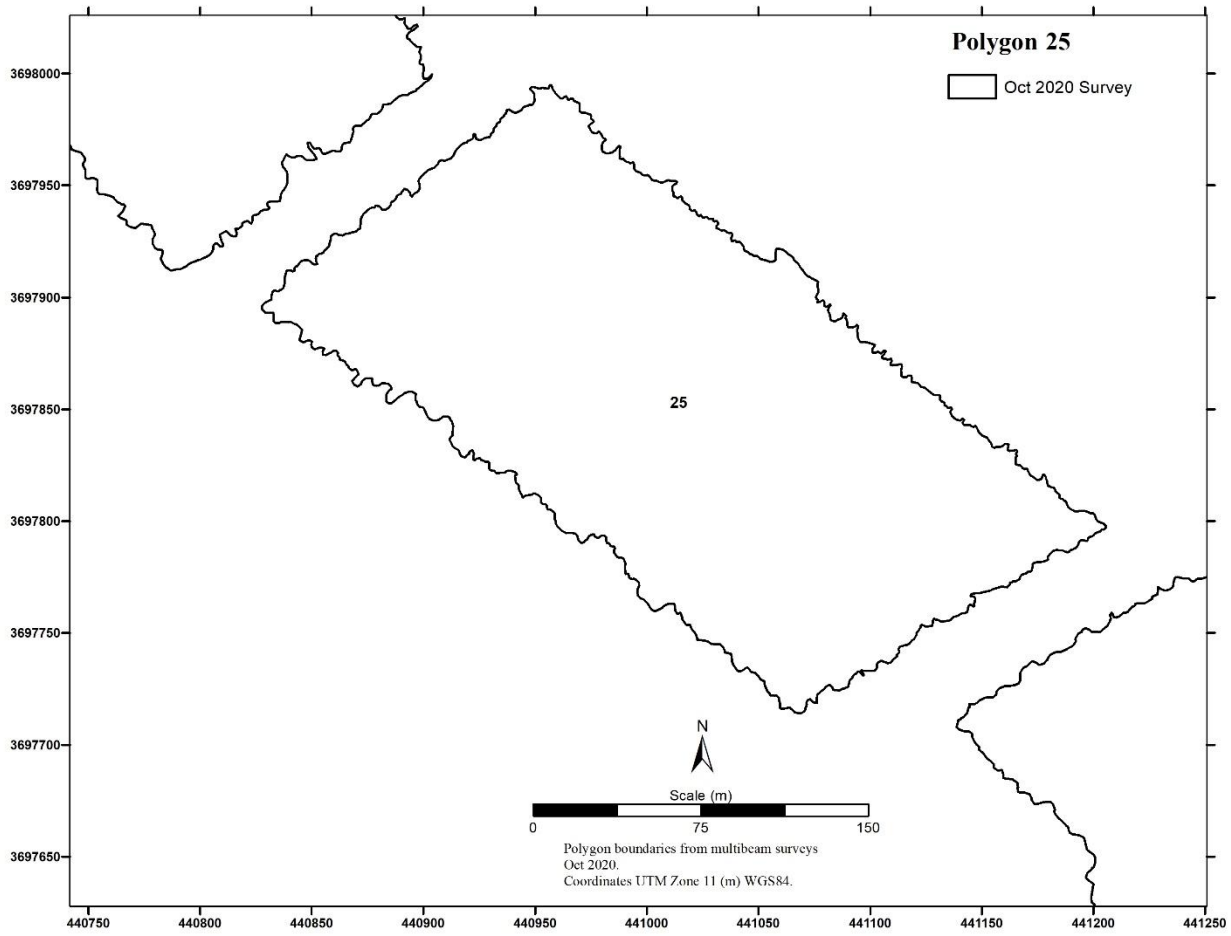

Figure C-7. Post-construction boundaries from October 2020 bathymetry data for Polygon 25.

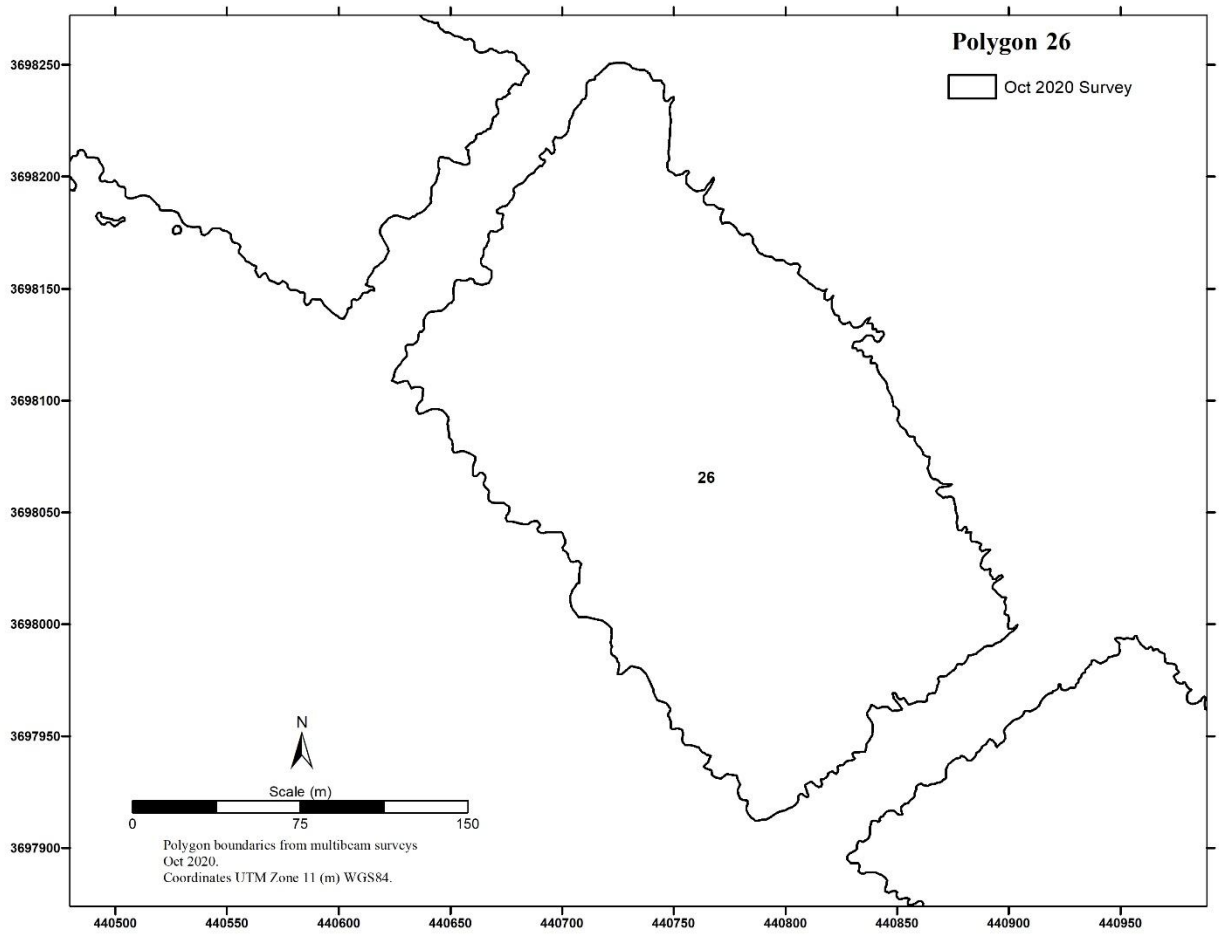

Figure C-8. Post-construction boundaries from October 2020 bathymetry data for Polygon 26.

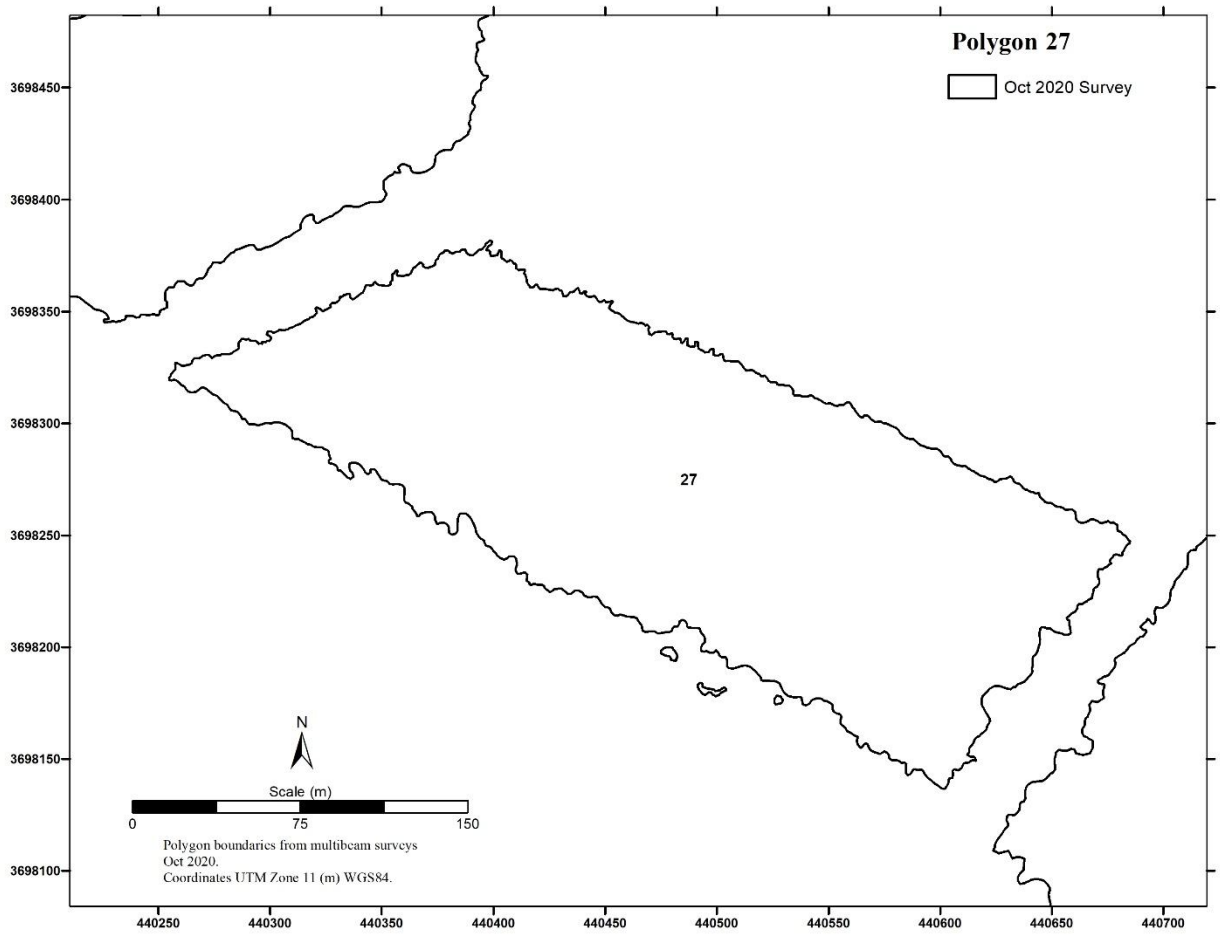

Figure C-9. Post-construction boundaries from October 2020 bathymetry data for Polygon 27.

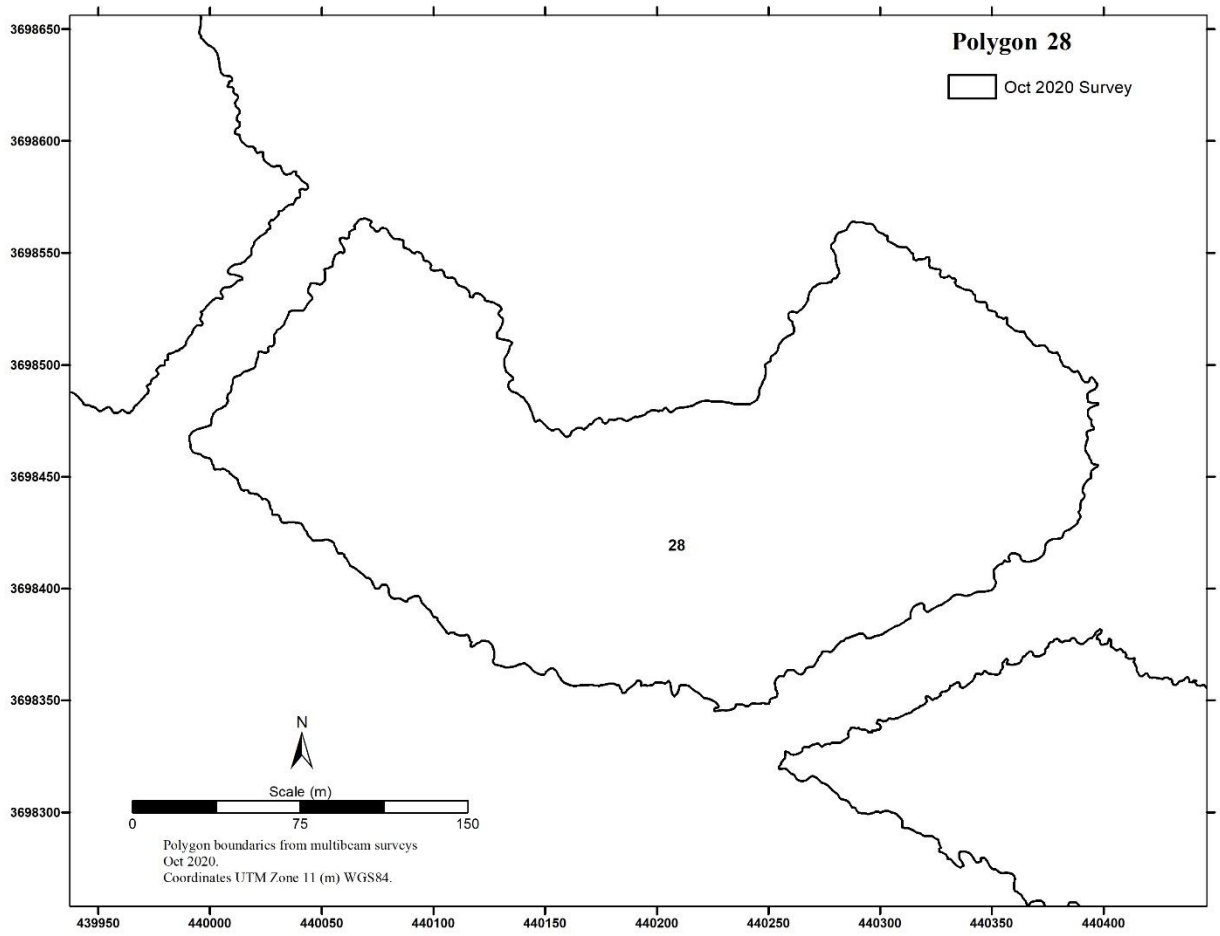

Figure C-10. Post-construction boundaries from October 2020 bathymetry data for Polygon 28.

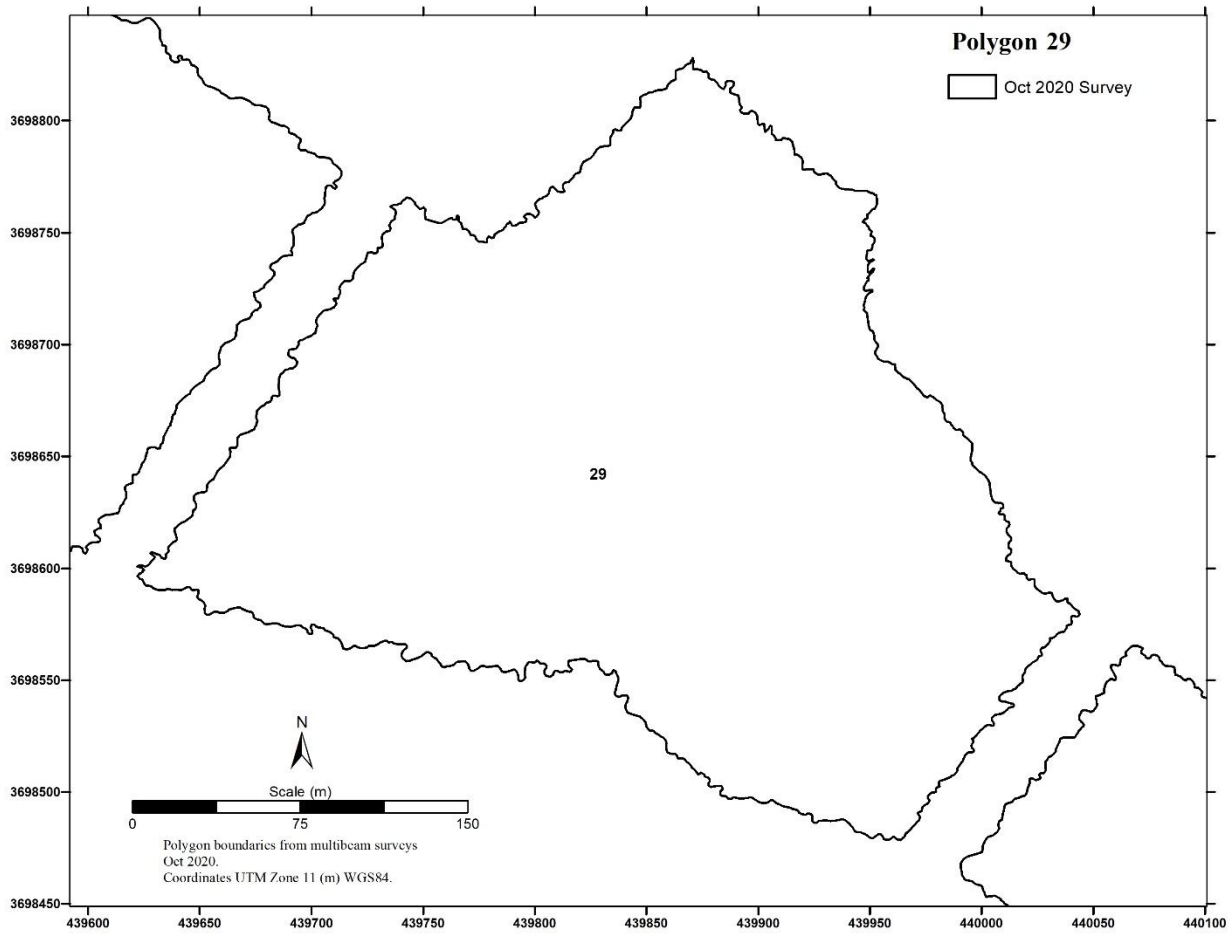

Figure C-11. Post-construction boundaries from October 2020 bathymetry data for Polygon 29.

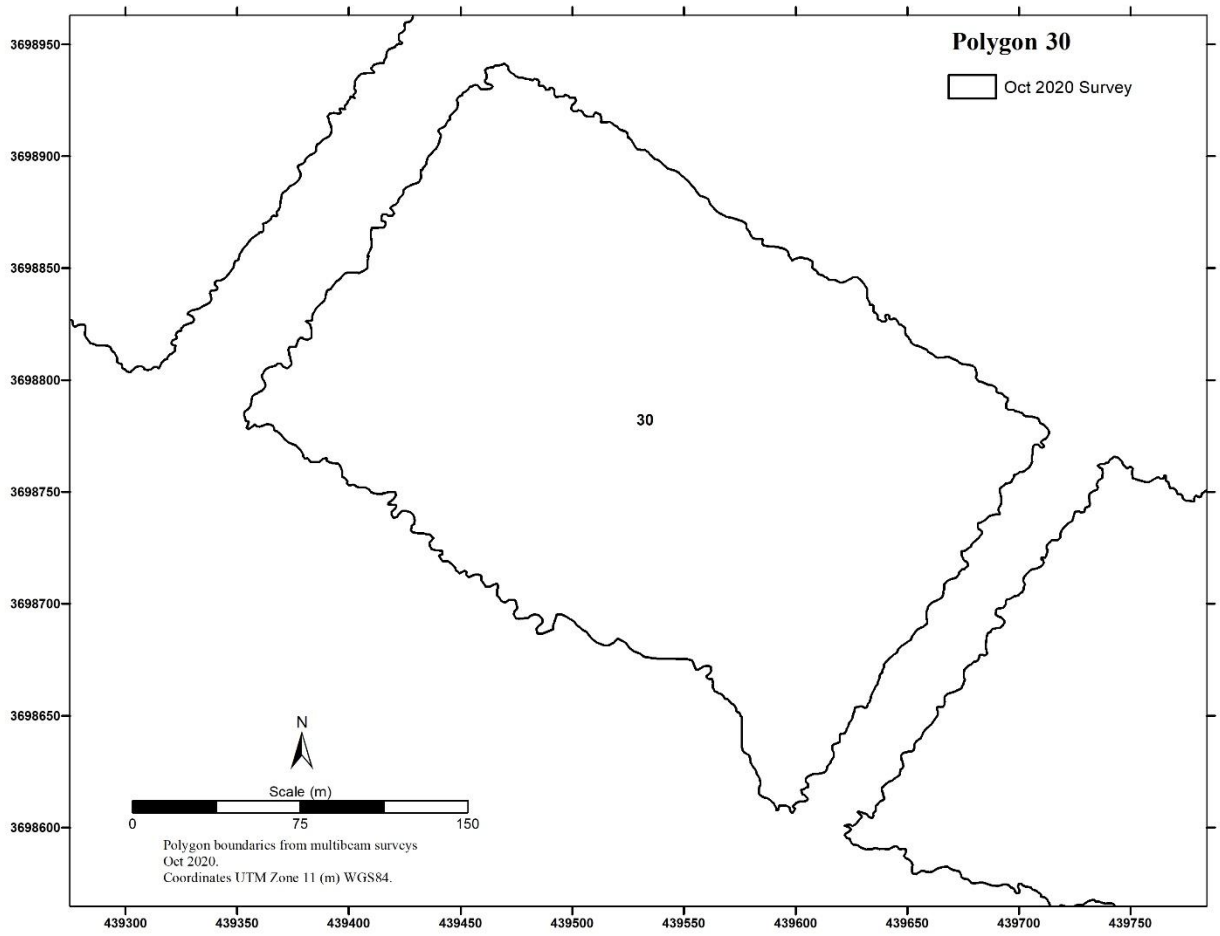

Figure C-12. Post-construction boundaries from October 2020 bathymetry data for Polygon 30.

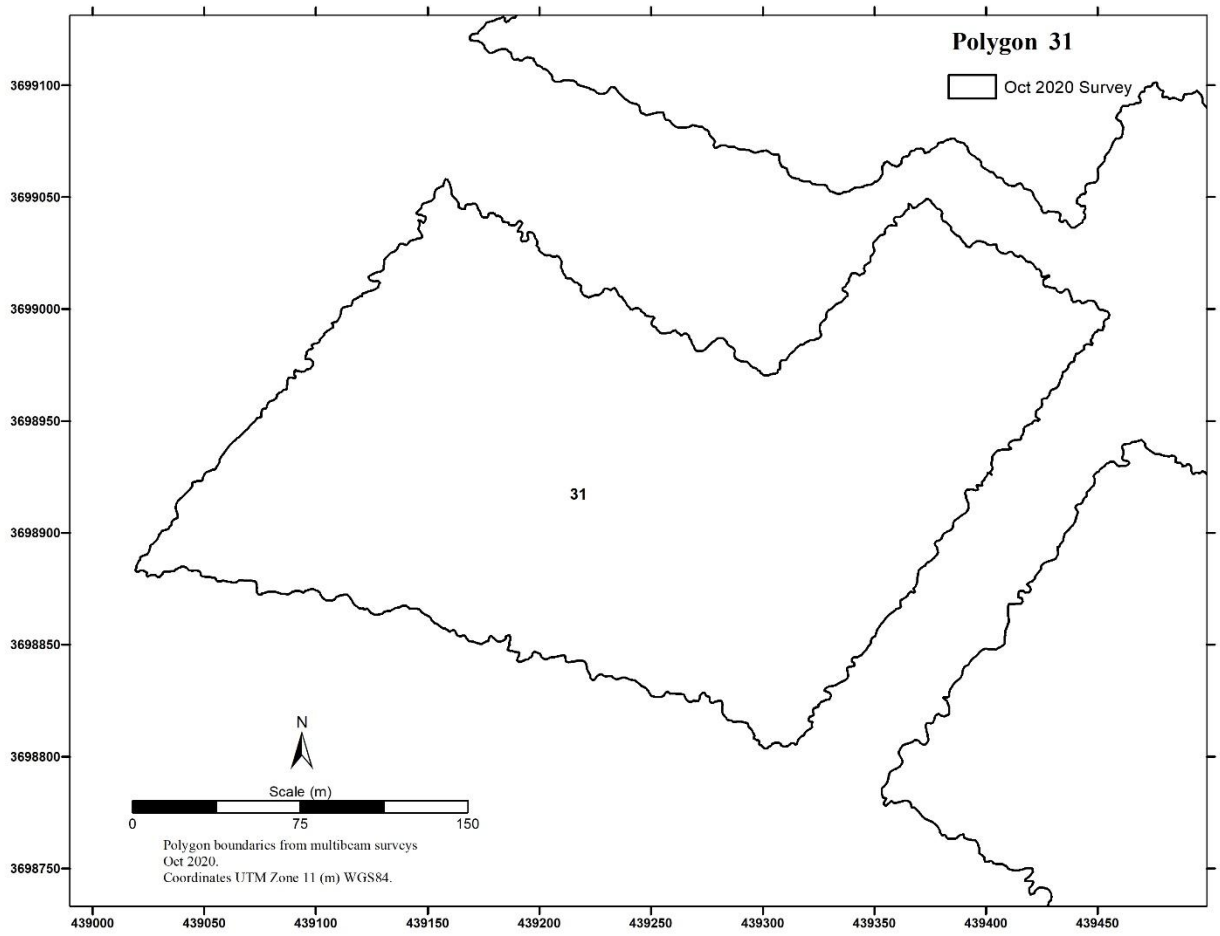

Figure C-13. Post-construction boundaries from October 2020 bathymetry data for Polygon 31.

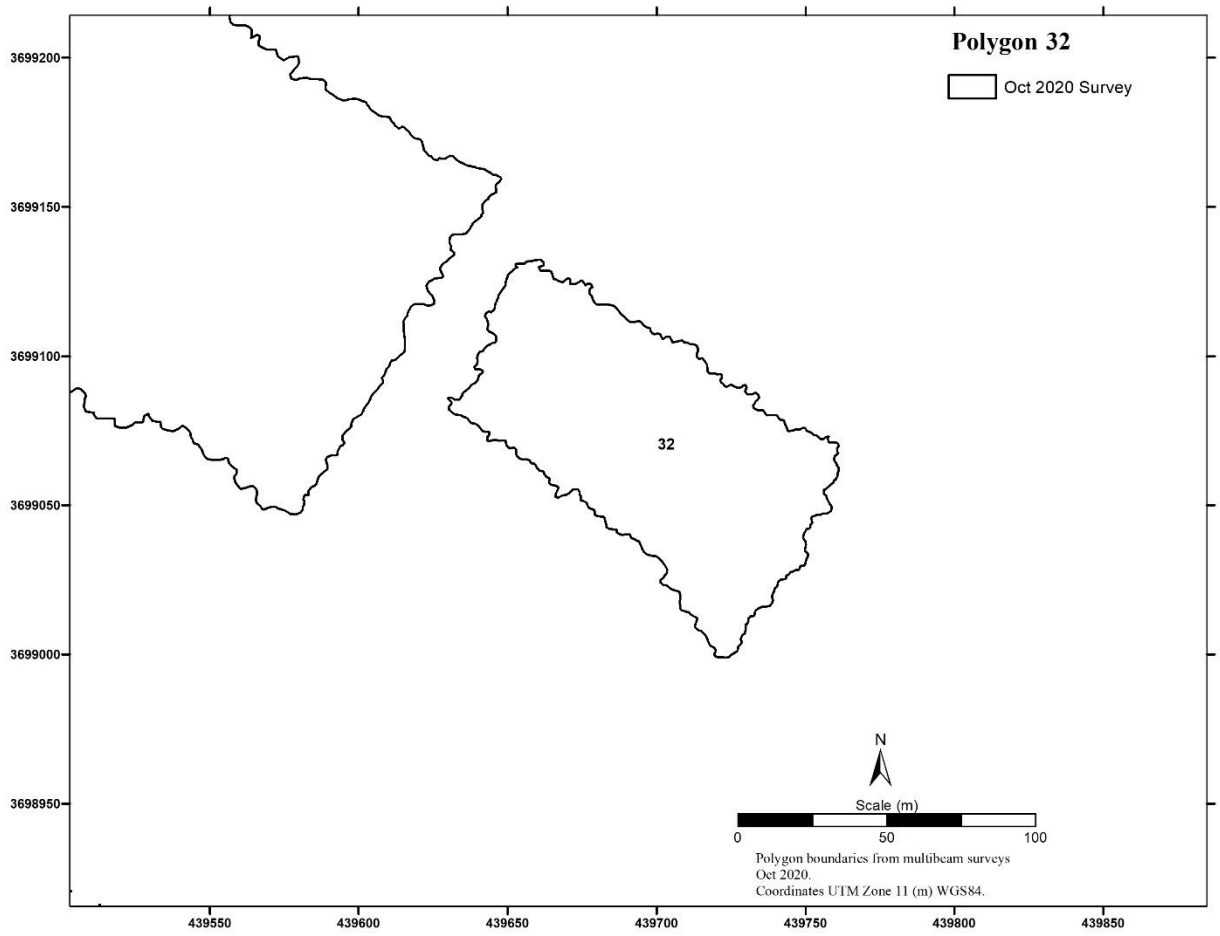

Figure C-14. Post-construction boundaries from October 2020 bathymetry data for Polygon 32.

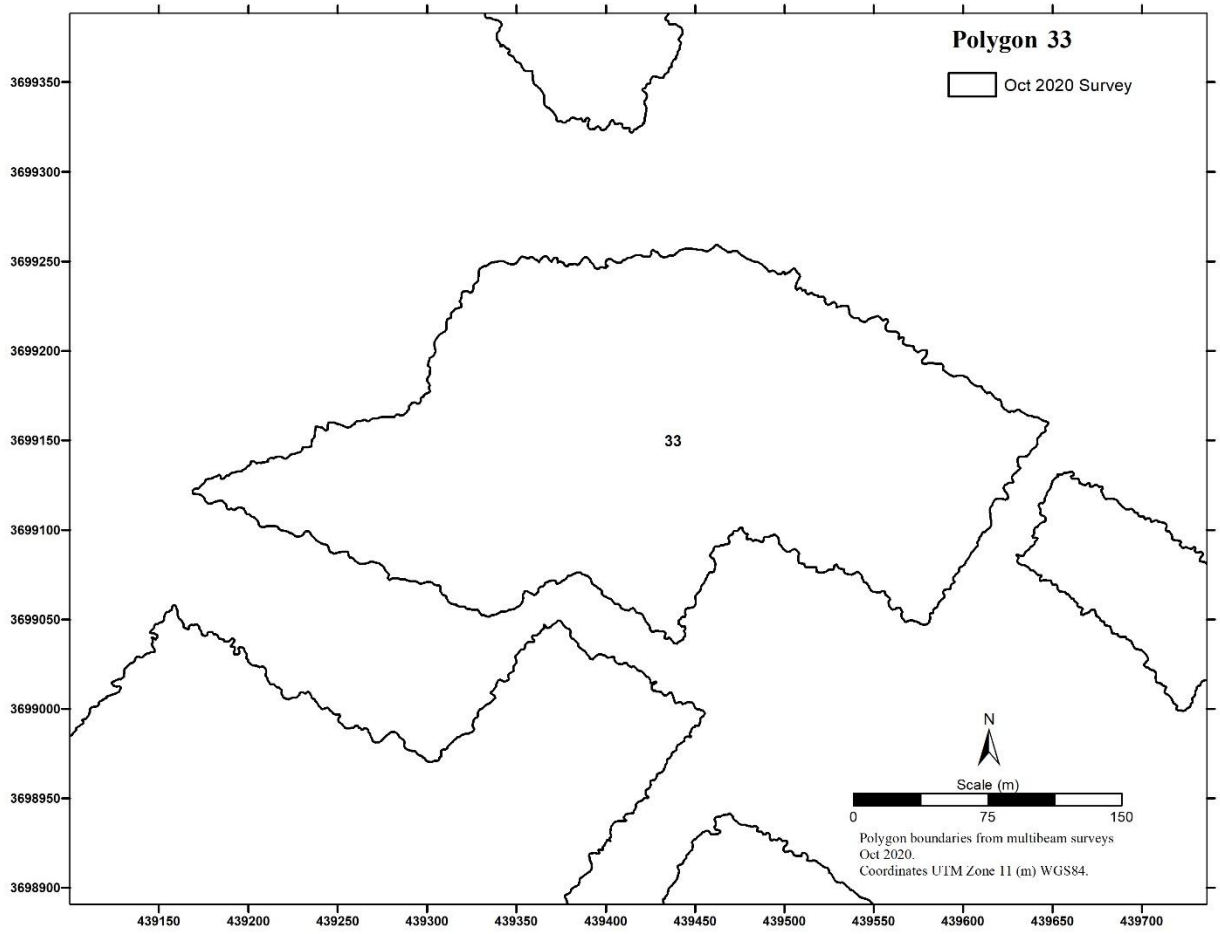

Figure C-15. Post-construction boundaries from October 2020 bathymetry data for Polygon 33.

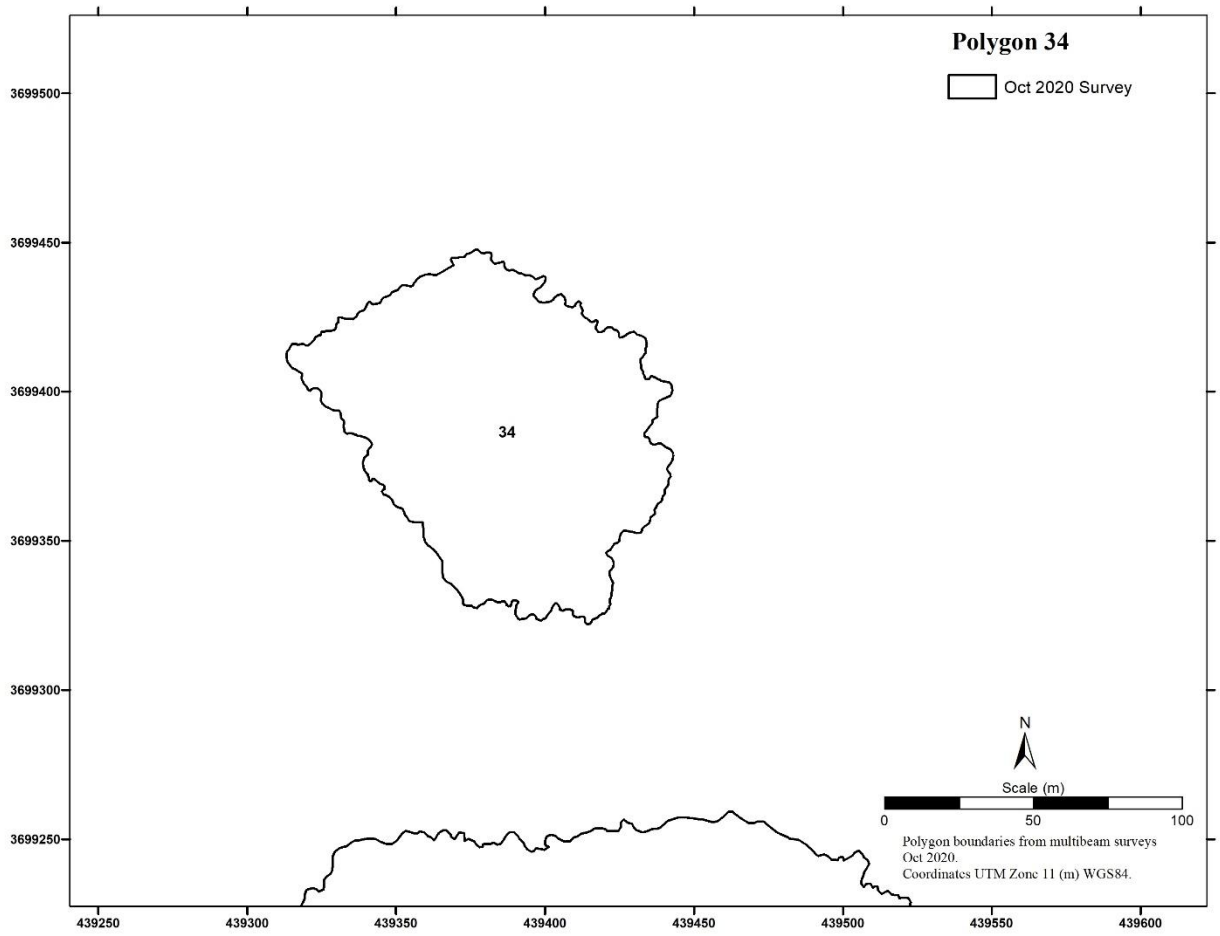

Figure C-16. Post-construction boundaries from October 2020 bathymetry data for Polygon 34.

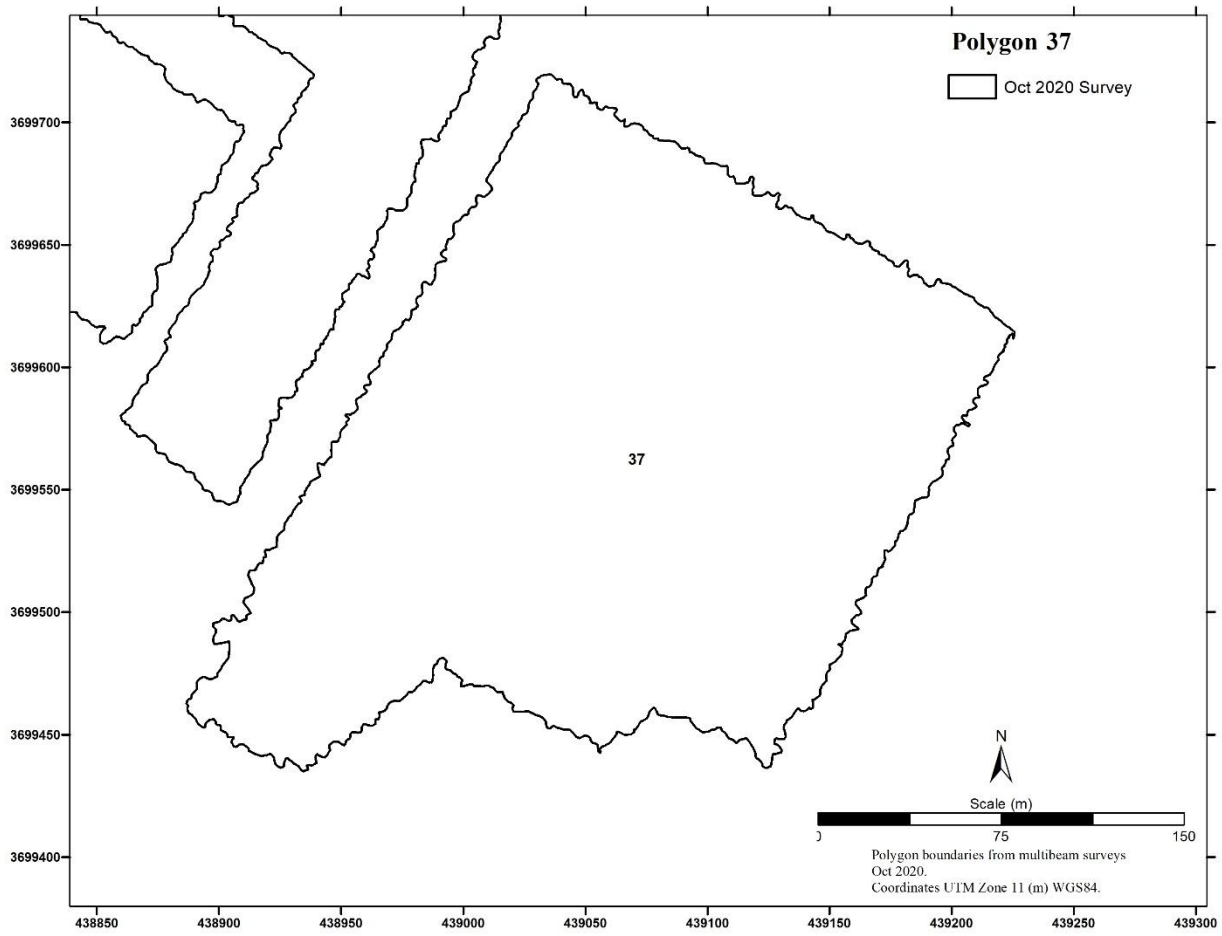

Figure C-17. Post-construction boundaries from October 2020 bathymetry data for Polygon 37.

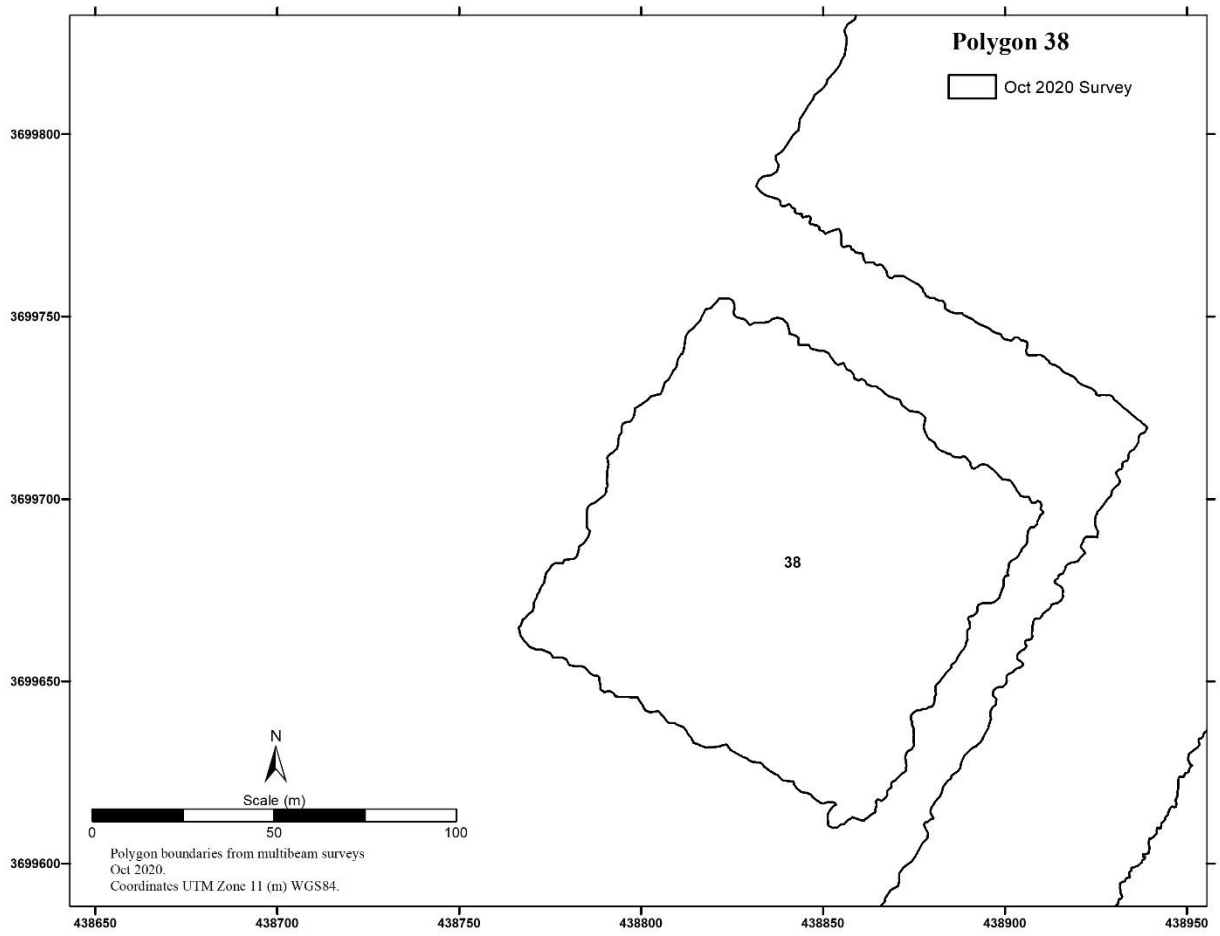

Figure C-18. Post-construction boundaries from October 2020 bathymetry data for Polygon 38.

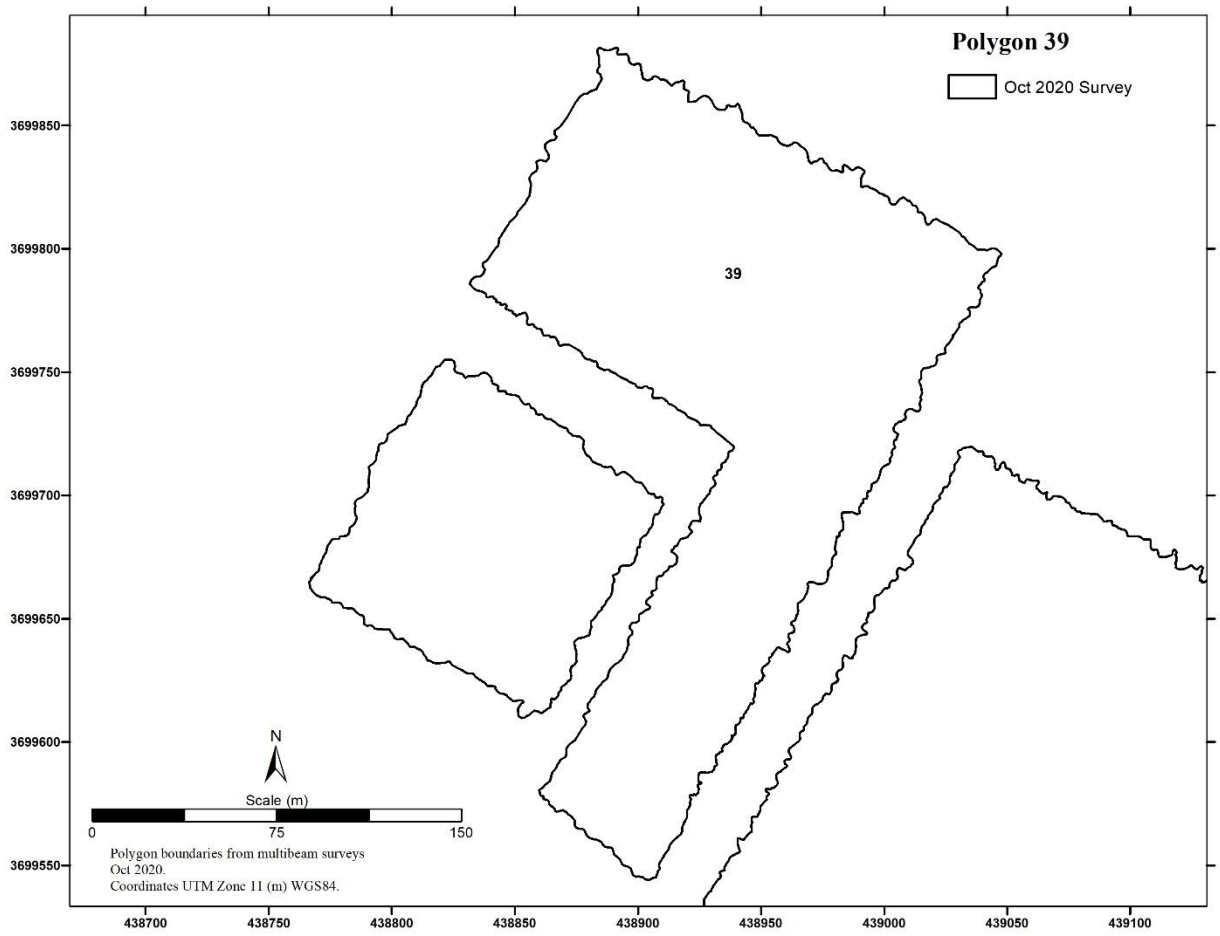

Figure C-19. Post-construction boundaries from October 2020 bathymetry data for Polygon 39.

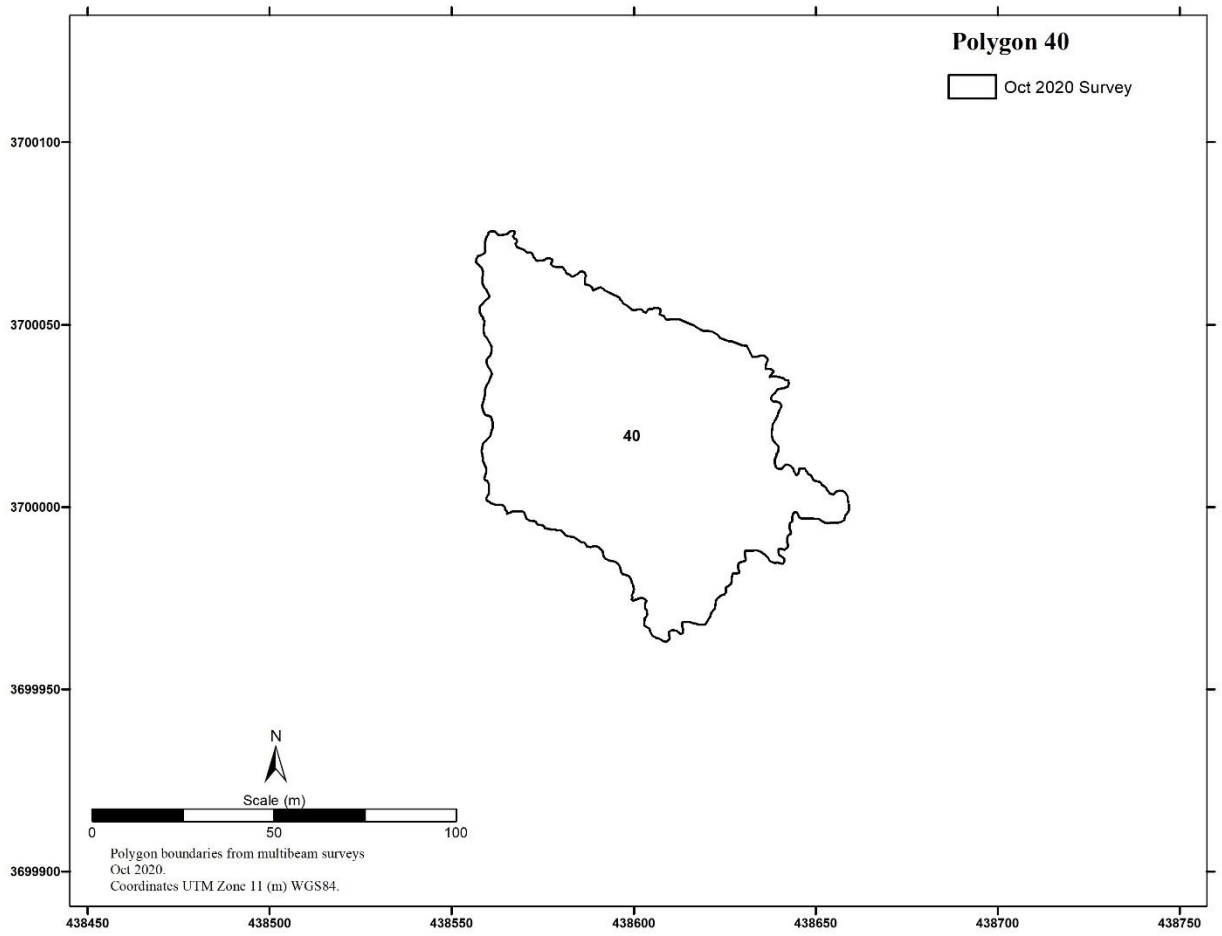

Figure C-20. Post-construction boundaries from October 2020 bathymetry data for Polygon 40.

APPENDIX D

BOUNDARIES FROM BATHYMETRIC DATA FOR MODULE BLOCKS 1-7 (OCTOBER 2020 MULTIBEAM SURVEY)

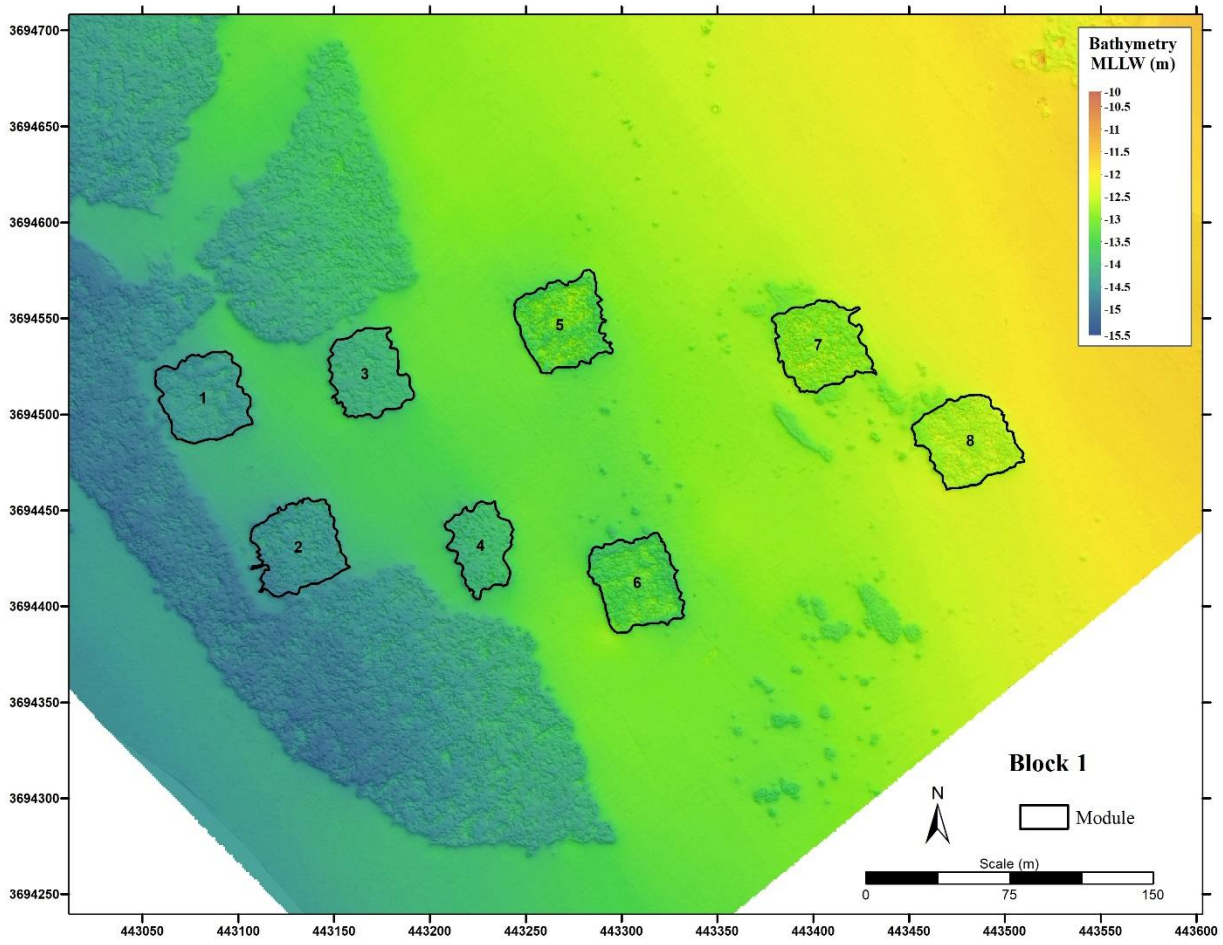

Figure D-1. Block 1 module boundaries from bathymetric data interpretation (October 2020 multibeam survey).

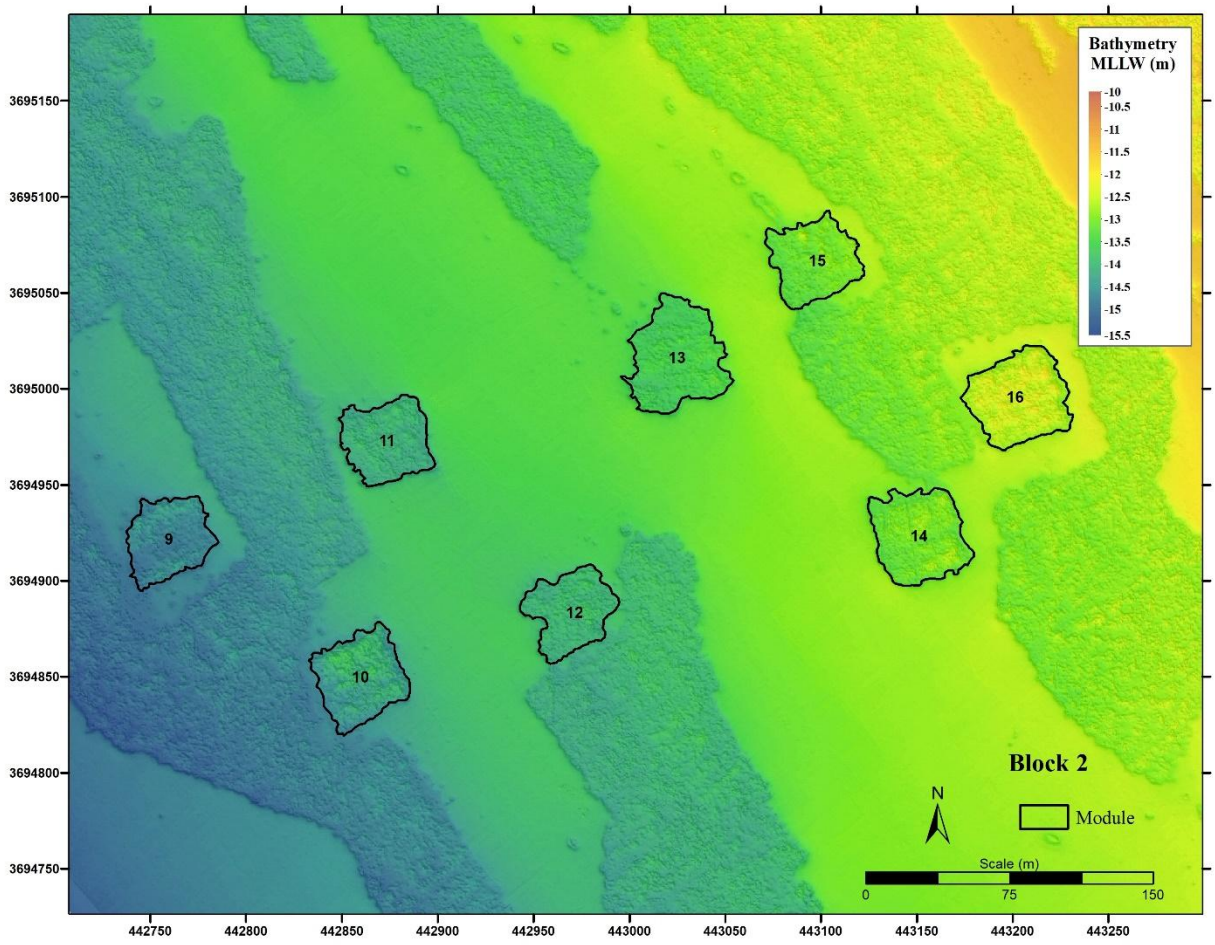

Figure D-2. Block 2 module boundaries from bathymetric data interpretation (October 2020 multibeam survey).

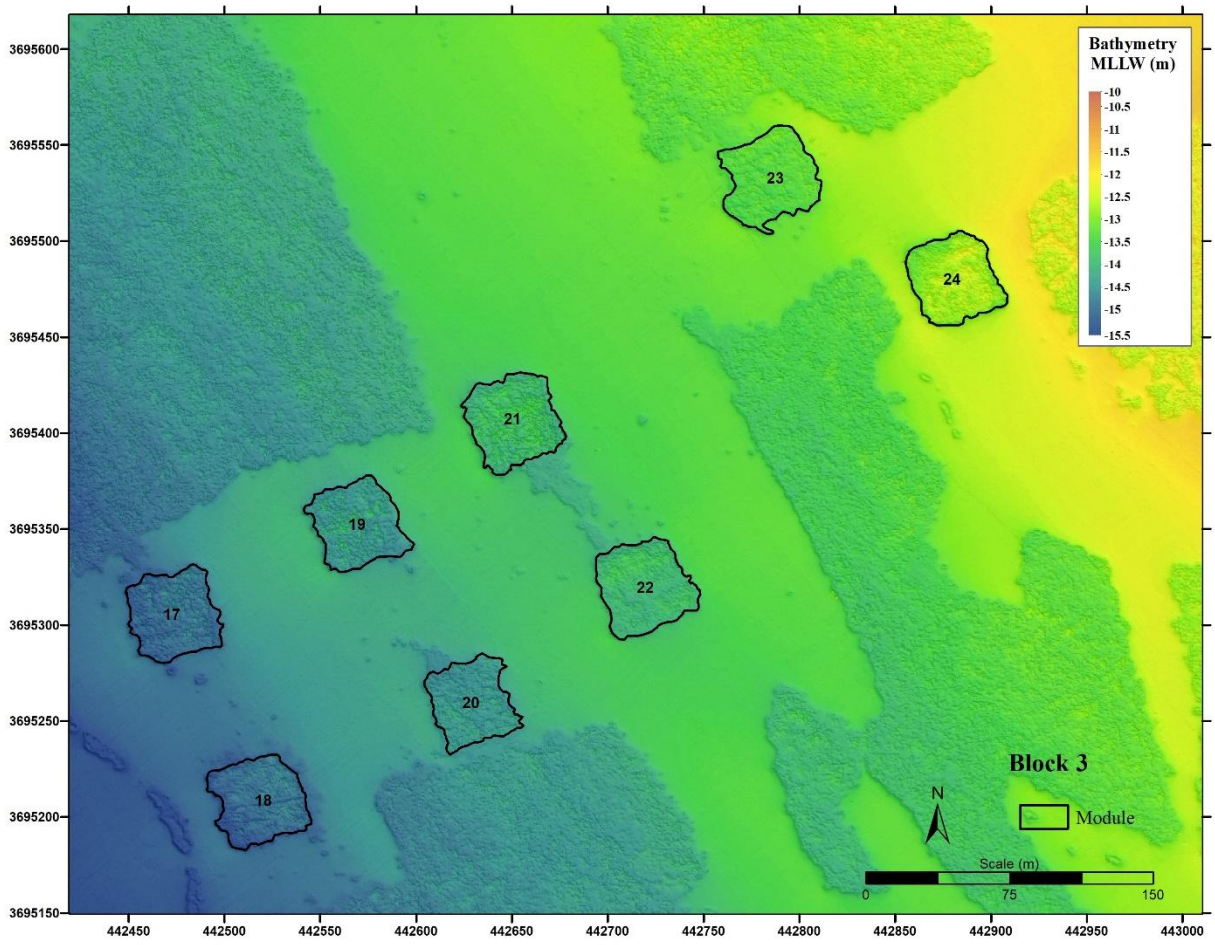

Figure D-3. Block 3 module boundaries from bathymetric data interpretation (October 2020 multibeam survey).

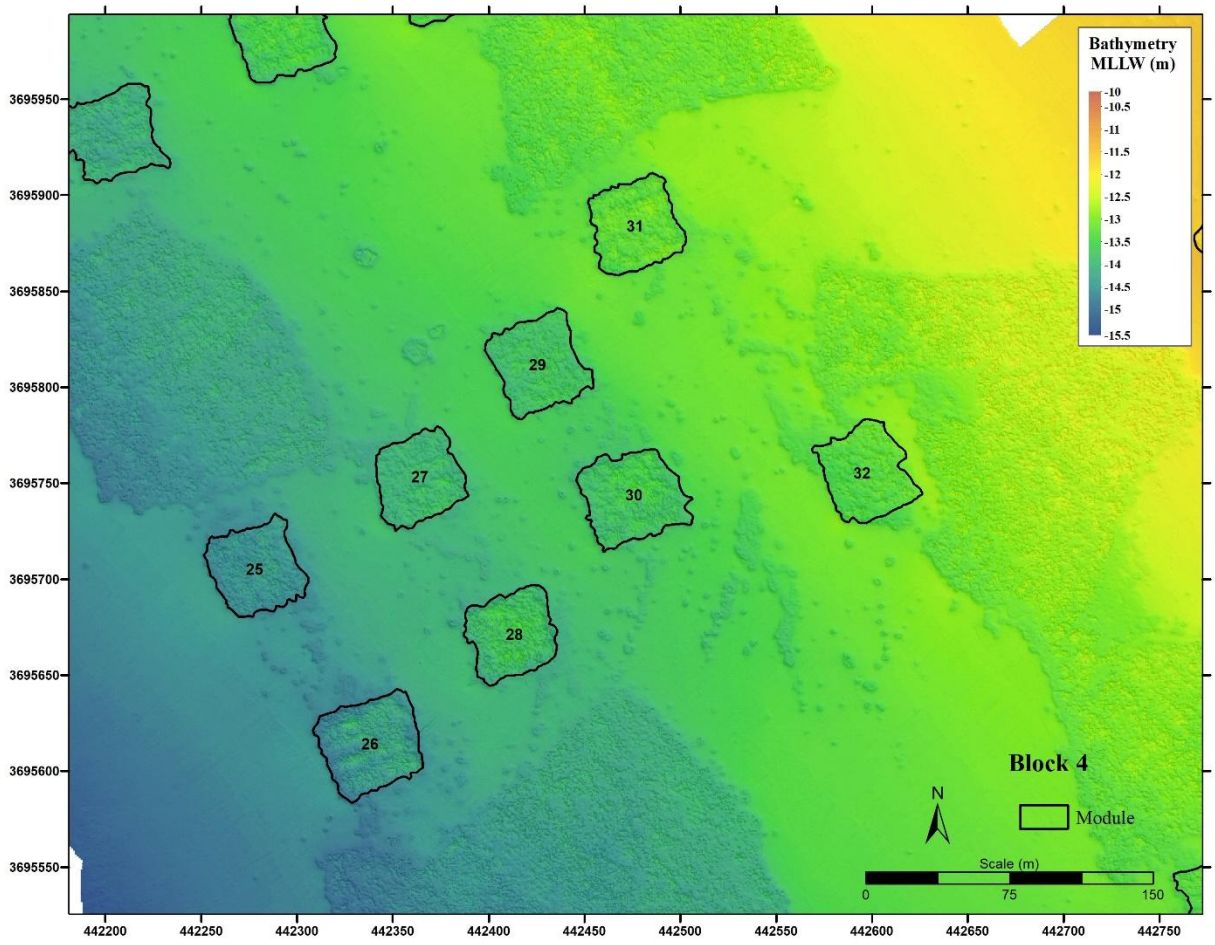

Figure D-4. Block 4 module boundaries from bathymetric data interpretation (October 2020 multibeam survey).

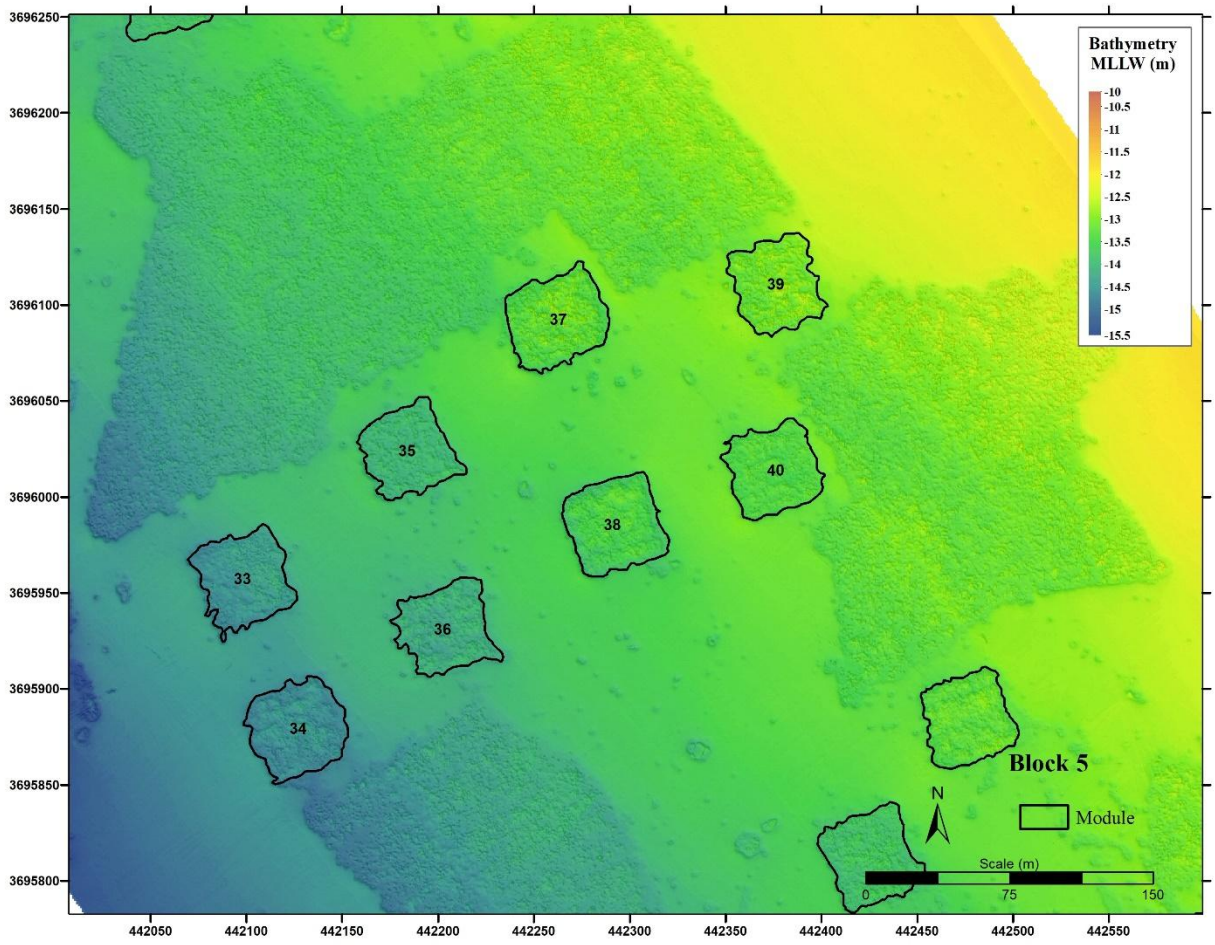

Figure D-5. Block 5 module boundaries from bathymetric data interpretation (October 2020 multibeam survey).

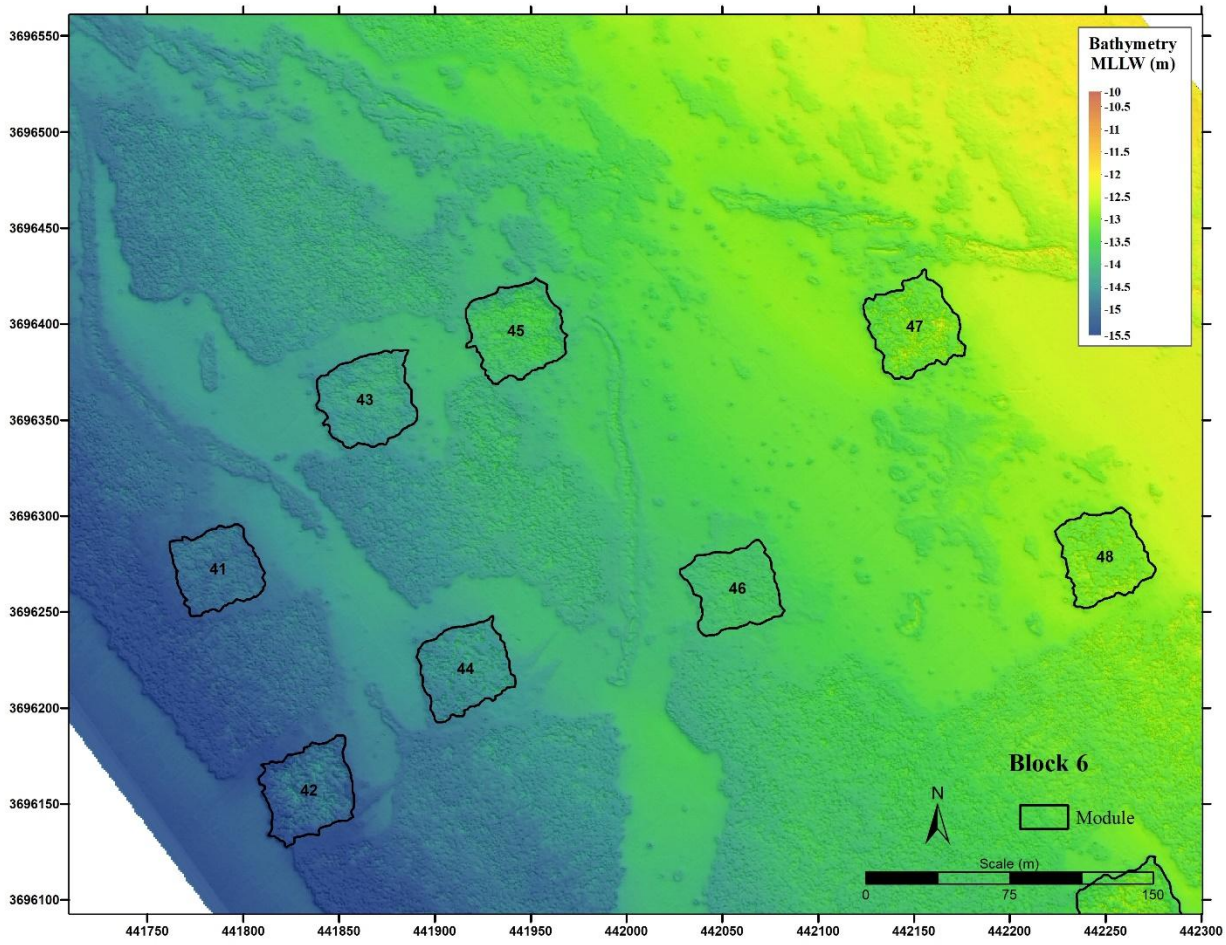

Figure D-6. Block 6 module boundaries from bathymetric data interpretation (October 2020 multibeam survey).

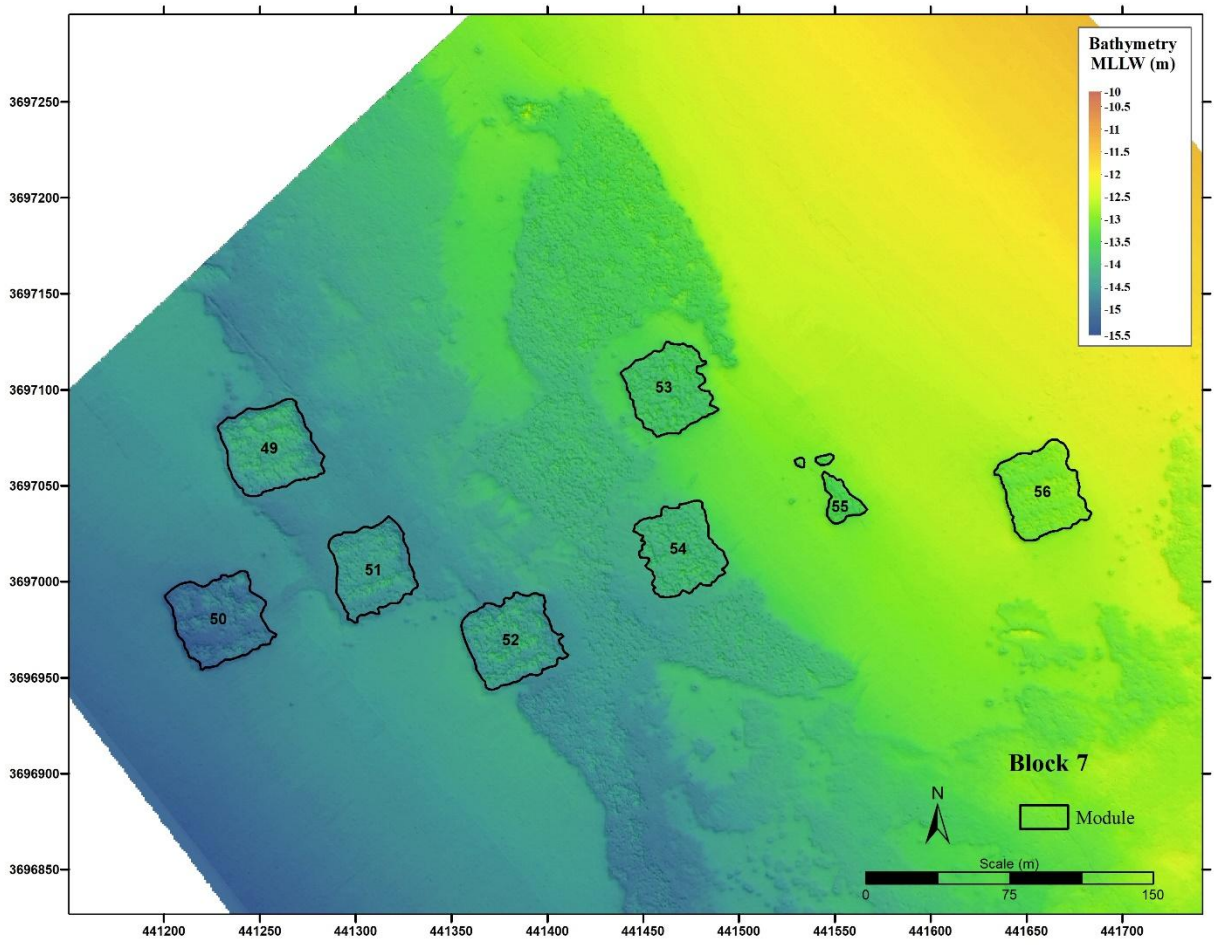

Figure D-7. Block 7 module boundaries from bathymetric data interpretation (October 2020 multibeam survey).

APPENDIX E

BOUNDARIES FROM BATHYMETRIC DATA FOR POLYGONS 1-17 (OCTOBER 2020 MULTIBEAM SURVEY)

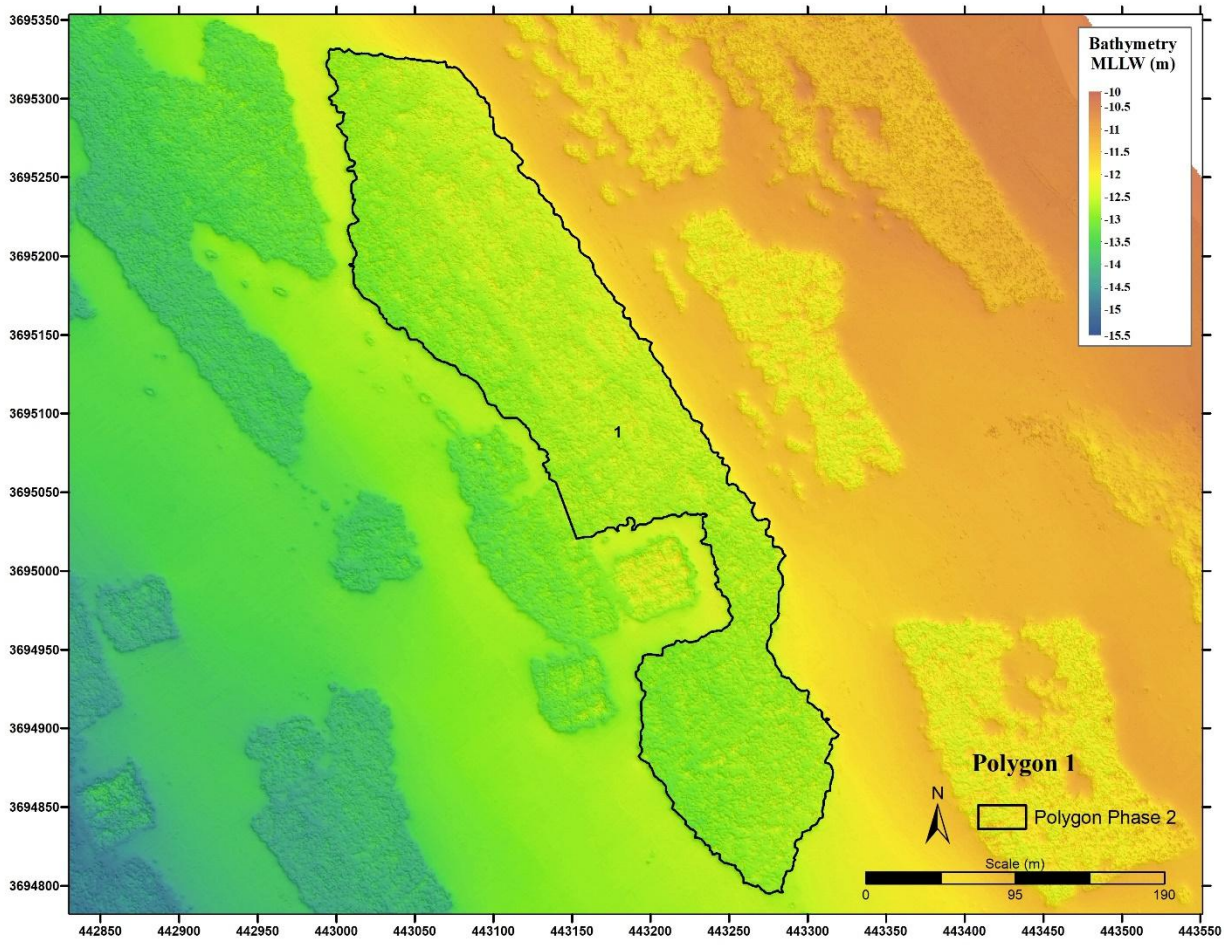

Figure E-1. Polygon 1 boundary from bathymetric data interpretation (October 2020 multibeam survey).

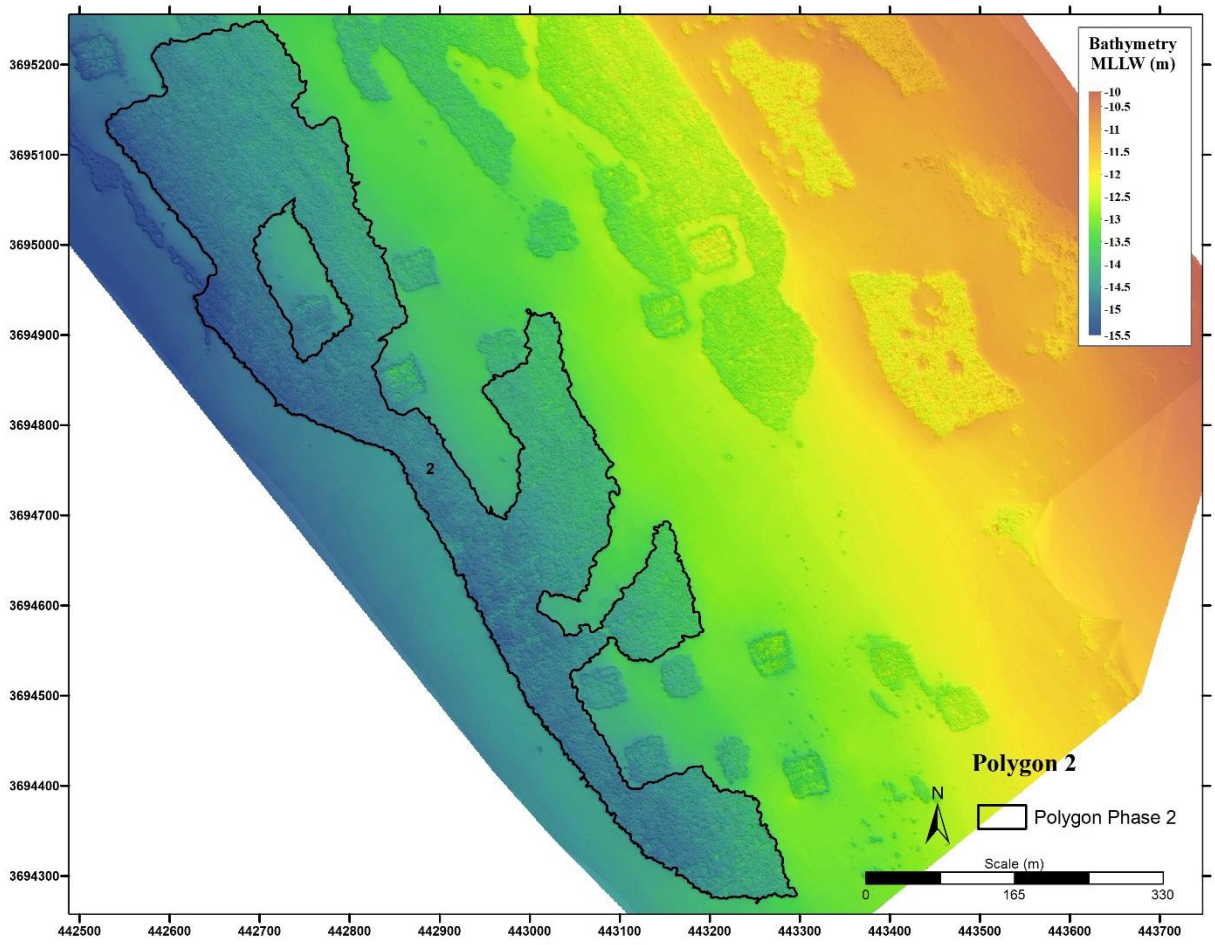

Figure E-2. Polygon 2 boundary from bathymetric data interpretation (October 2020 multibeam survey).

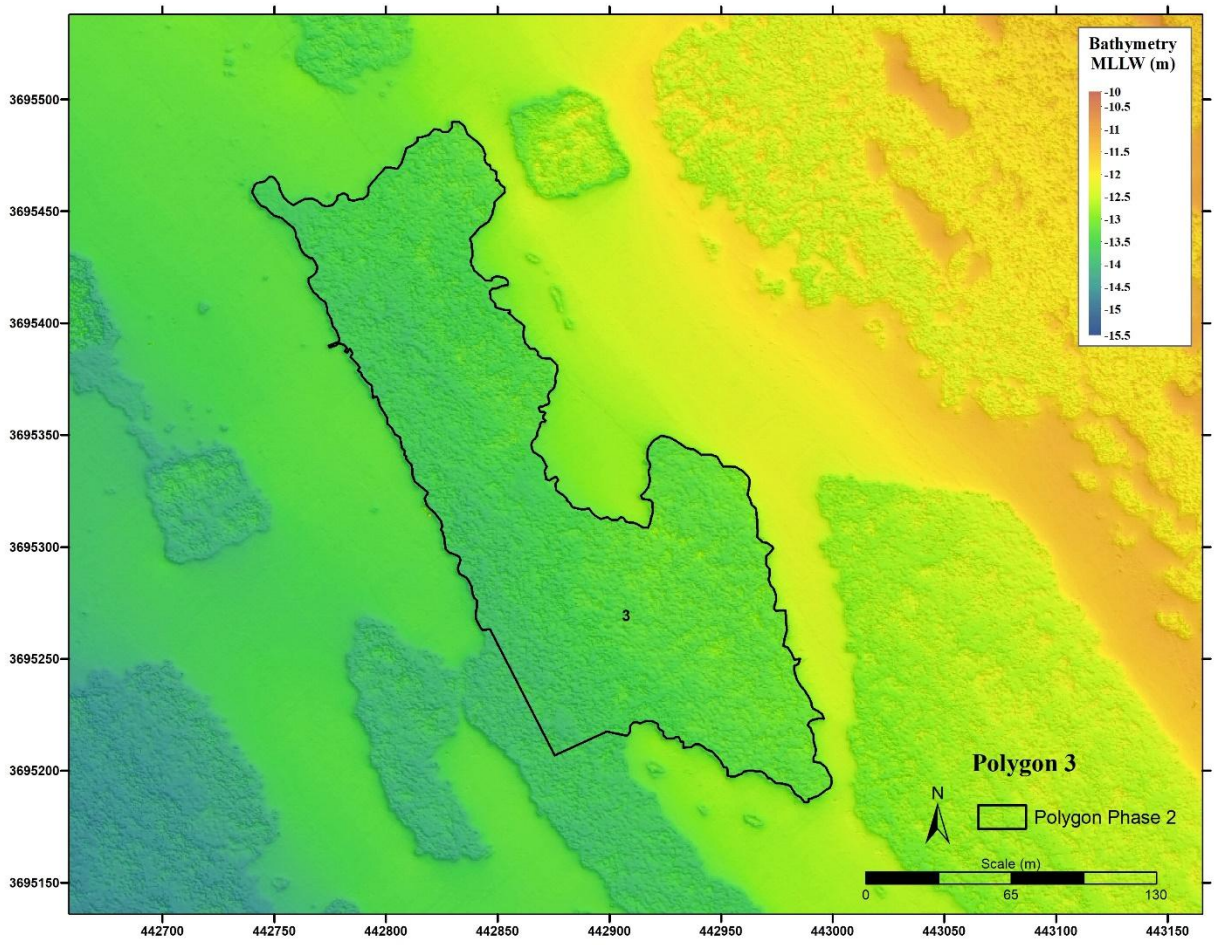

Figure E-3. Polygon 3 boundary from bathymetric data interpretation (October 2020 multibeam survey).

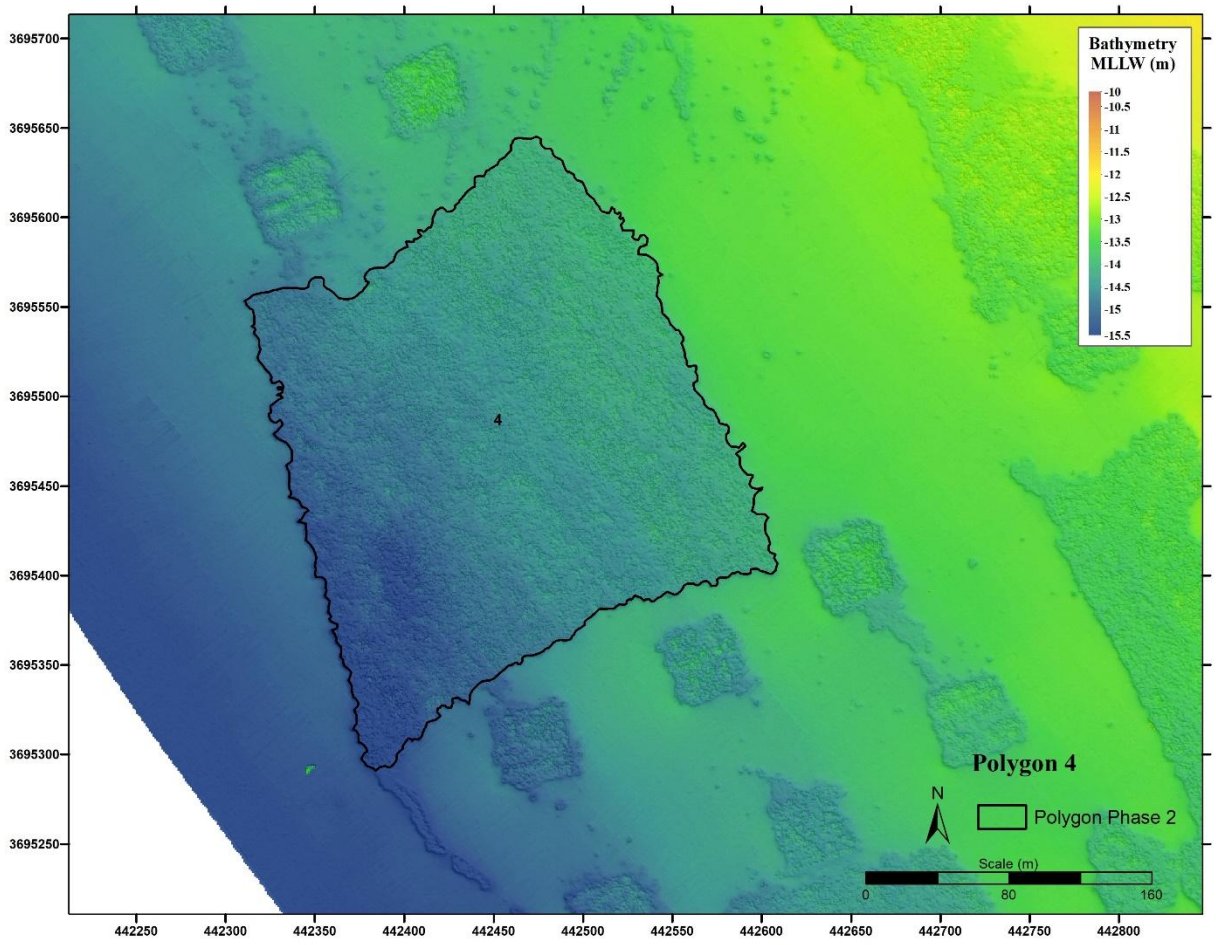

Figure E-4. Polygon 4 boundary from bathymetric data interpretation (October 2020 multibeam survey).

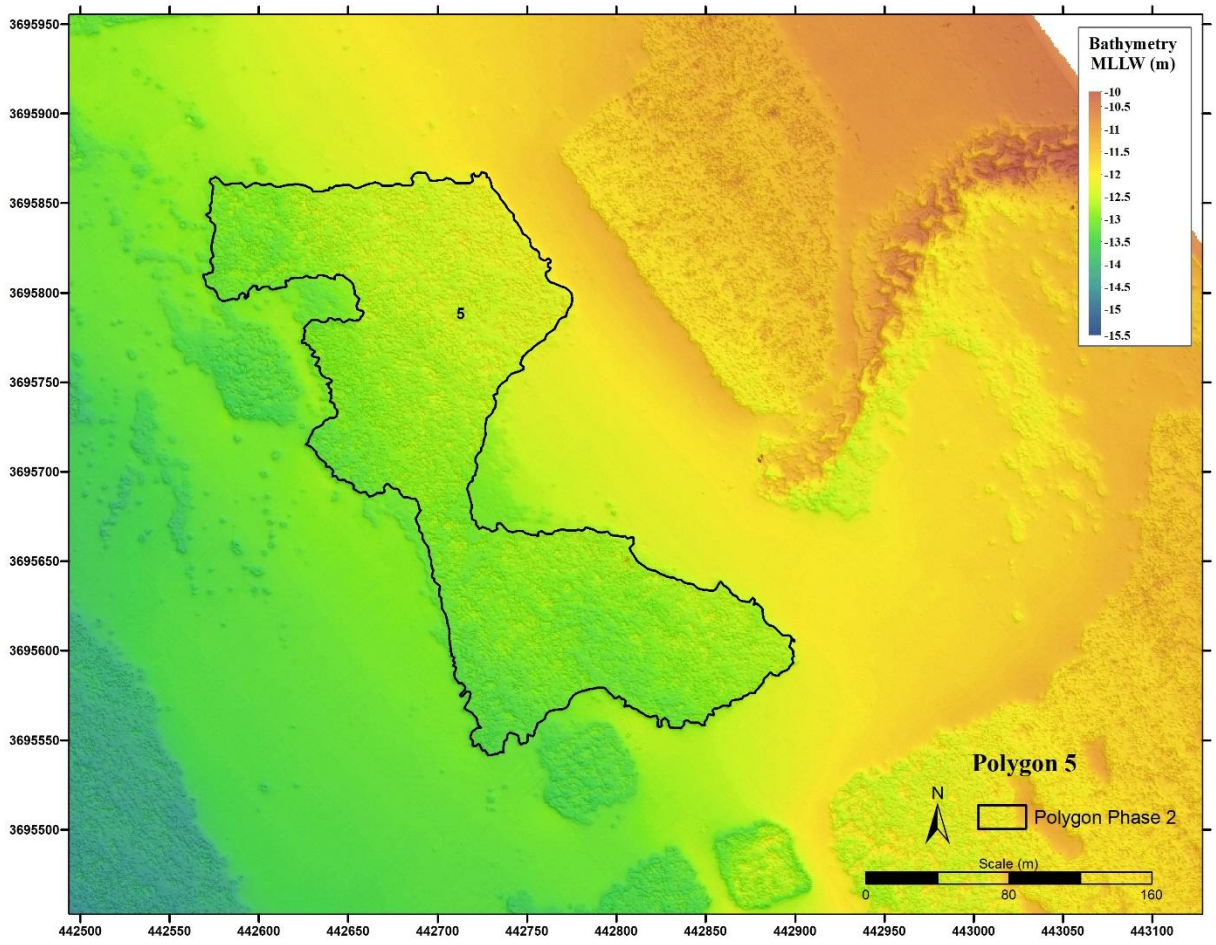

Figure E-5. Polygon 5 boundary from bathymetric data interpretation (October 2020 multibeam survey).

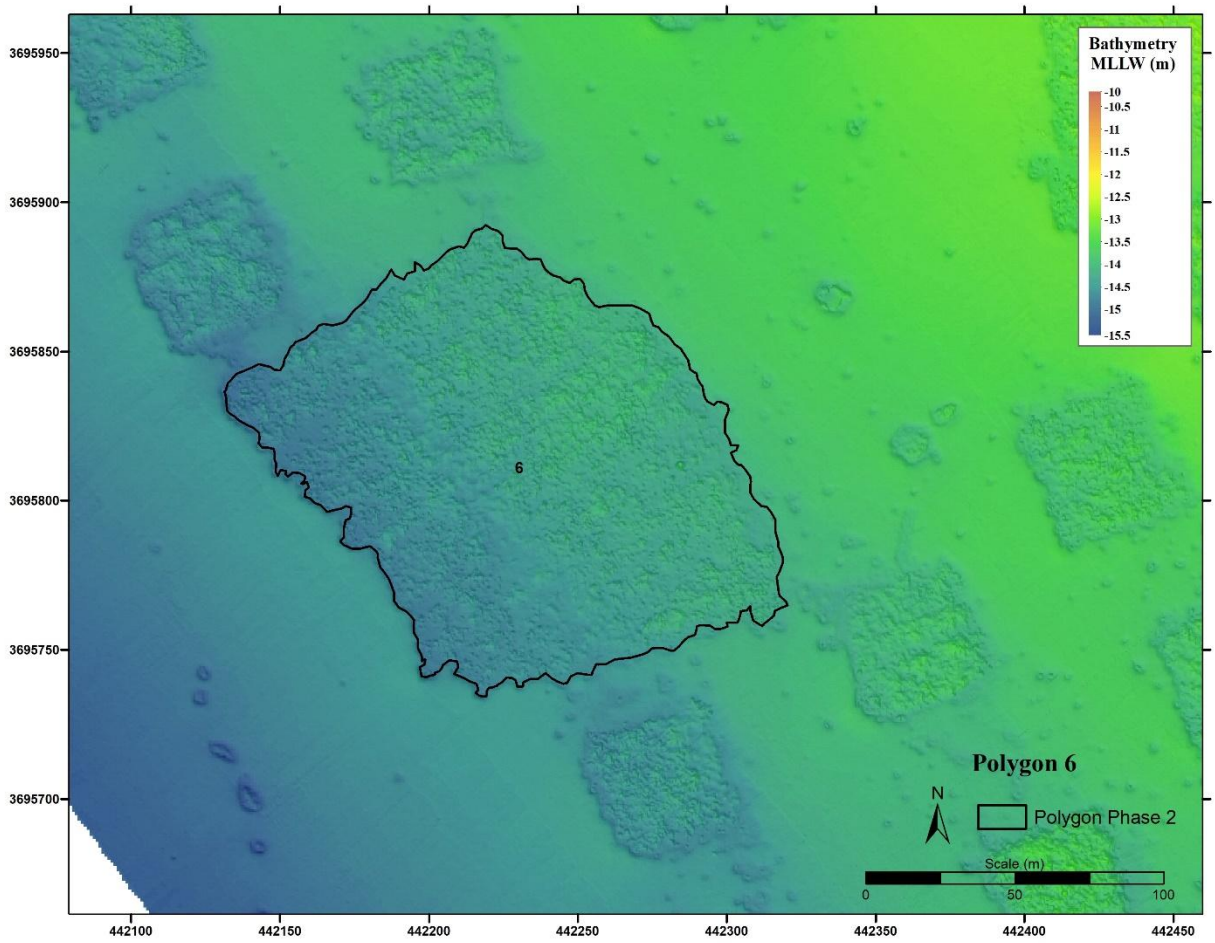

Figure E-6. Polygon 6 boundary from bathymetric data interpretation (October 2020 multibeam survey).

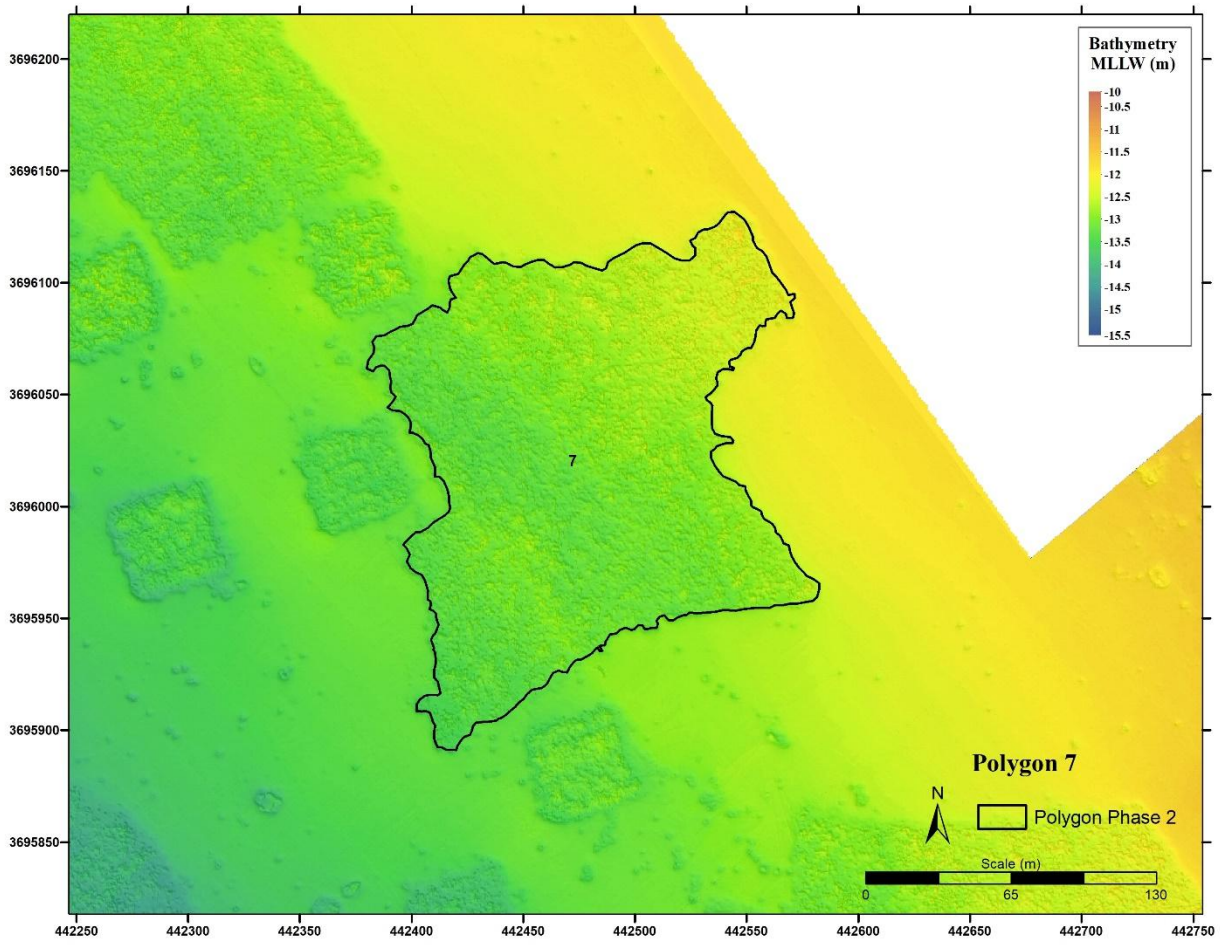

Figure E-7. Polygon 7 boundary from bathymetric data interpretation (October 2020 multibeam survey).

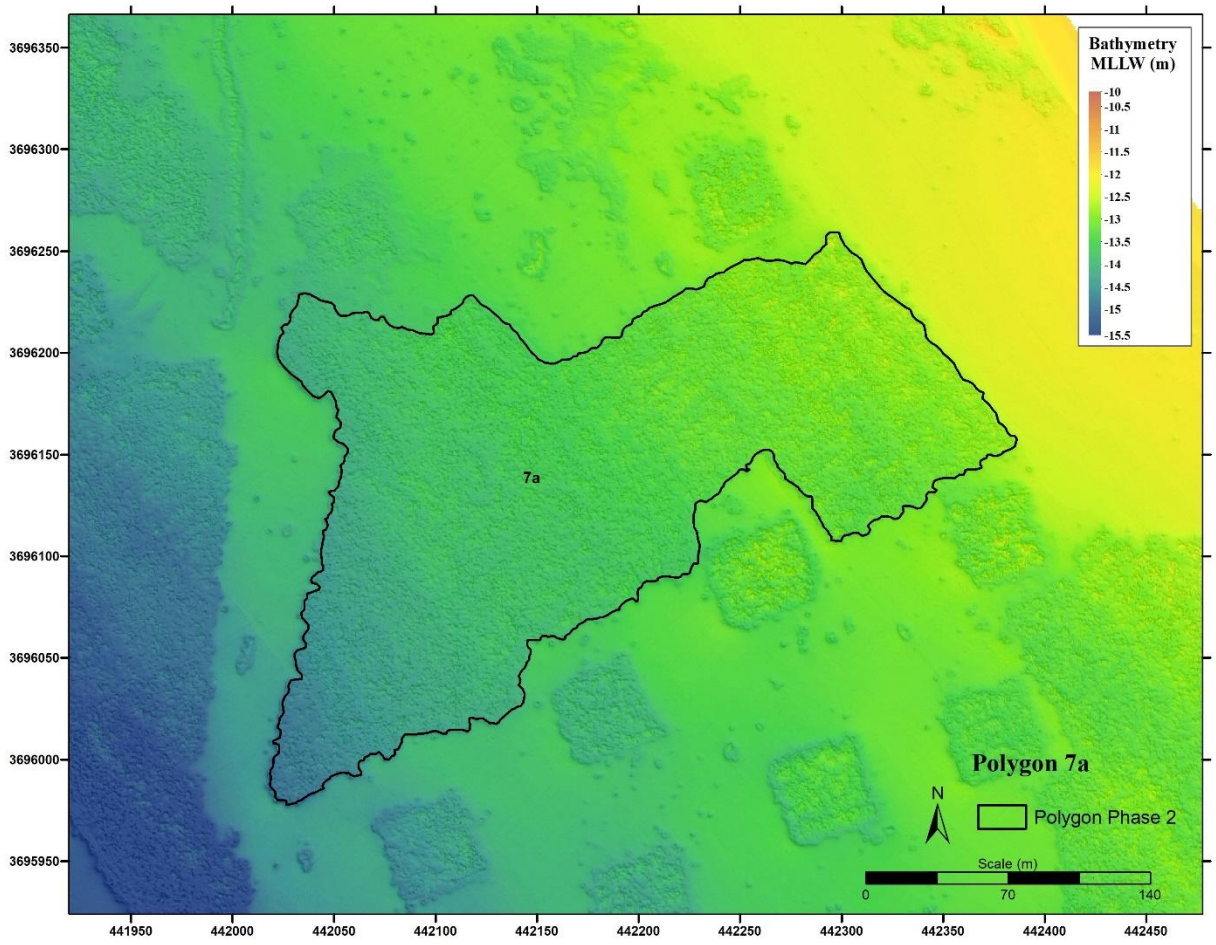

Figure E-8. Polygon 7a boundary from bathymetric data interpretation (October 2020 multibeam survey).

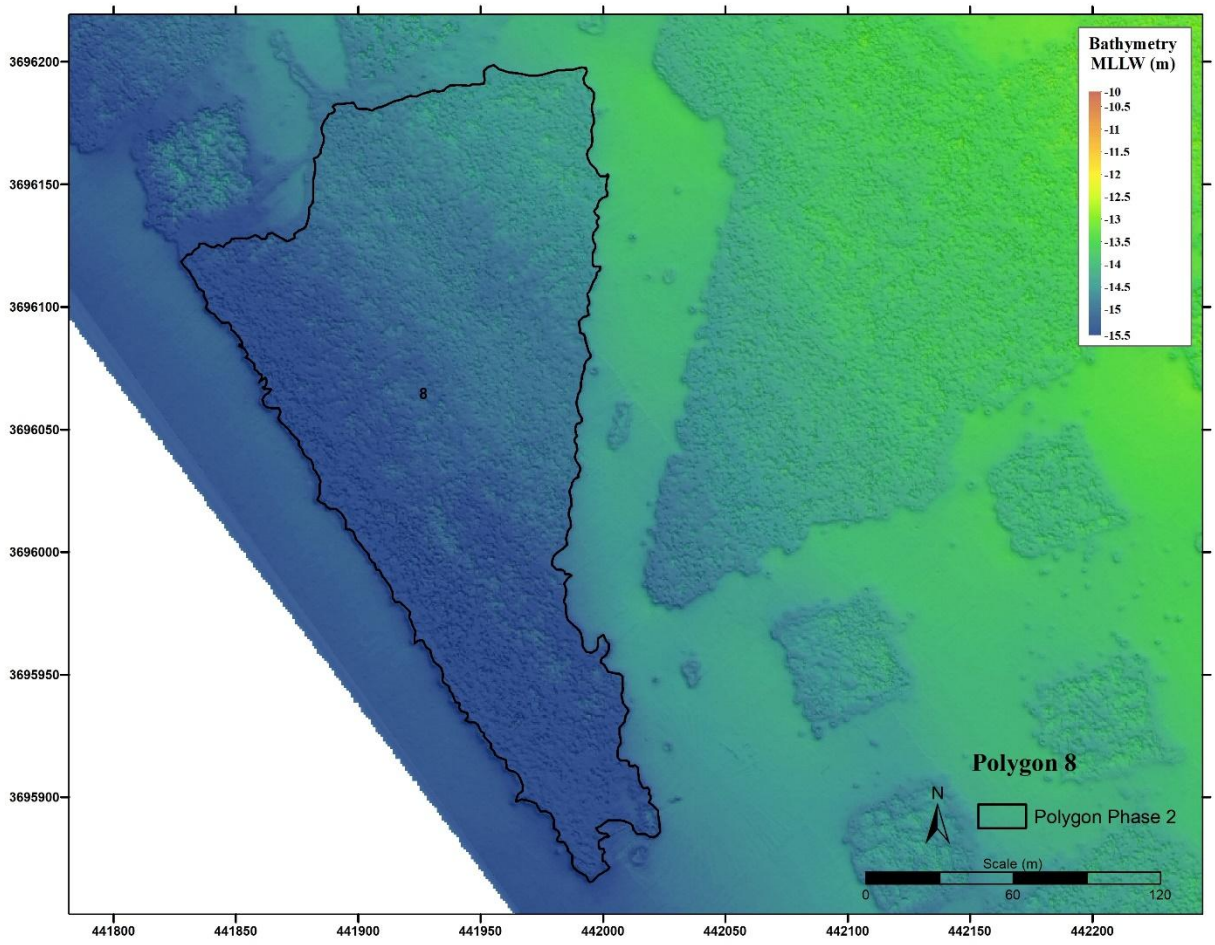

Figure E-9. Polygon 8 boundary from bathymetric data interpretation (October 2020 multibeam survey).

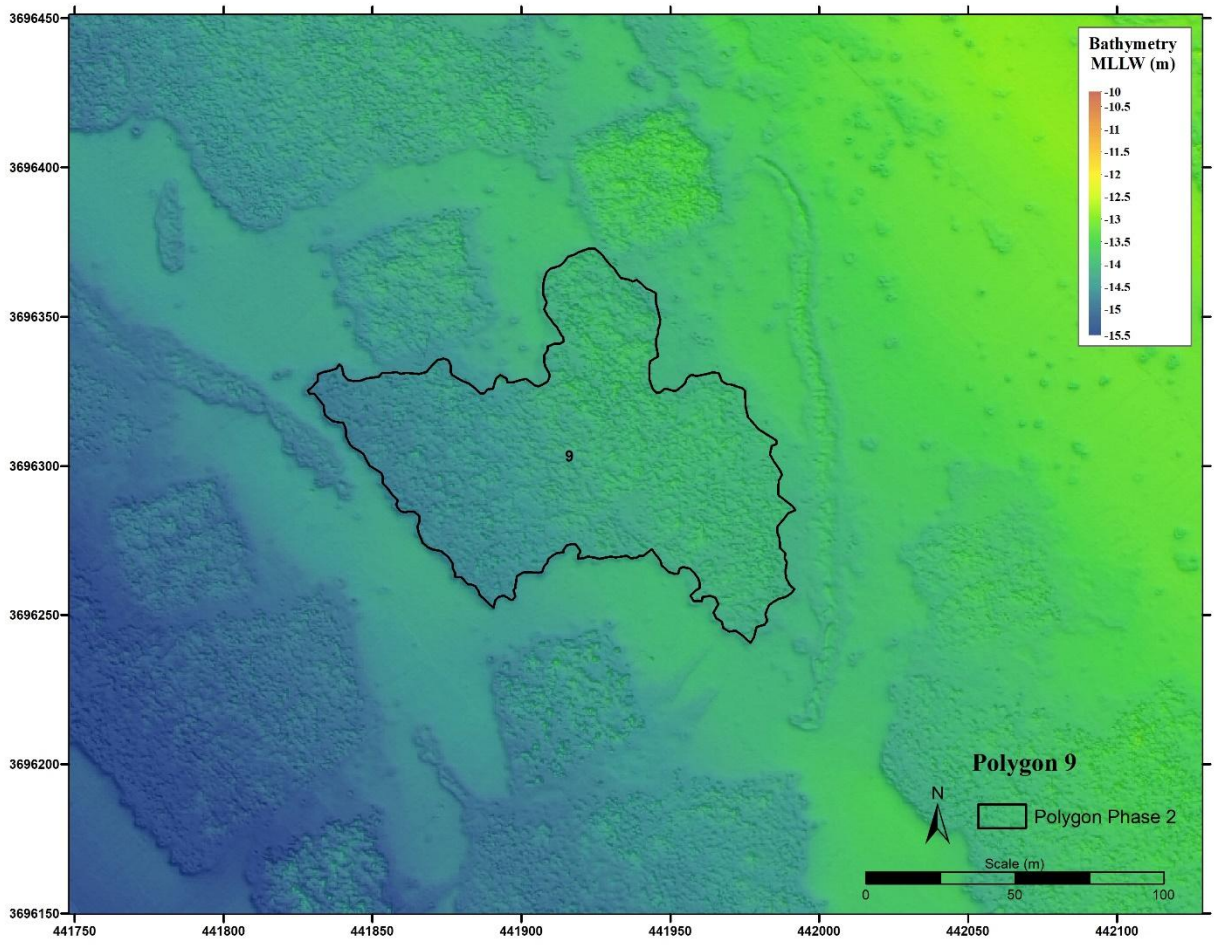

Figure E-10. Polygon 9 boundary from bathymetric data interpretation (October 2020 multibeam survey).

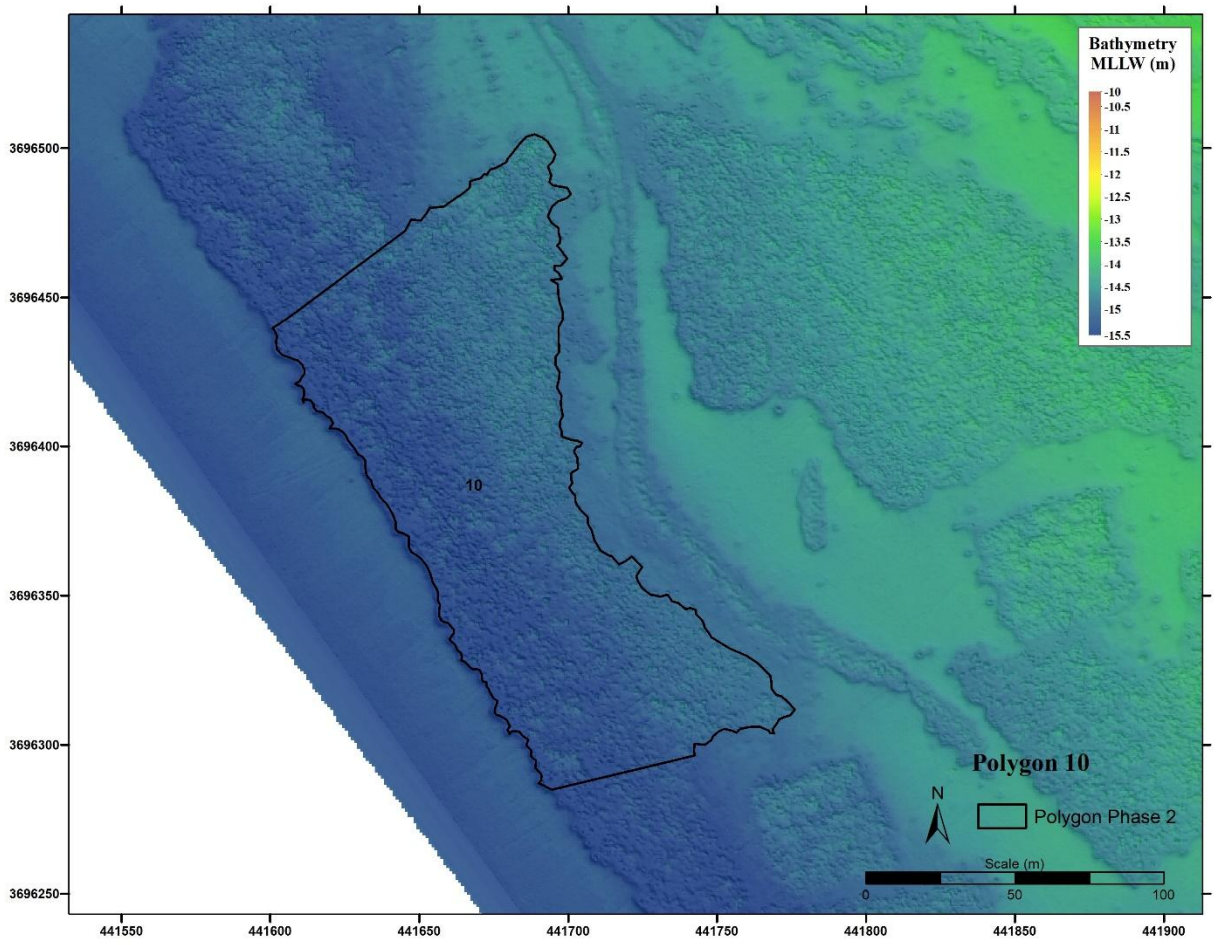

Figure E-11. Polygon 10 boundary from bathymetric data interpretation (October 2020 multibeam survey).

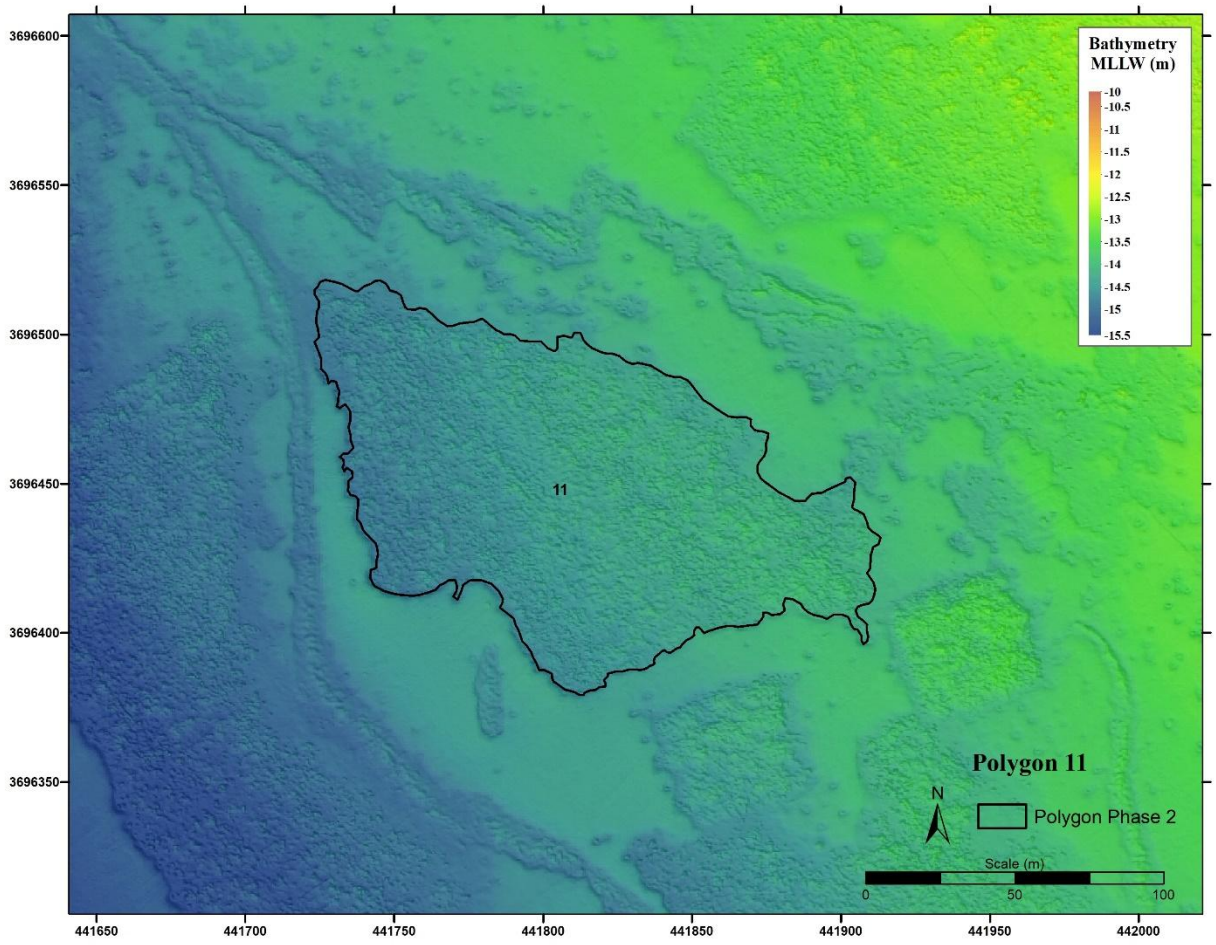

Figure E-12. Polygon 11 boundary from bathymetric data interpretation (October 2020 multibeam survey).

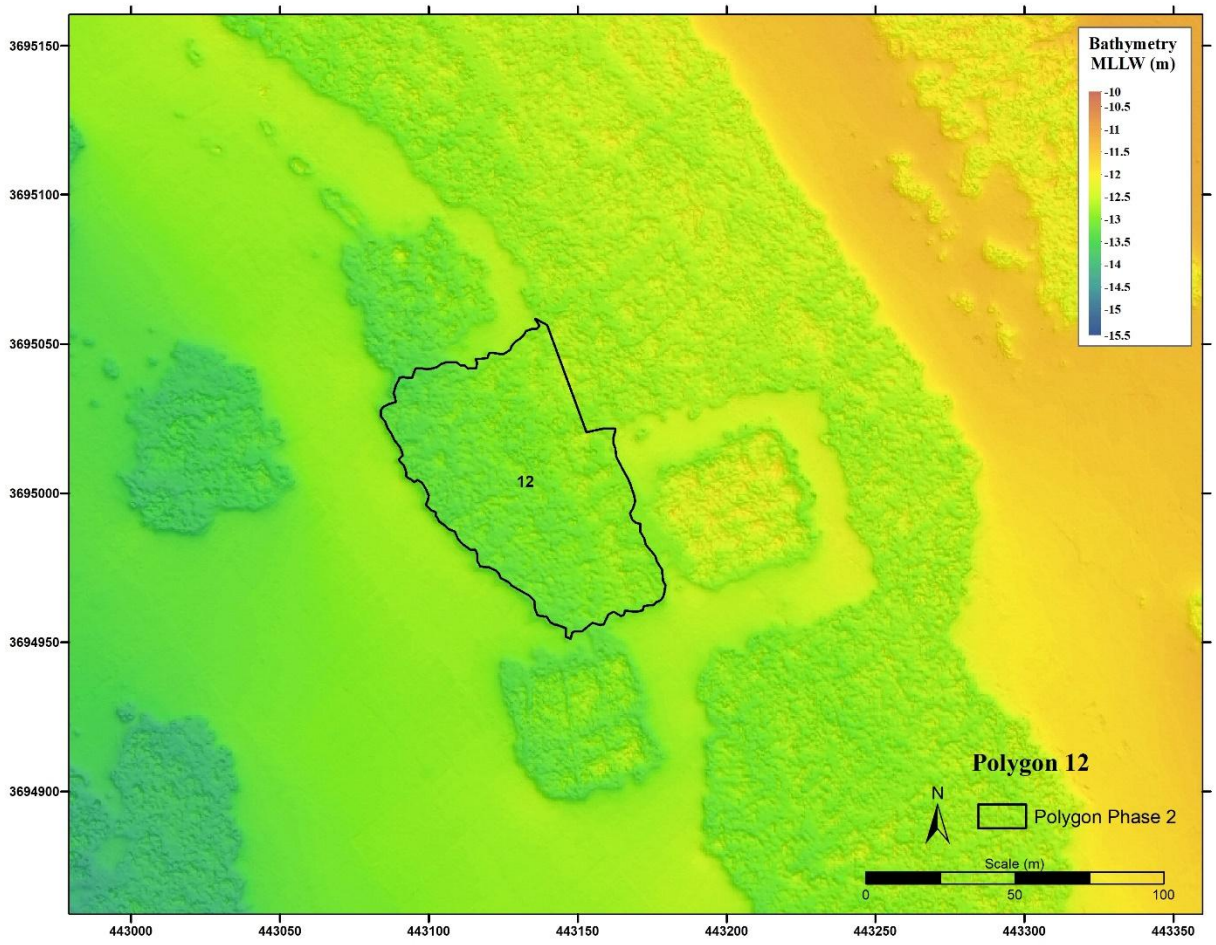

Figure E-13. Polygon 12 boundary from bathymetric data interpretation (October 2020 multibeam survey).

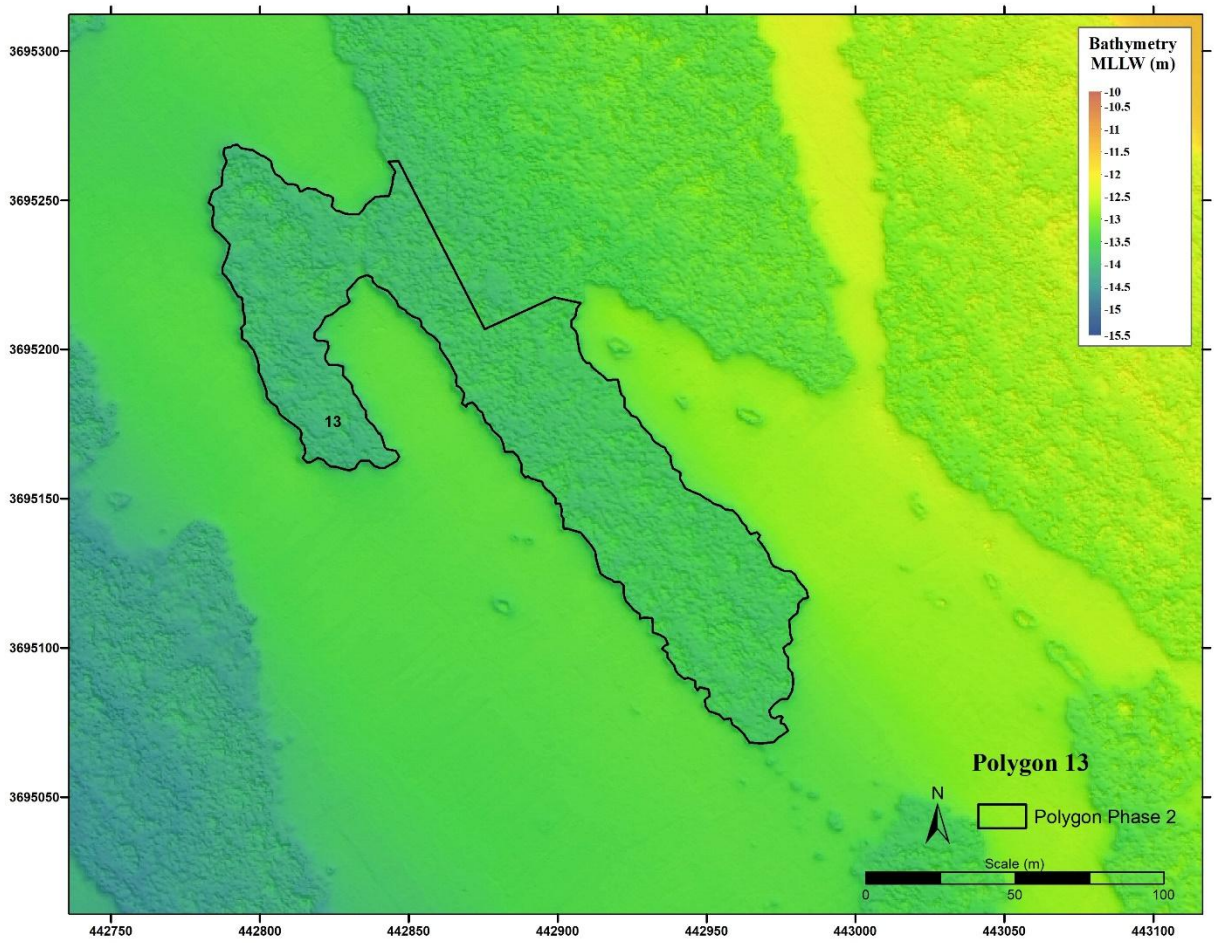

Figure E-14. Polygon 13 boundary from bathymetric data interpretation (October 2020 multibeam survey).

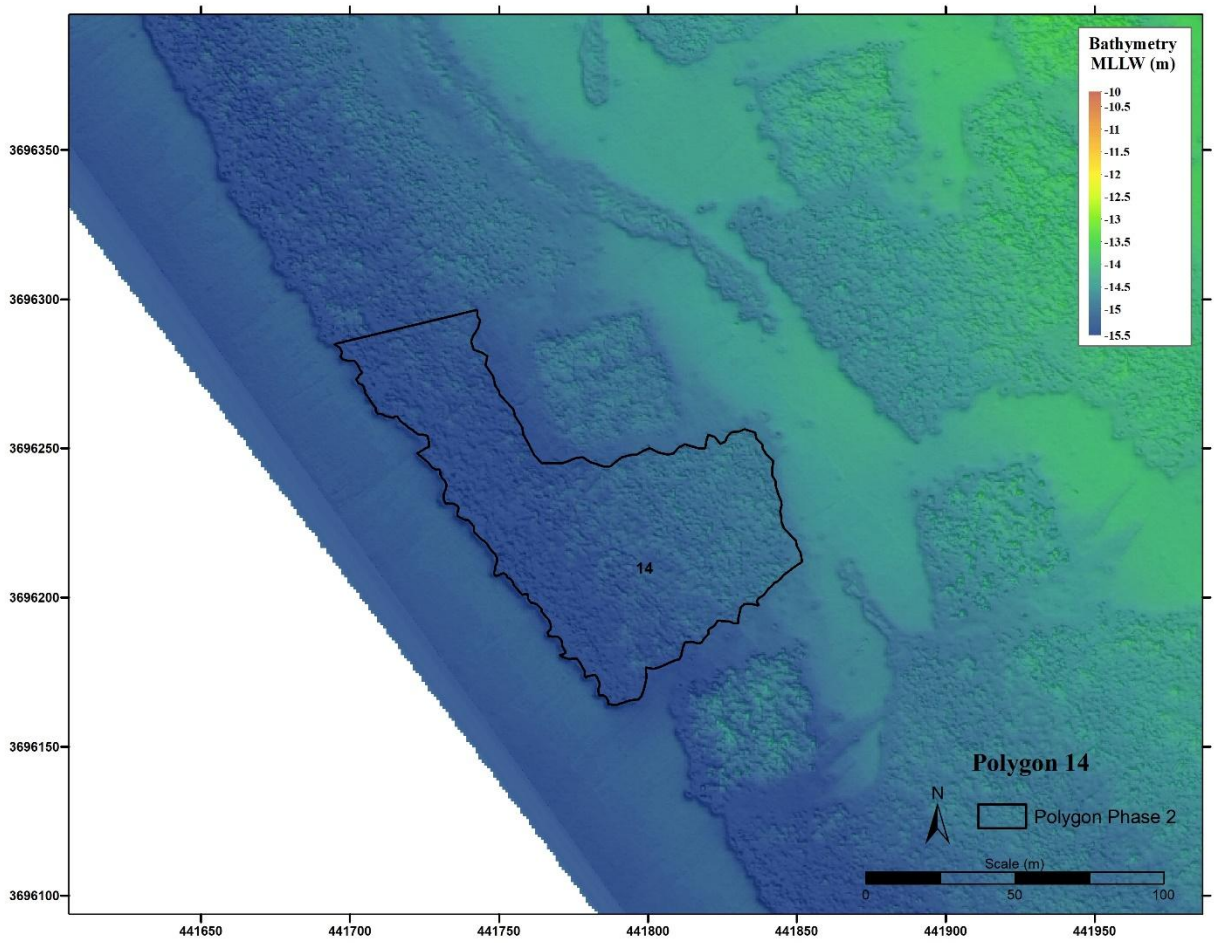

Figure E-15. Polygon 14 boundary from bathymetric data interpretation (October 2020 multibeam survey).

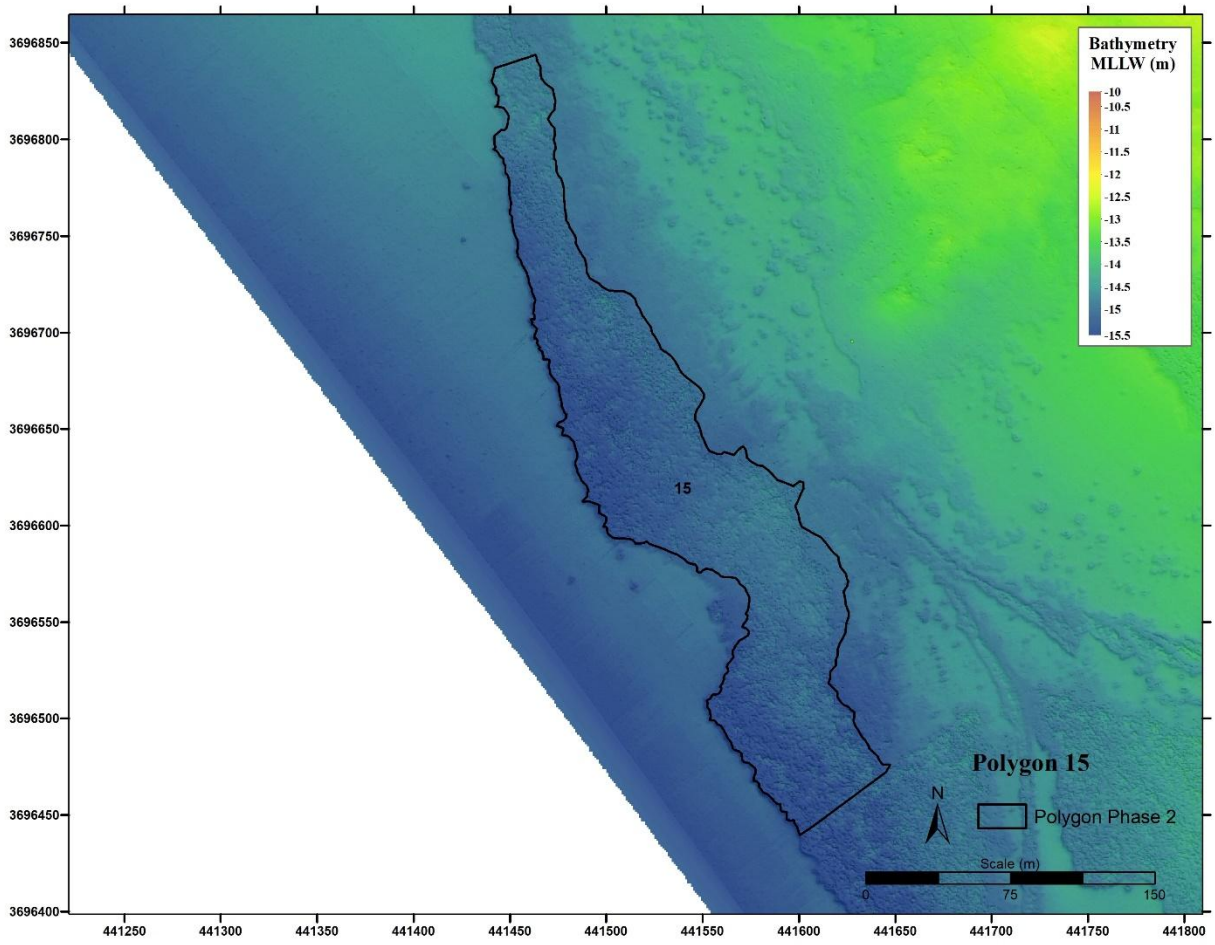

Figure E-16. Polygon 15 boundary from bathymetric data interpretation (October 2020 multibeam survey).

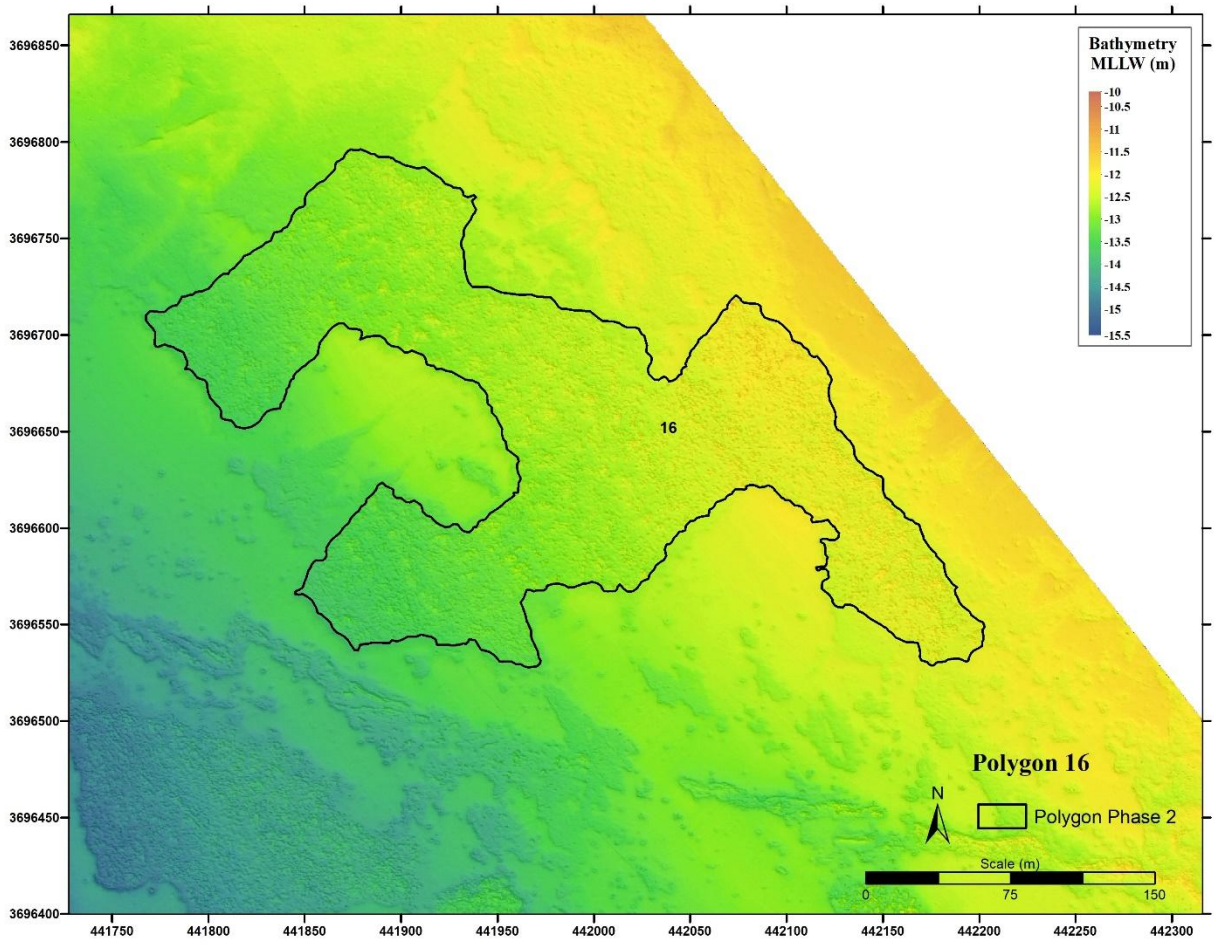

Figure E-17. Polygon 16 boundary from bathymetric data interpretation (October 2020 multibeam survey).

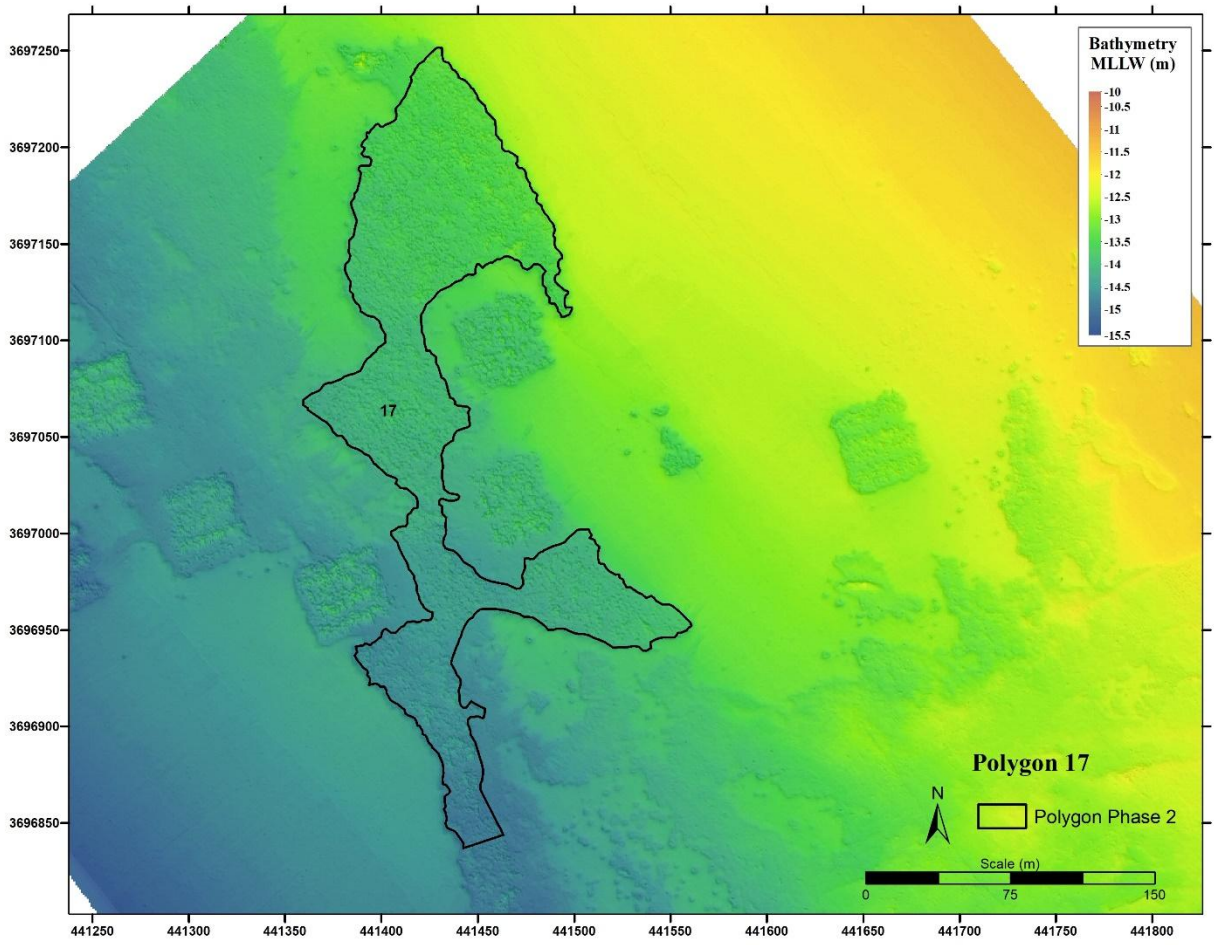

Figure E-18. Polygon 17 boundary from bathymetric data interpretation (October 2020 multibeam survey).

APPENDIX F

BOUNDARIES FROM BATHYMETRIC DATA FOR POLYGONS 18-40 (OCTOBER 2020 MULTIBEAM SURVEY)

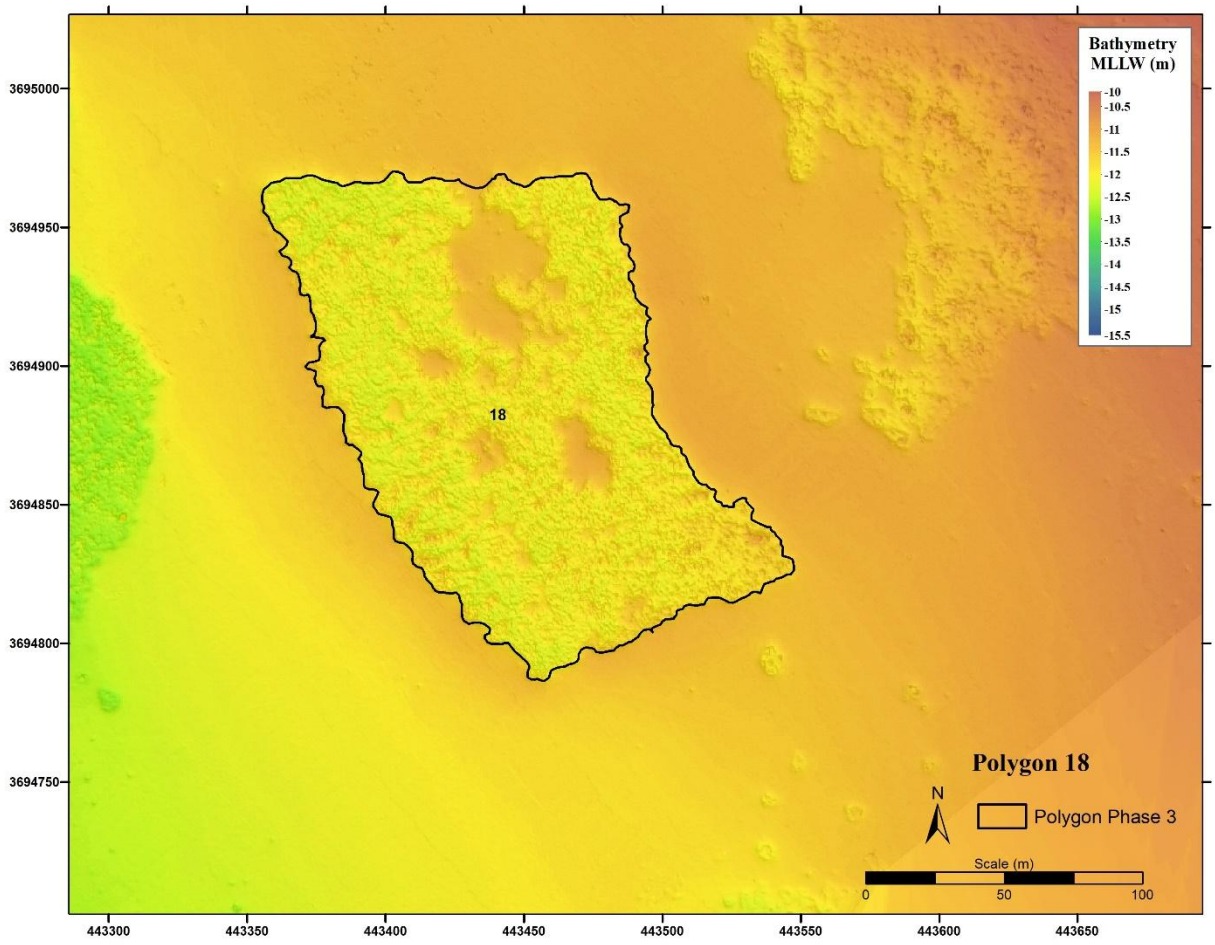

Figure F-1. Polygon 18 boundary from bathymetric data interpretation (October 2020 multibeam survey).

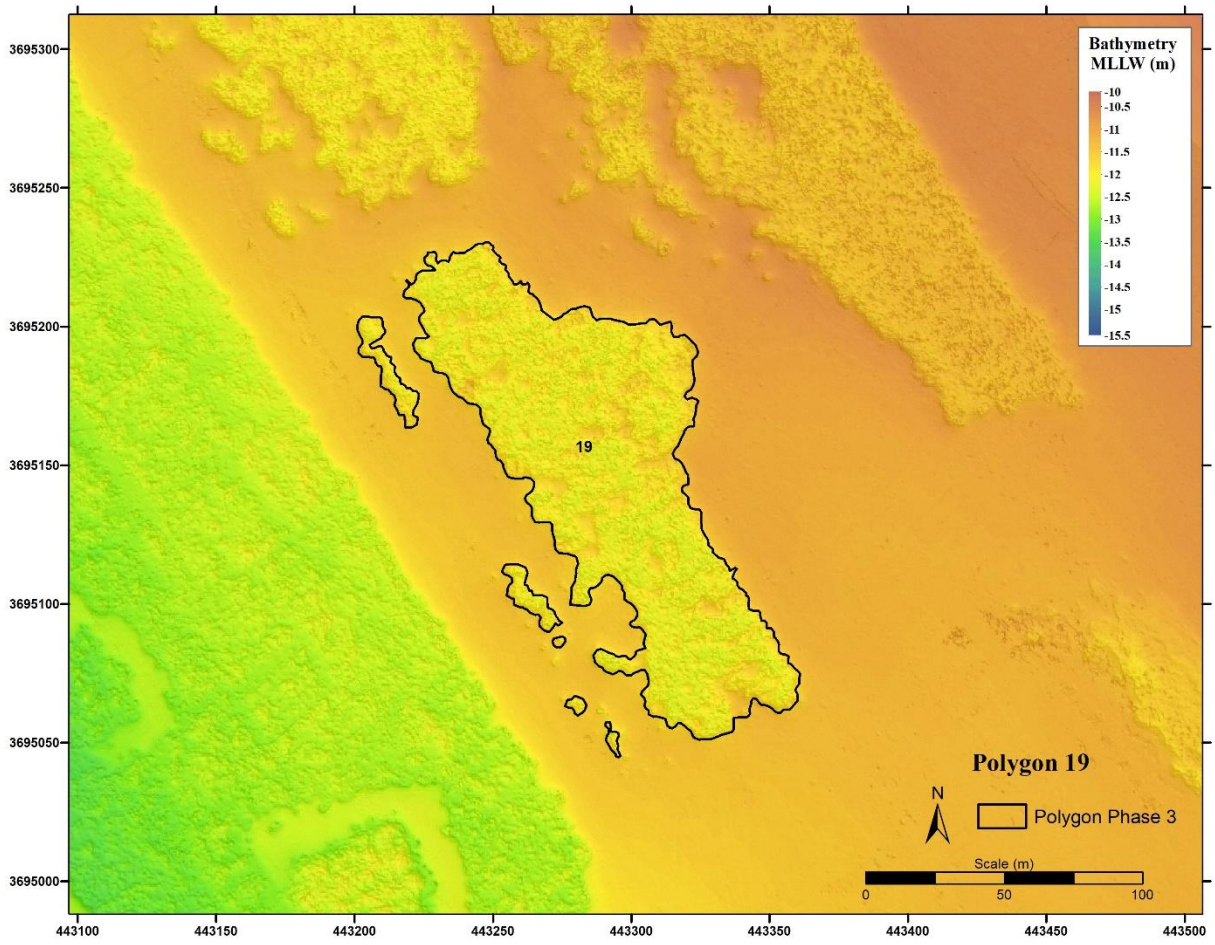

Figure F-2. Polygon 19 boundary from bathymetric data interpretation (October 2020 multibeam survey).

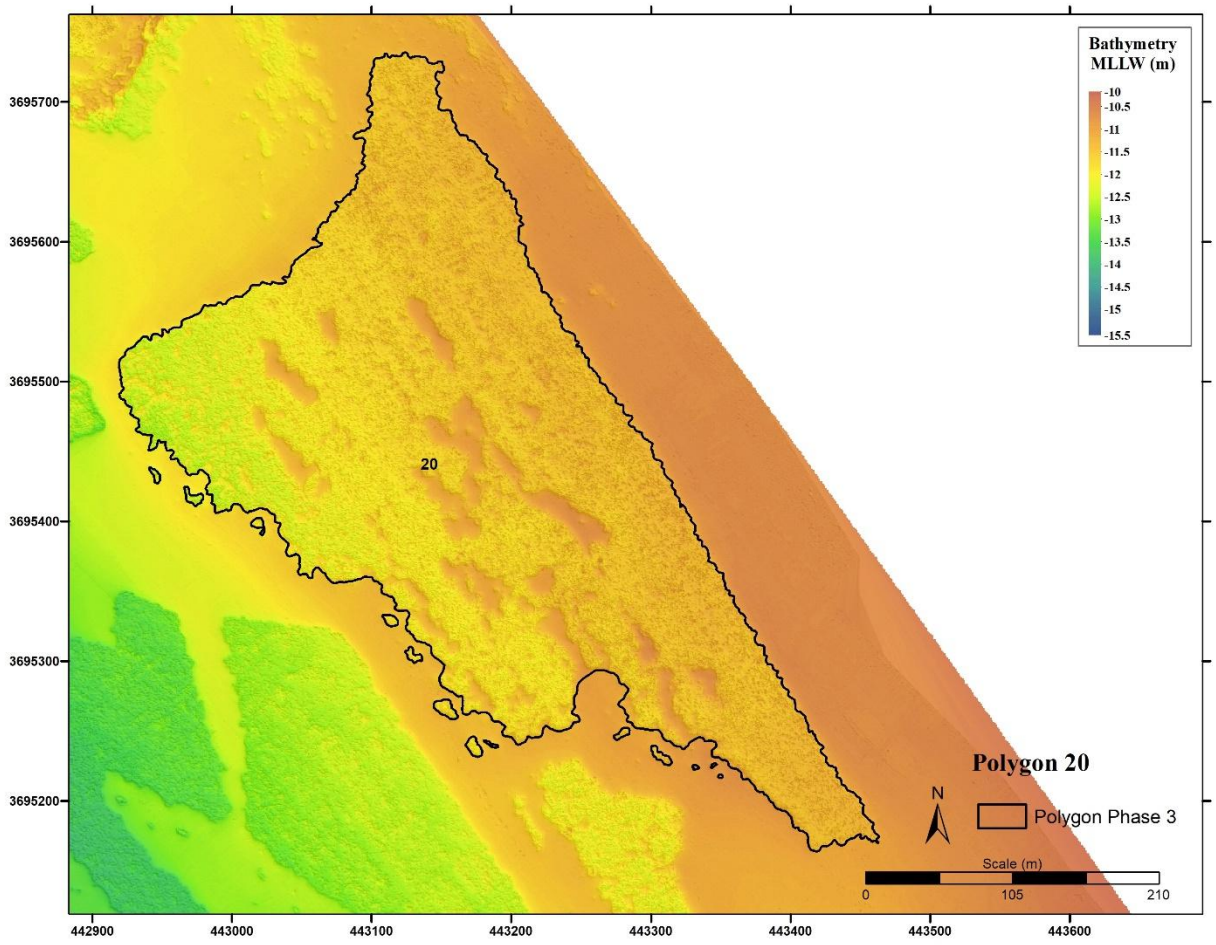

Figure F-3. Polygon 20 boundary from bathymetric data interpretation (October 2020 multibeam survey).

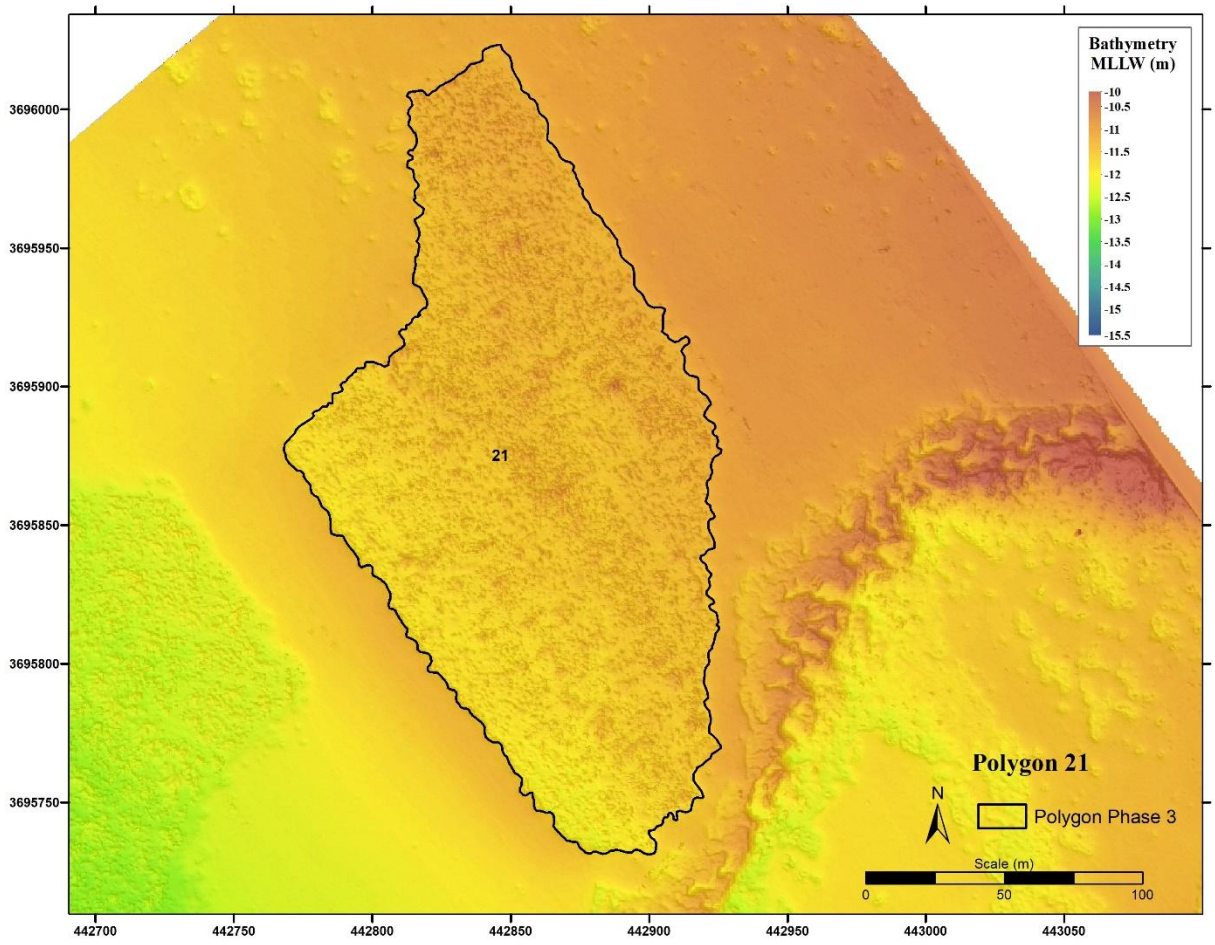

Figure F-4. Polygon 21 boundary from bathymetric data interpretation (October 2020 multibeam survey).

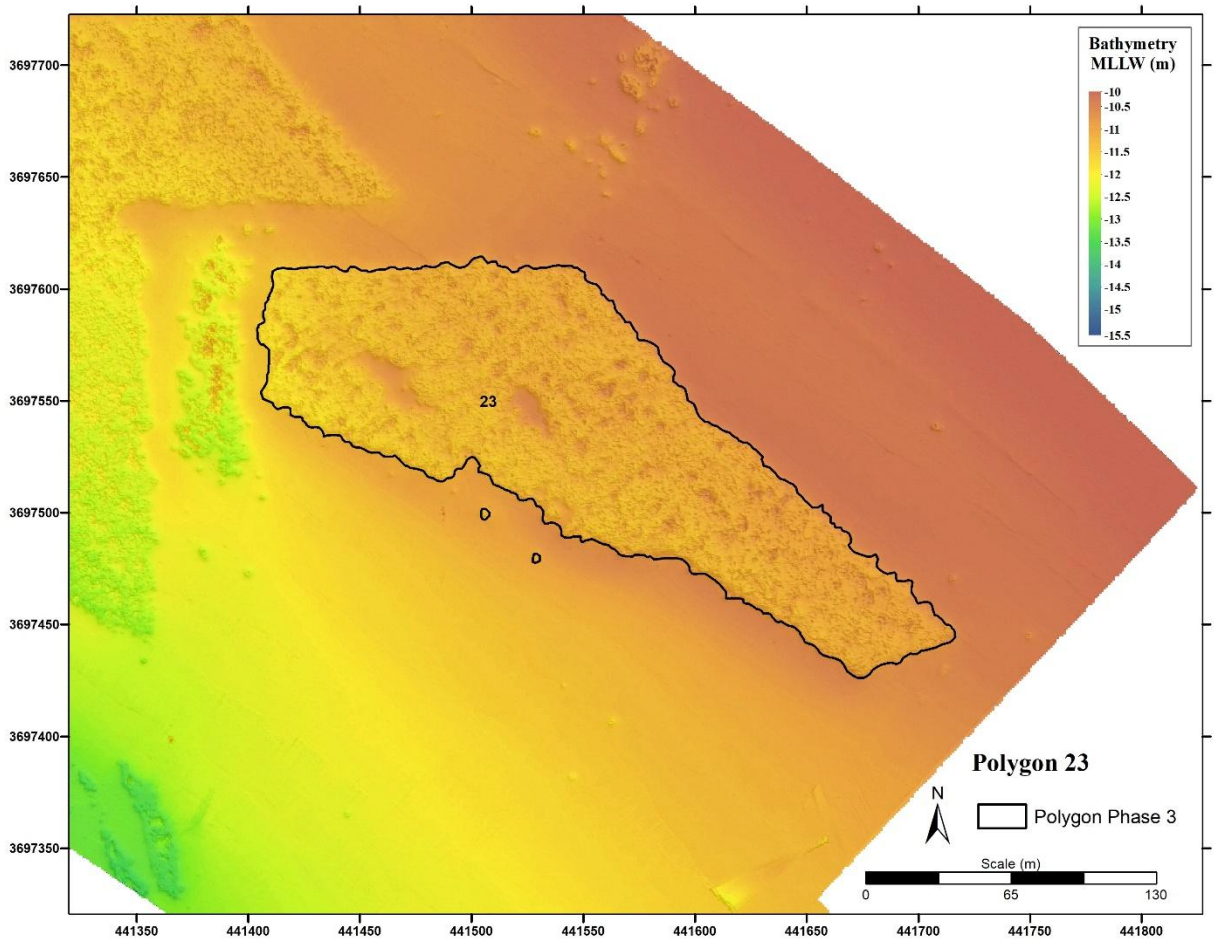

Figure F-5. Polygon 23 boundary from bathymetric data interpretation (October 2020 multibeam survey).

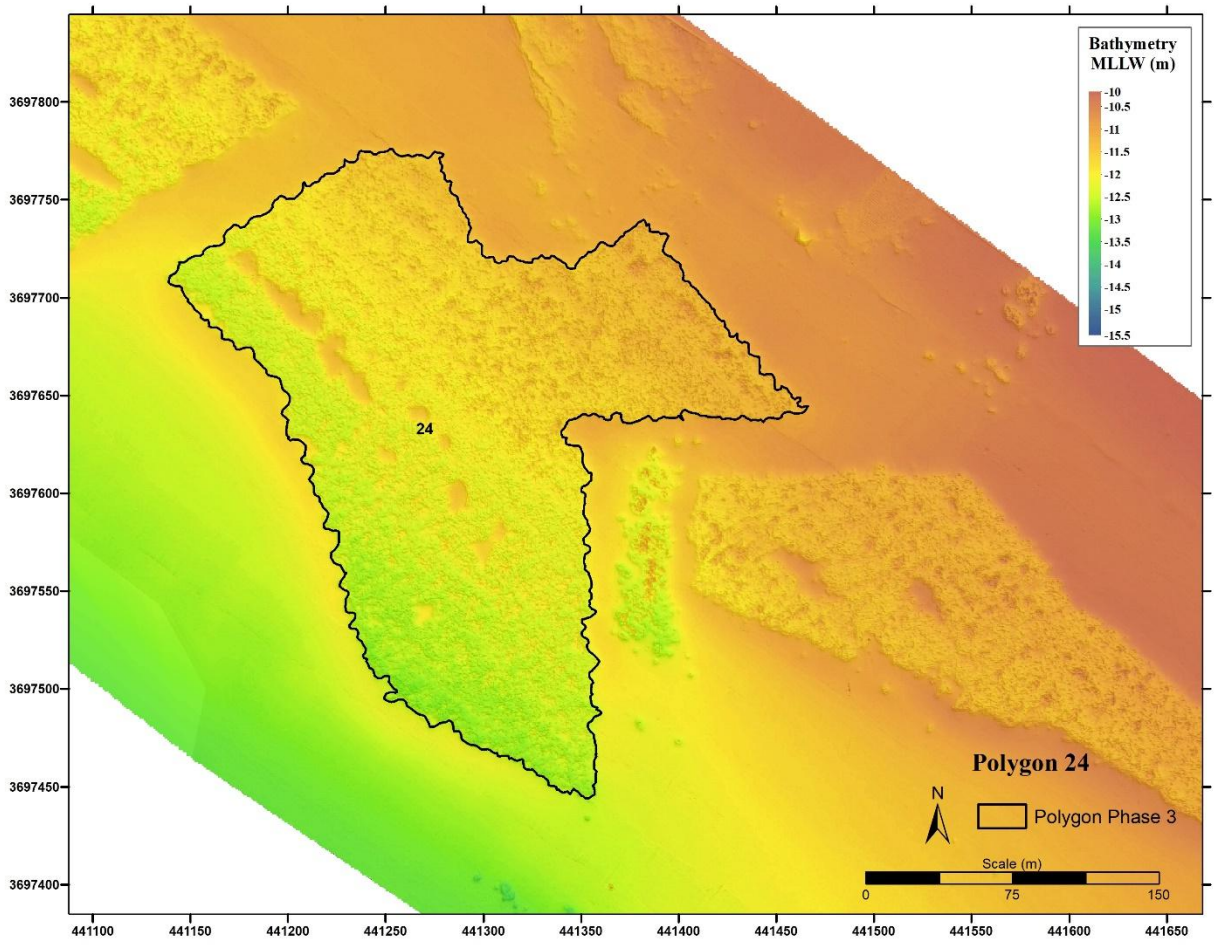

Figure F-6. Polygon 24 boundary from bathymetric data interpretation (October 2020 multibeam survey).

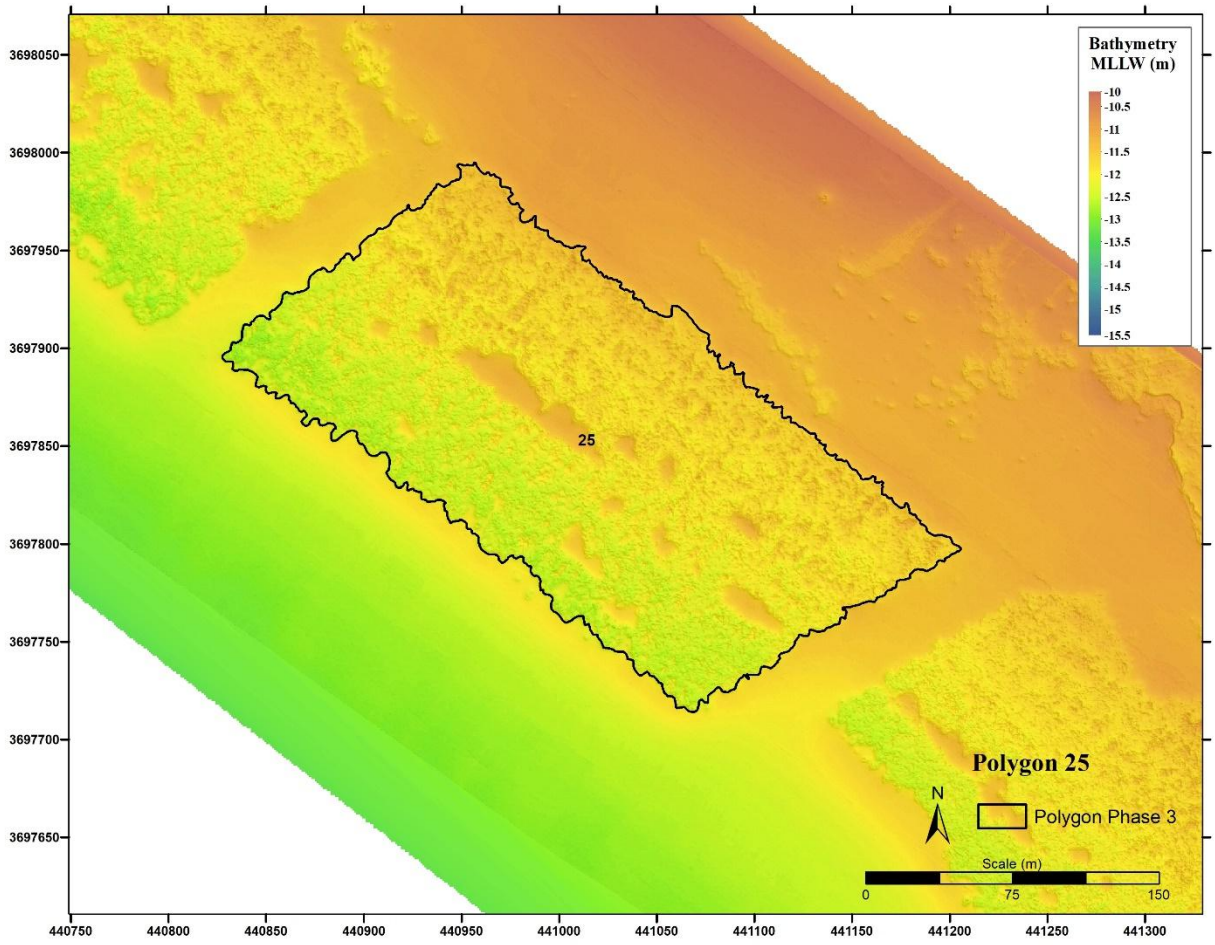

Figure F-7. Polygon 25 boundary from bathymetric data interpretation (October 2020 multibeam survey).

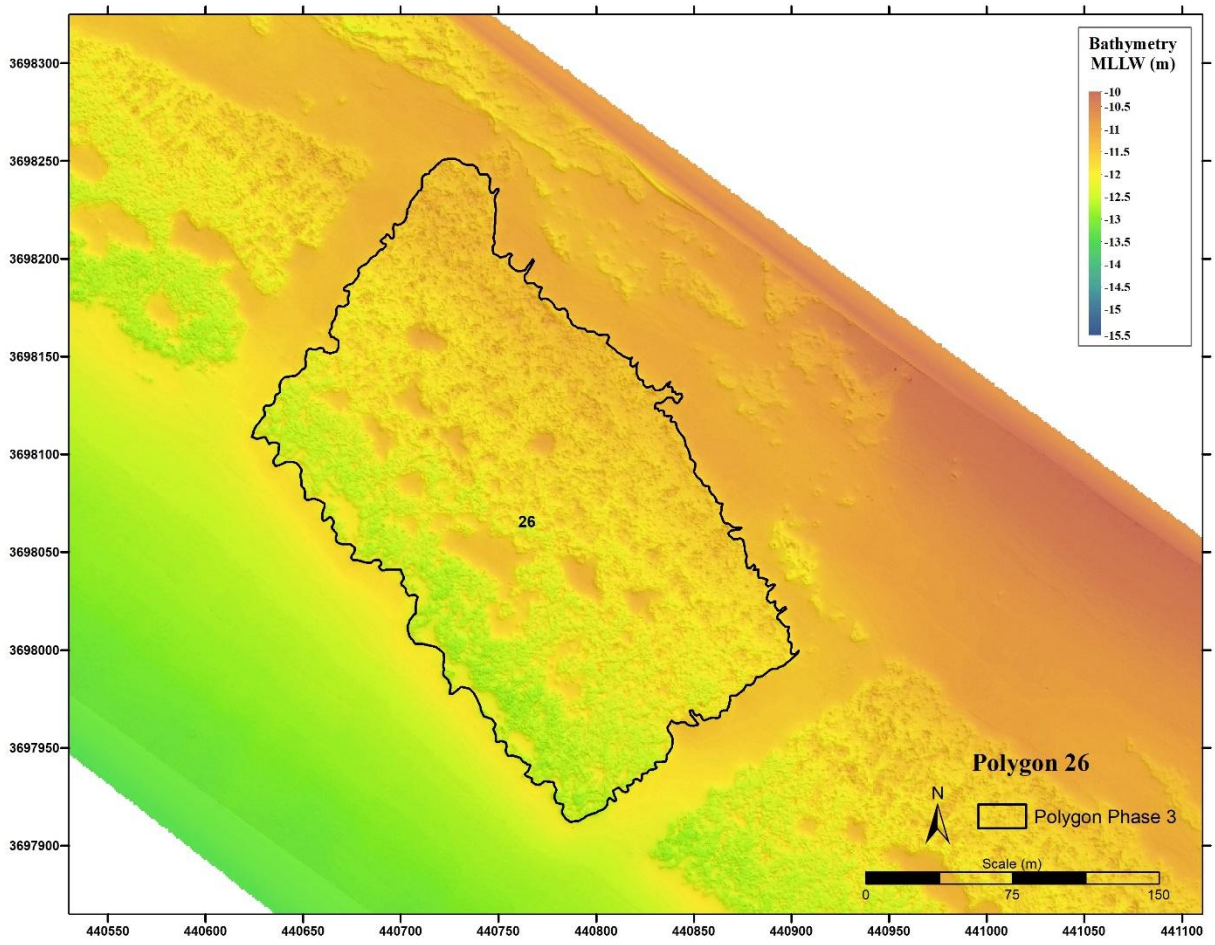

Figure F-8. Polygon 26 boundary from bathymetric data interpretation (October 2020 multibeam survey).

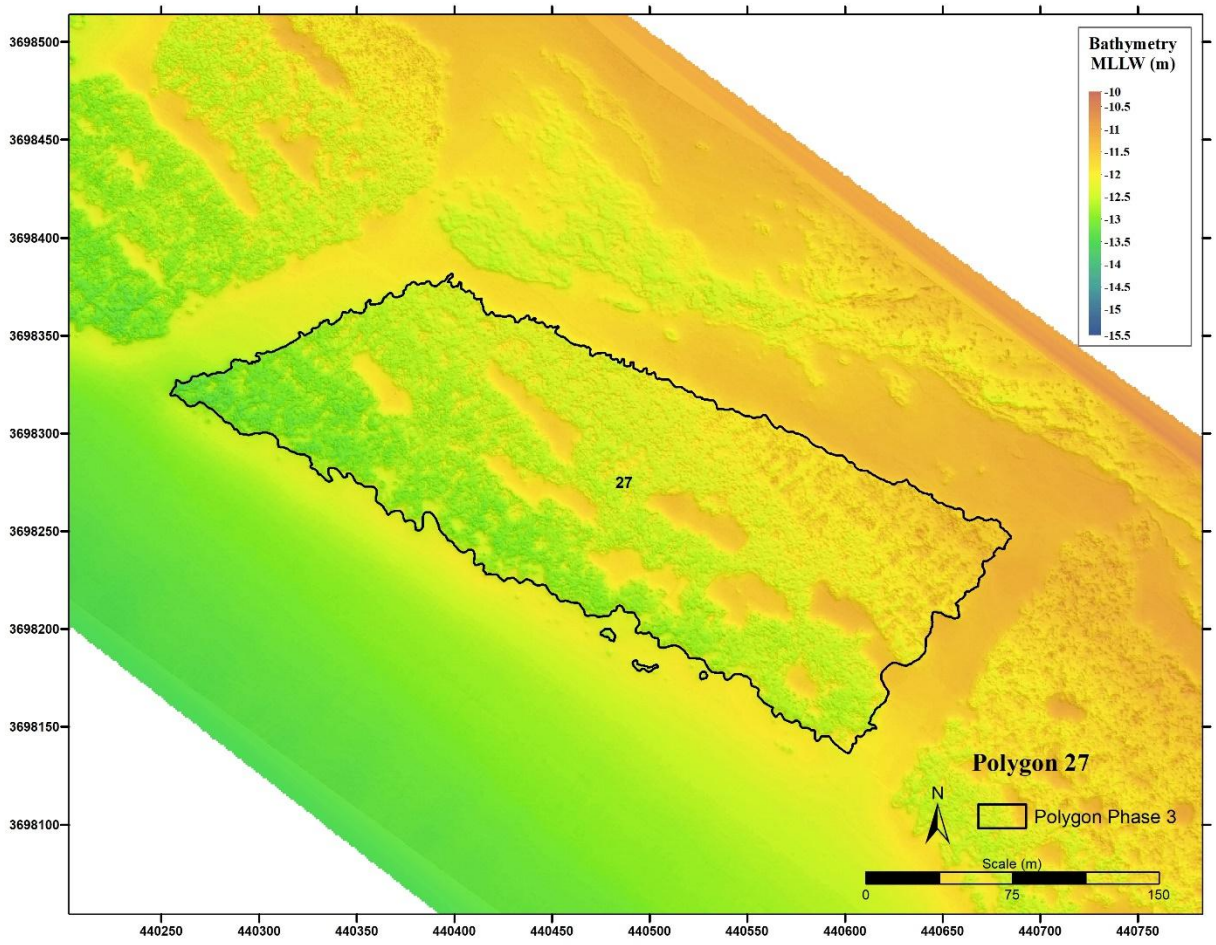

Figure F-9. Polygon 27 boundary from bathymetric data interpretation (October 2020 multibeam survey).

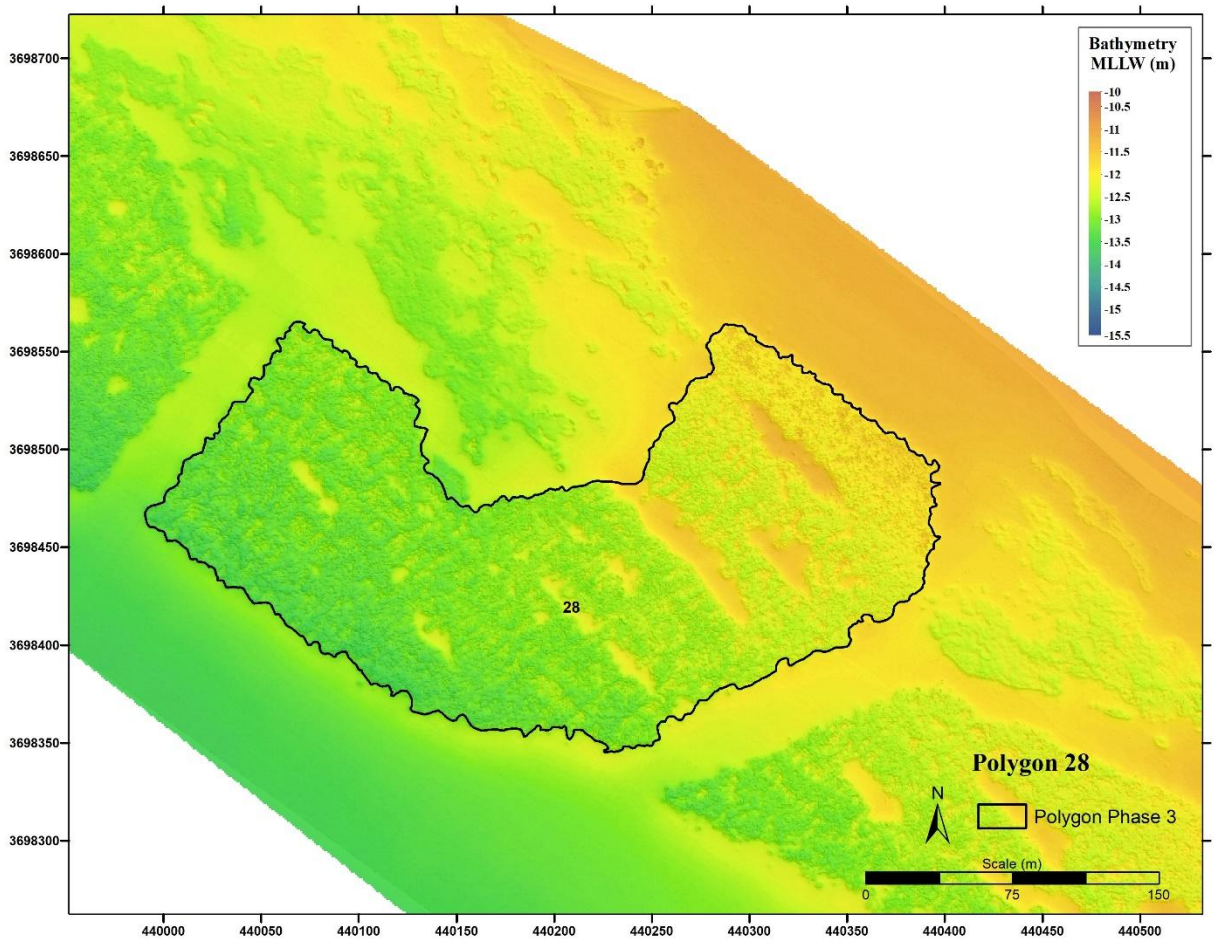

Figure F-10. Polygon 28 boundary from bathymetric data interpretation (October 2020 multibeam survey).

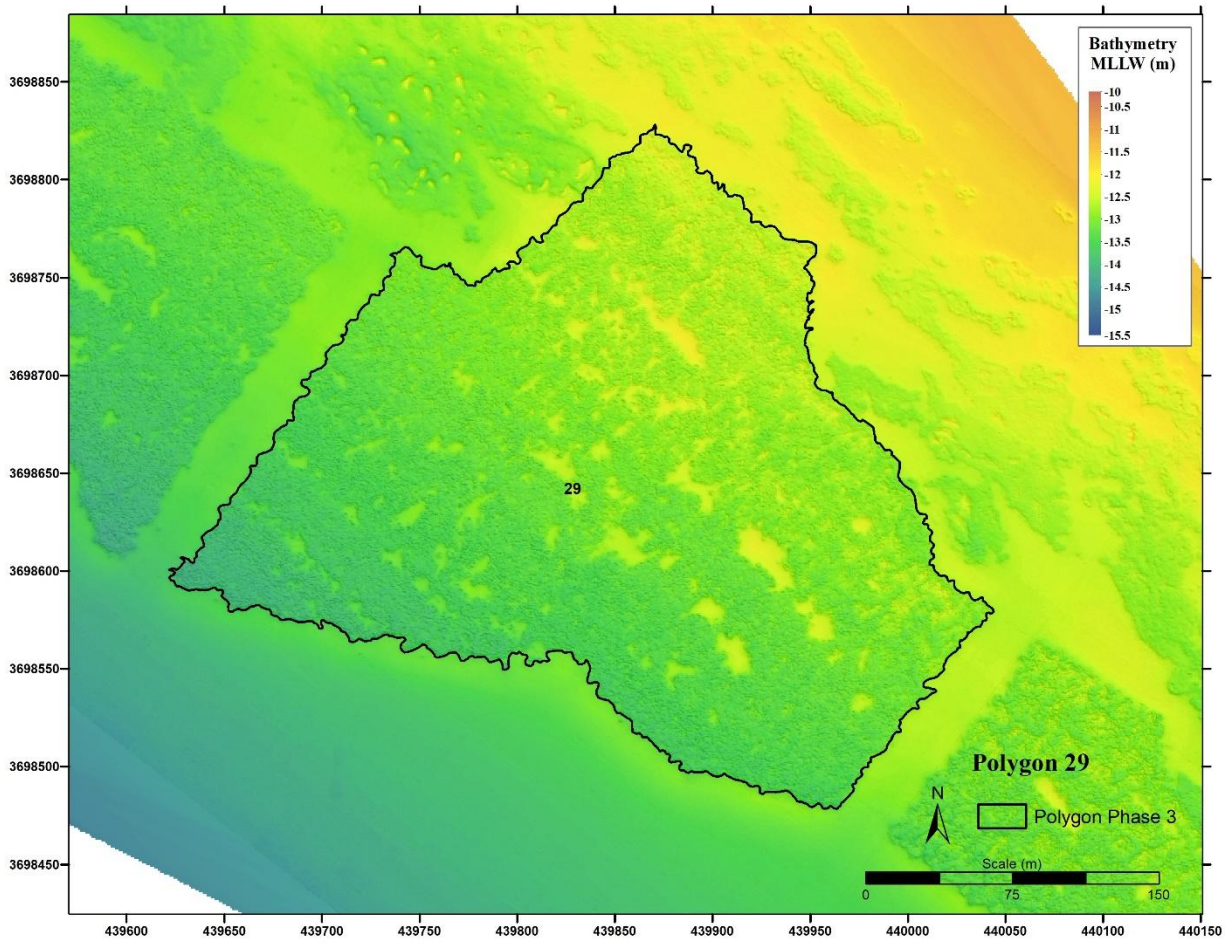

Figure F-11. Polygon 29 boundary from bathymetric data interpretation (October 2020 multibeam survey).

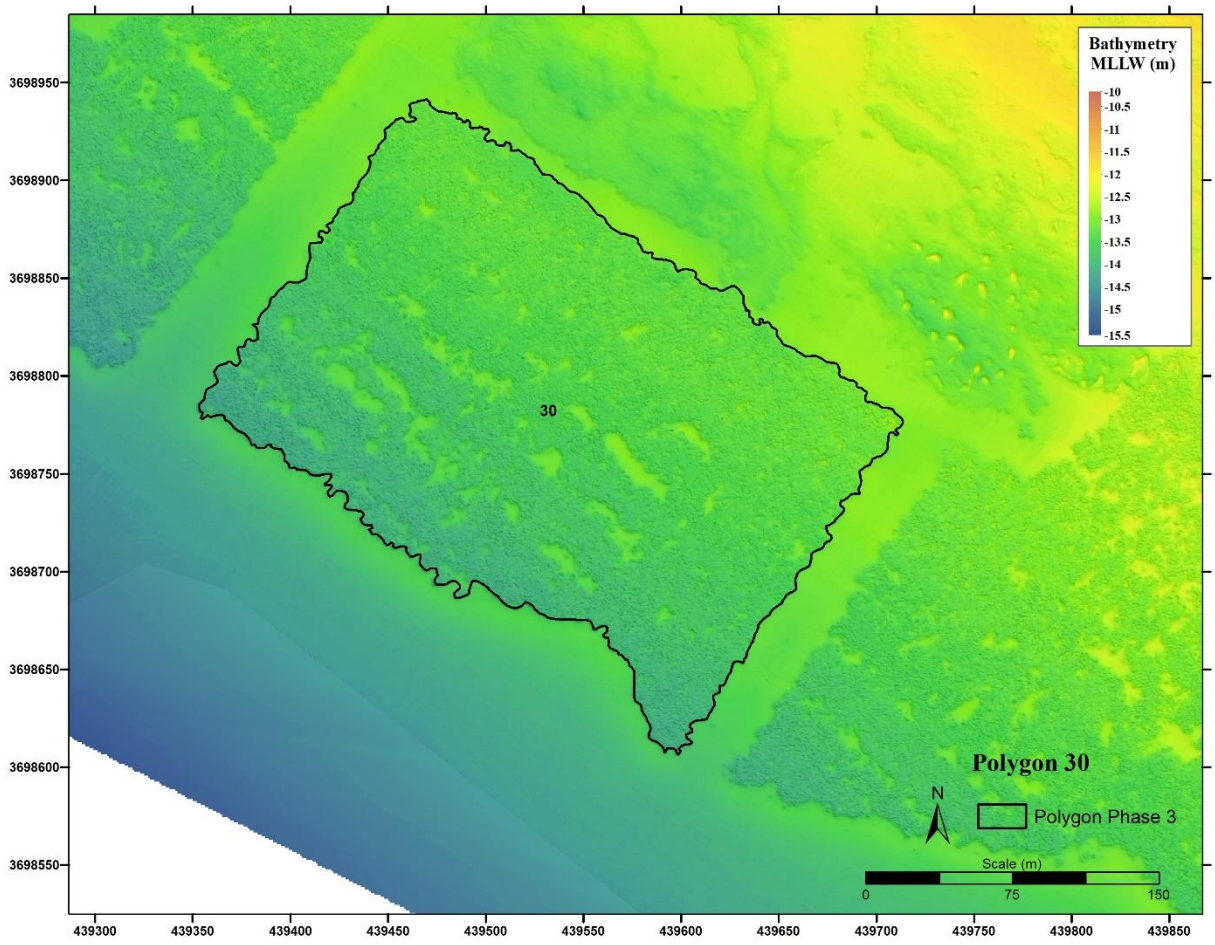

Figure F-12. Polygon 30 boundary from bathymetric data interpretation (October 2020 multibeam survey).

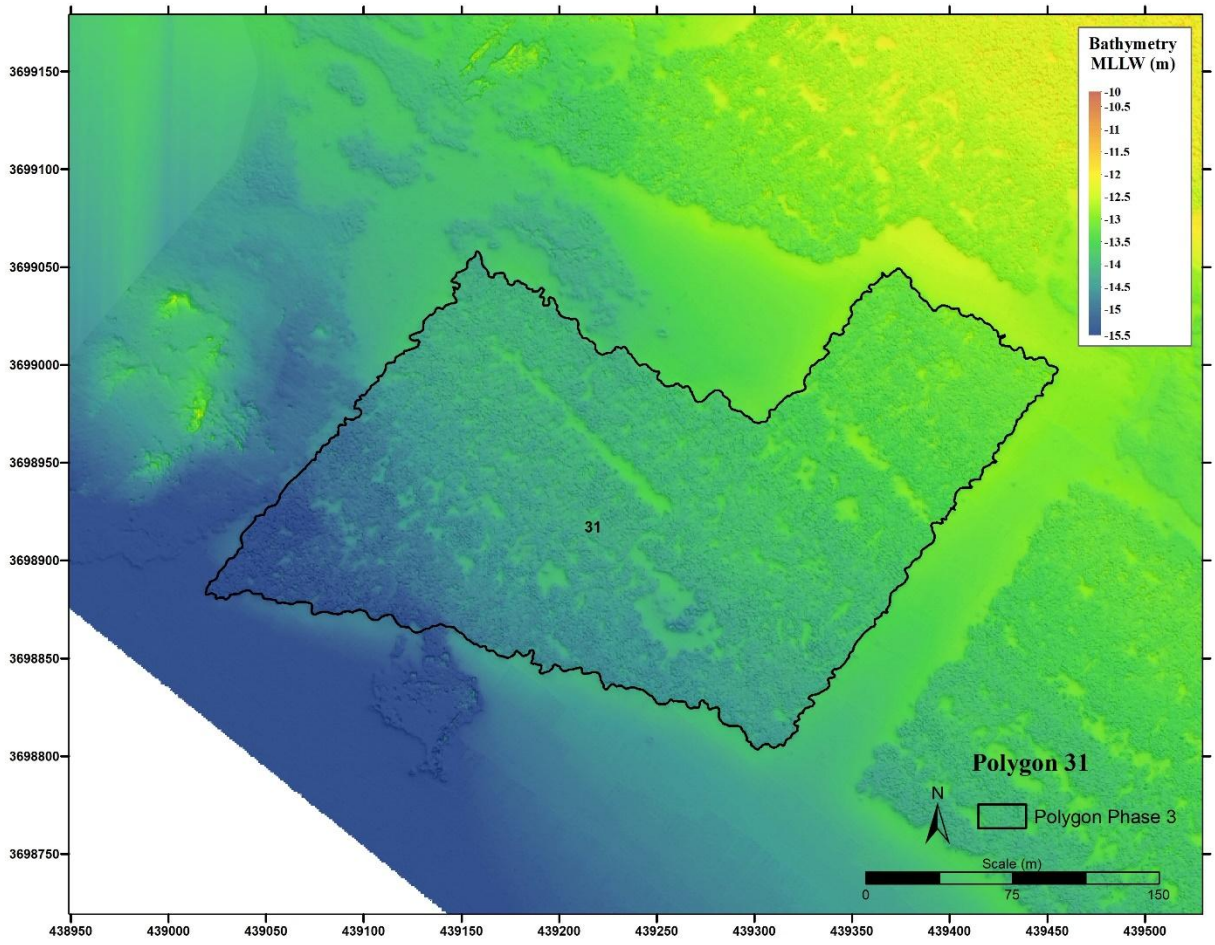

Figure F-13. Polygon 31 boundary from bathymetric data interpretation (October 2020 multibeam survey).

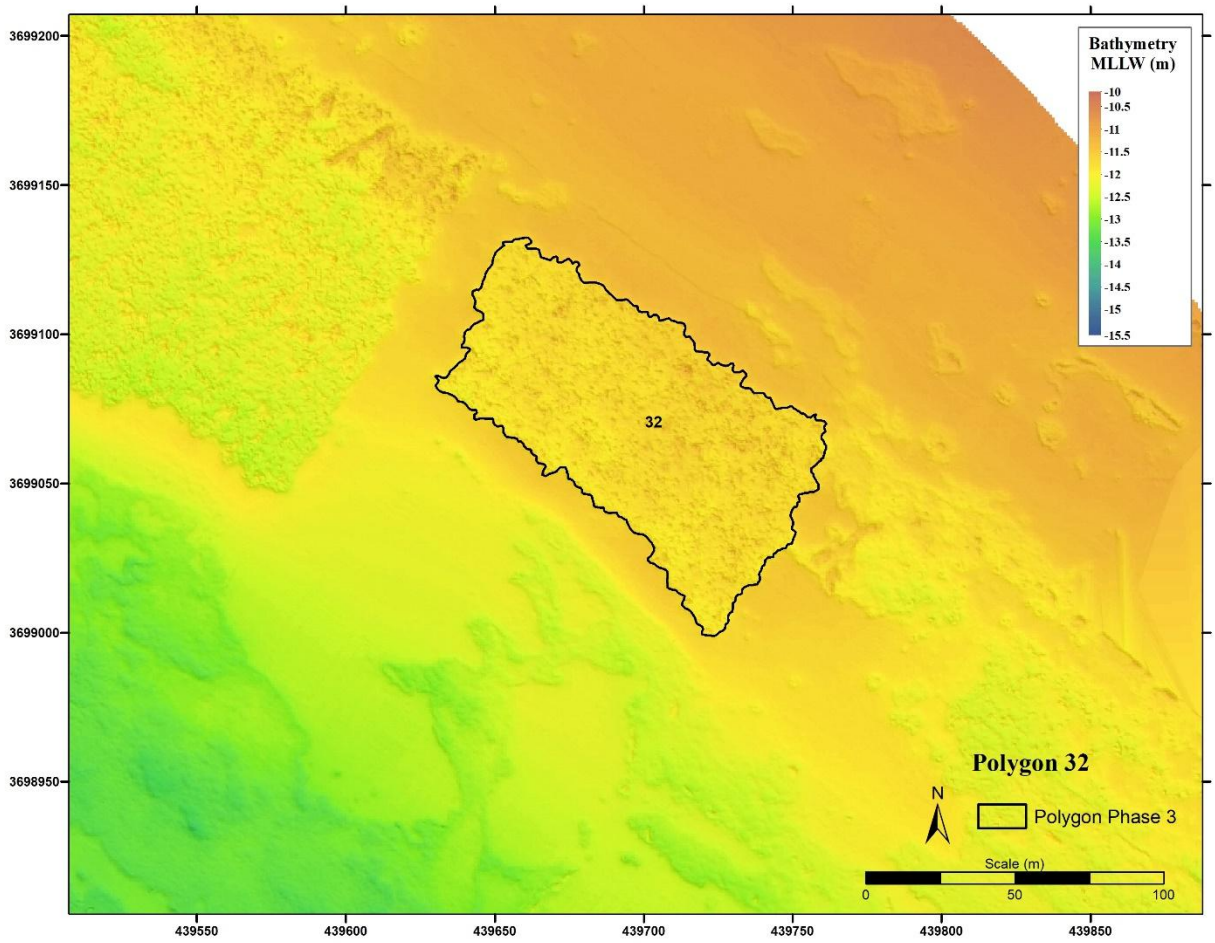

Figure F-14. Polygon 32 boundary from bathymetric data interpretation (October 2020 multibeam survey).

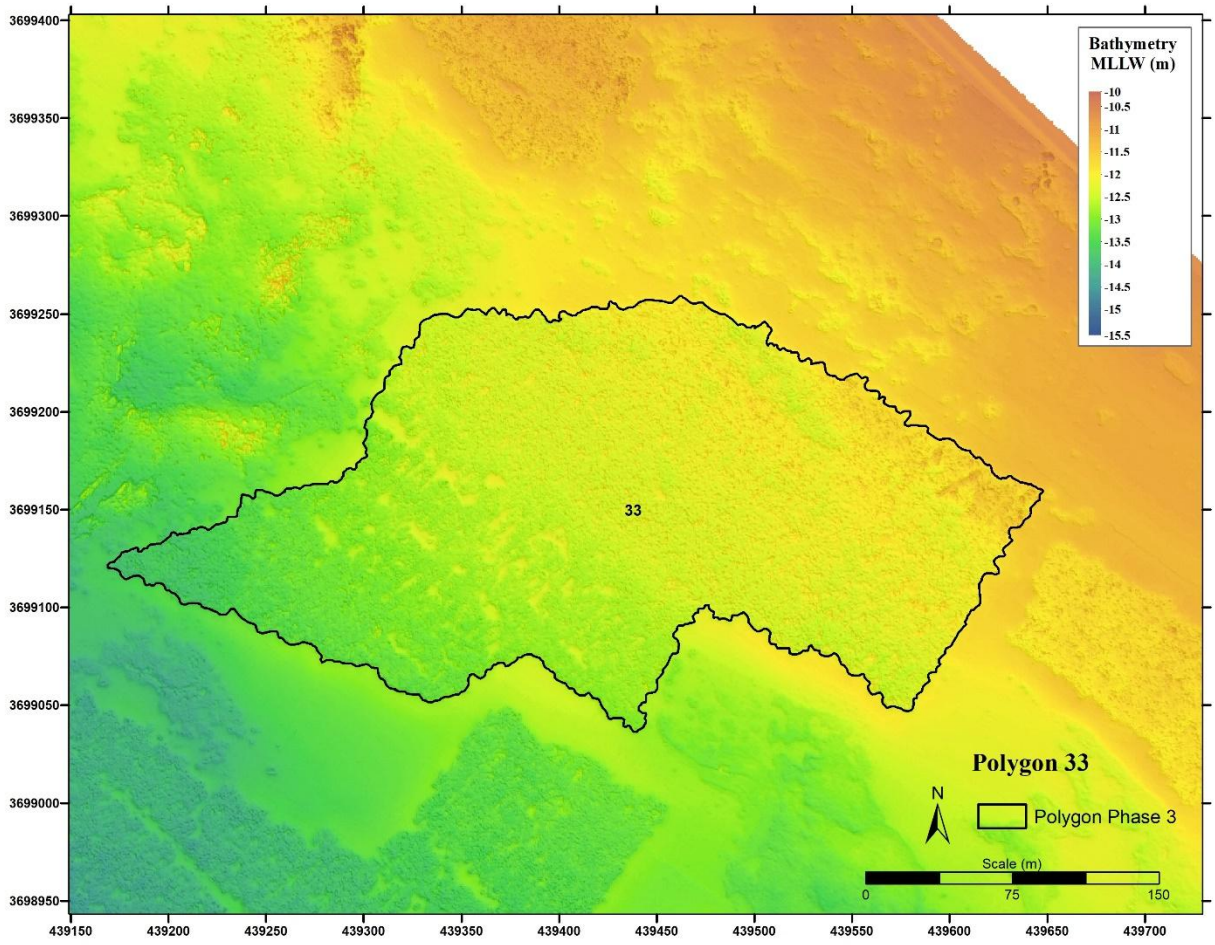

Figure F-15. Polygon 33 boundary from bathymetric data interpretation (October 2020 multibeam survey).

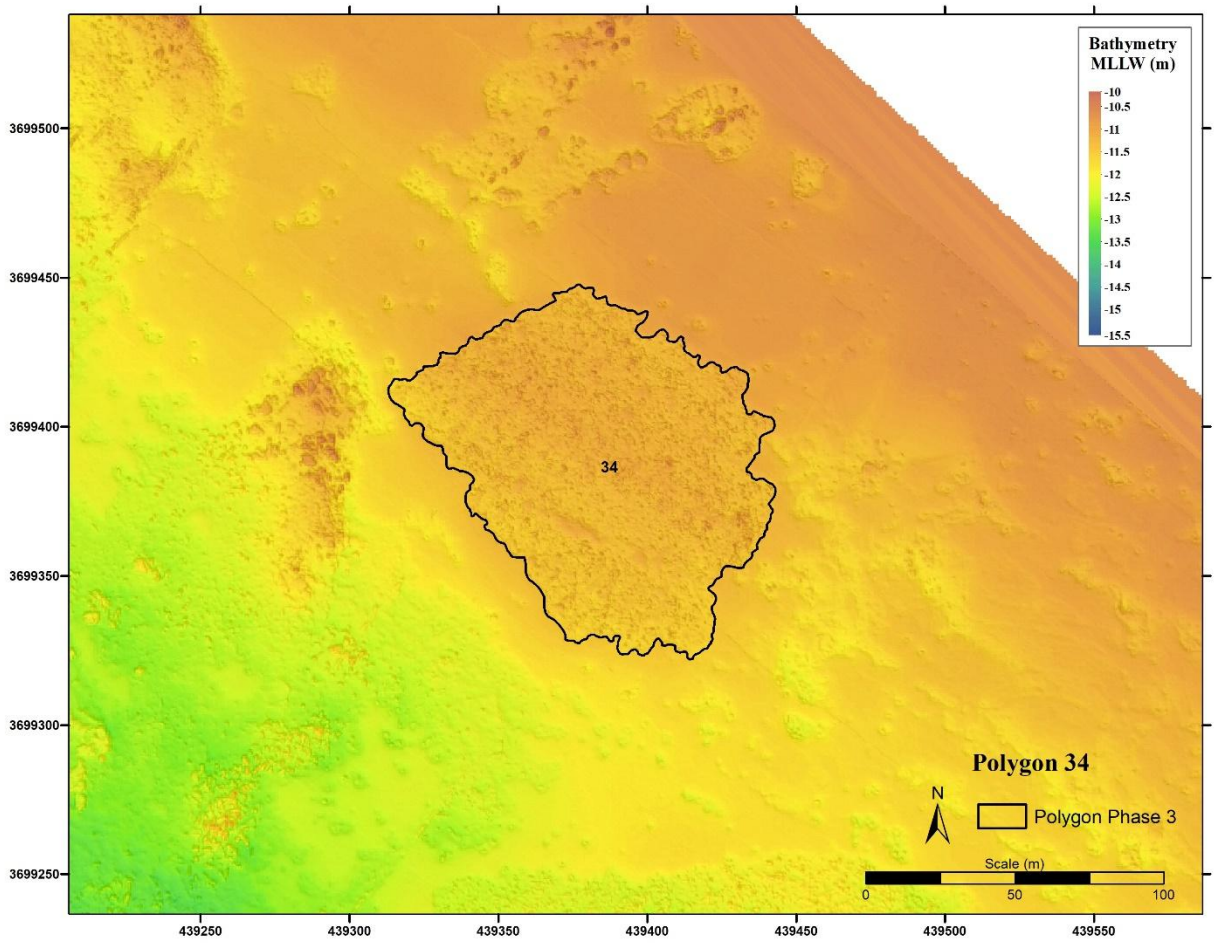

Figure F-16. Polygon 34 boundary from bathymetric data interpretation (October 2020 multibeam survey).

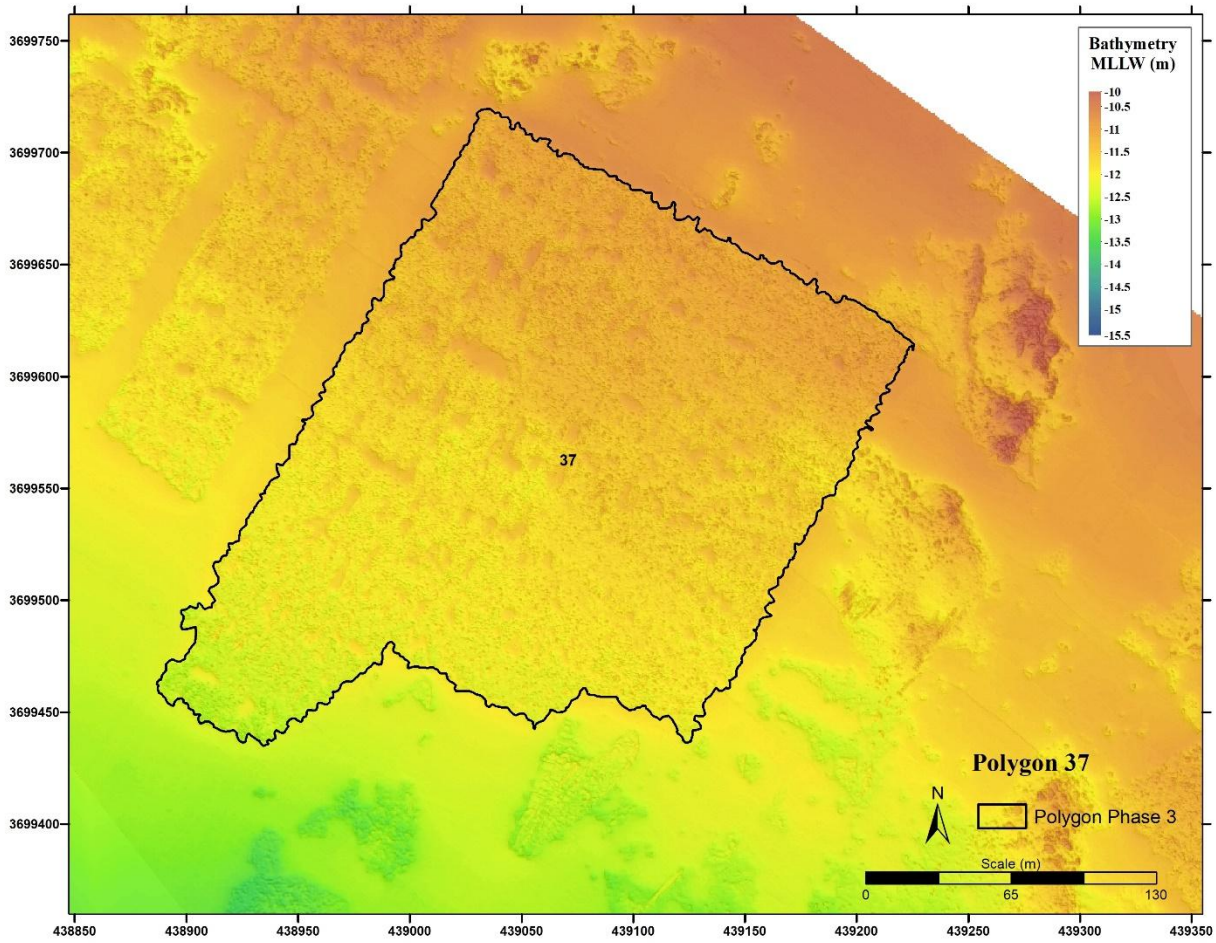

Figure F-17. Polygon 37 boundary from bathymetric data interpretation (October 2020 multibeam survey).

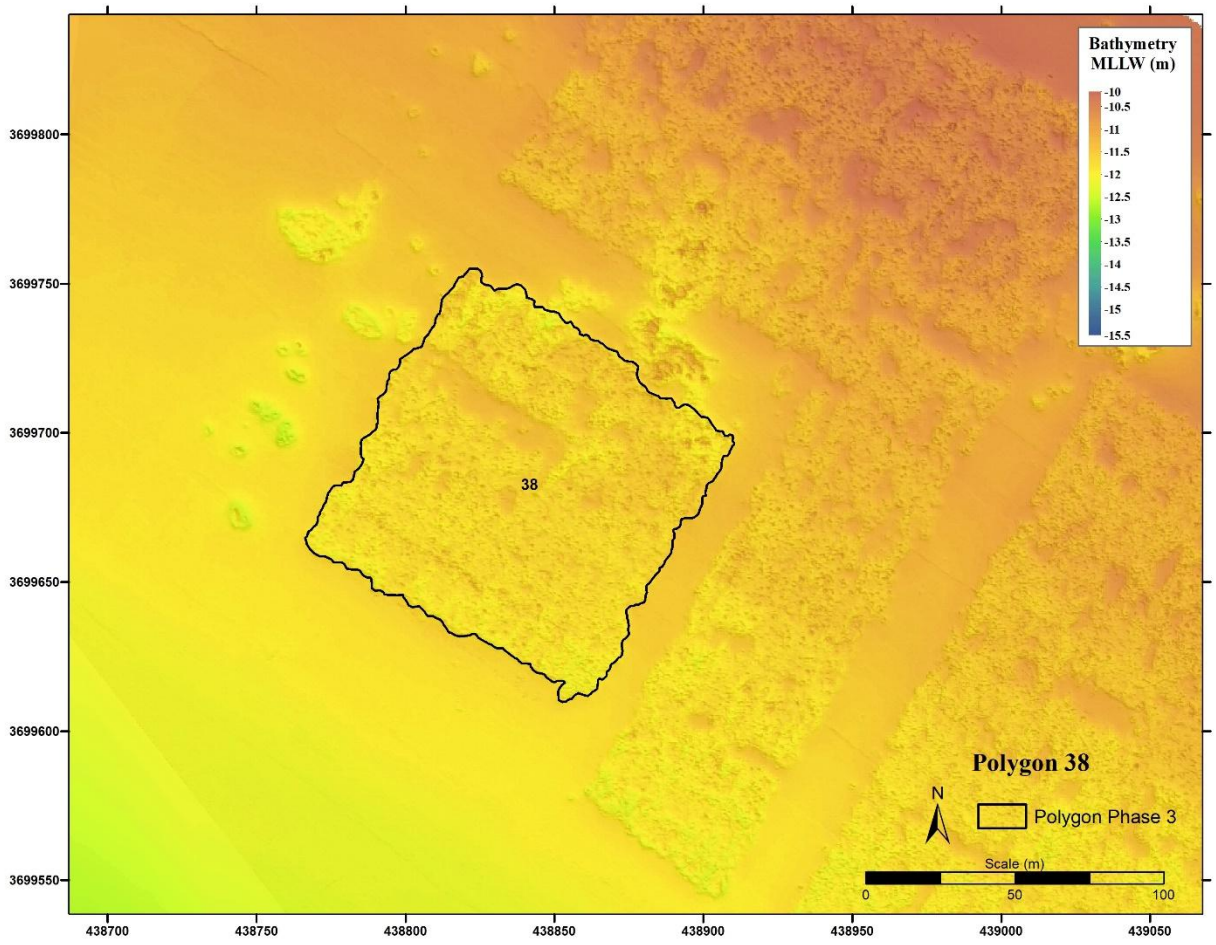

Figure F-18. Polygon 38 boundary from bathymetric data interpretation (October 2020 multibeam survey).

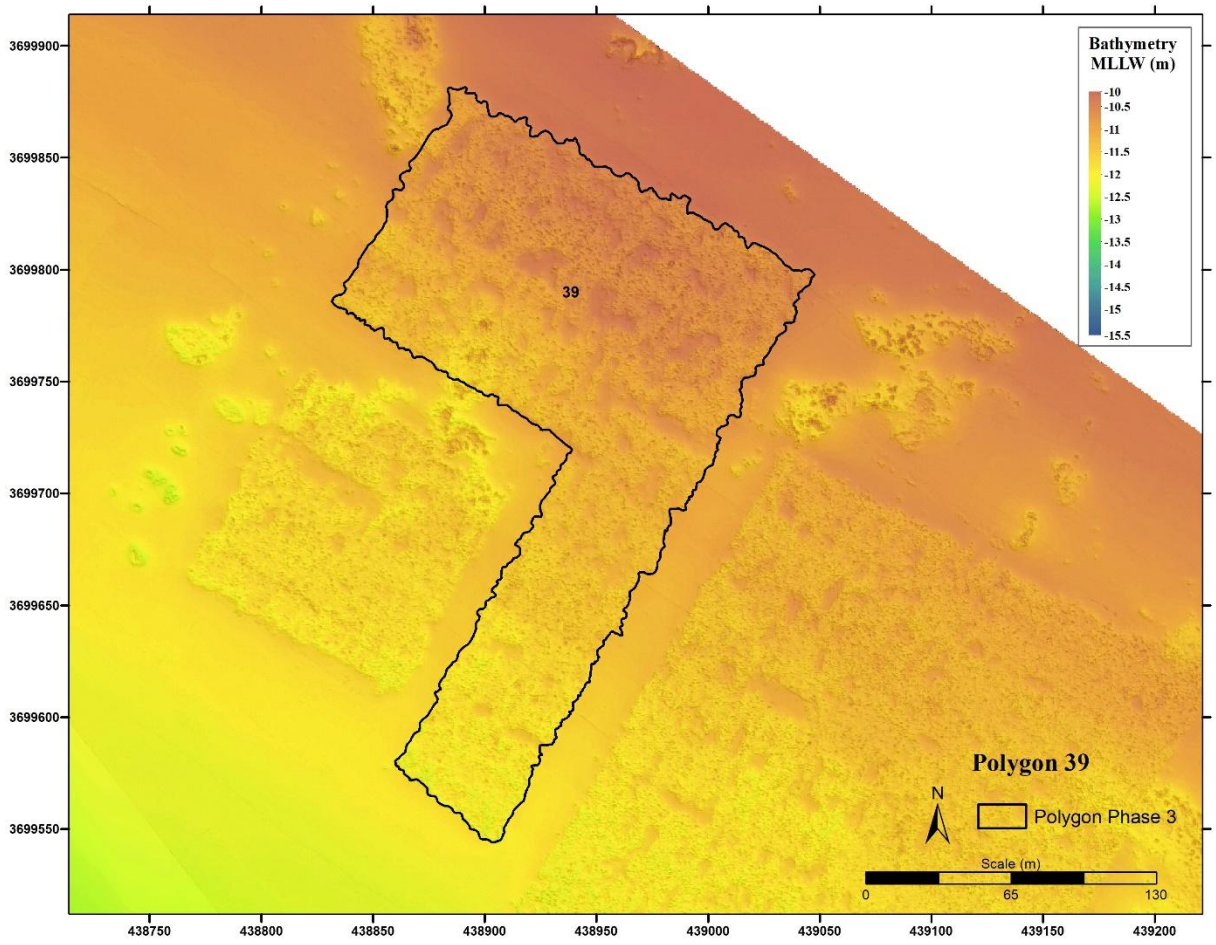

Figure F-19. Polygon 39 boundary from bathymetric data interpretation (October 2020 multibeam survey).

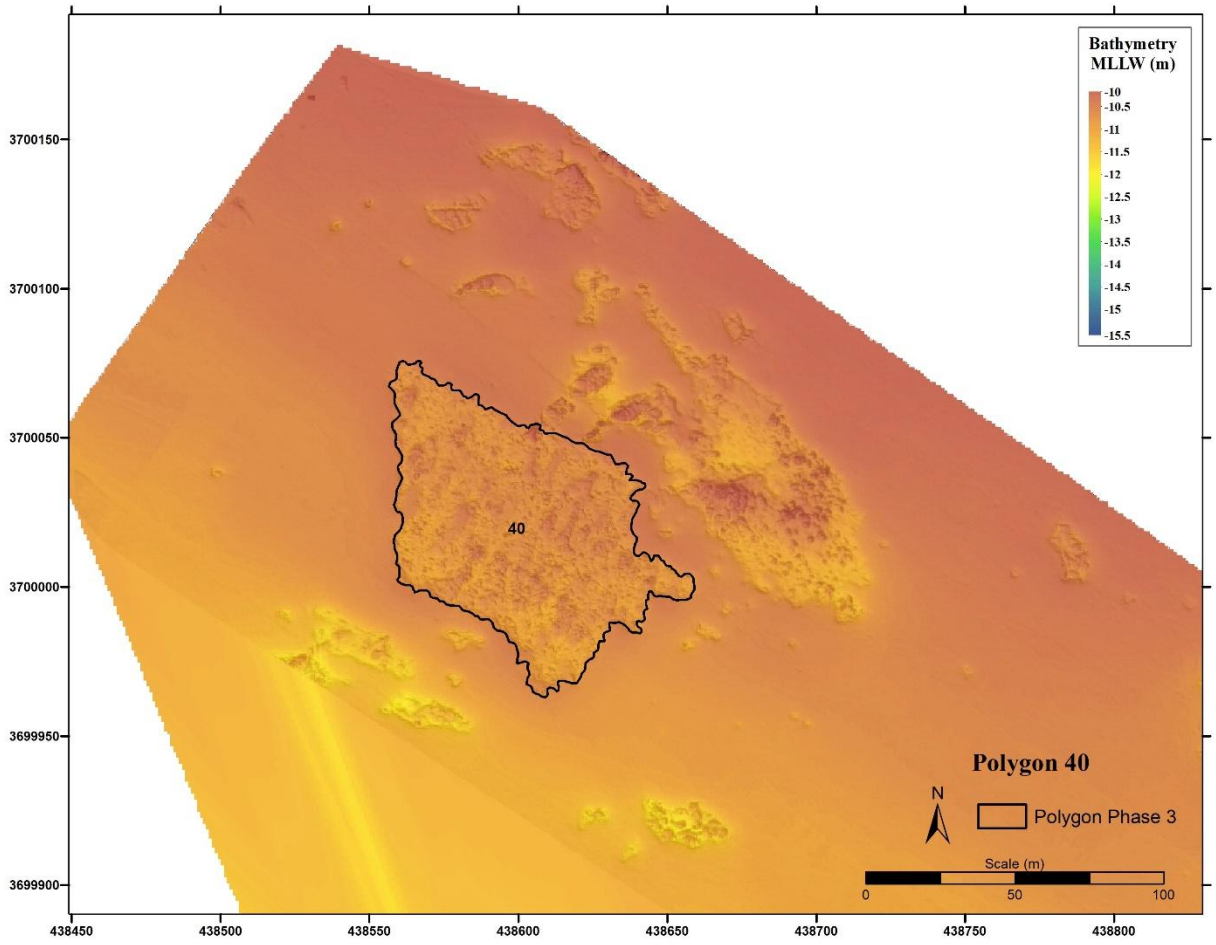

Figure F-20. Polygon 40 boundary from bathymetric data interpretation (October 2020 multibeam survey).

APPENDIX G

SUMMARY OF SURVEY DATA IN LARGE-SCALE DRAWINGS (OCTOBER 2020 MULTIBEAM SURVEY)

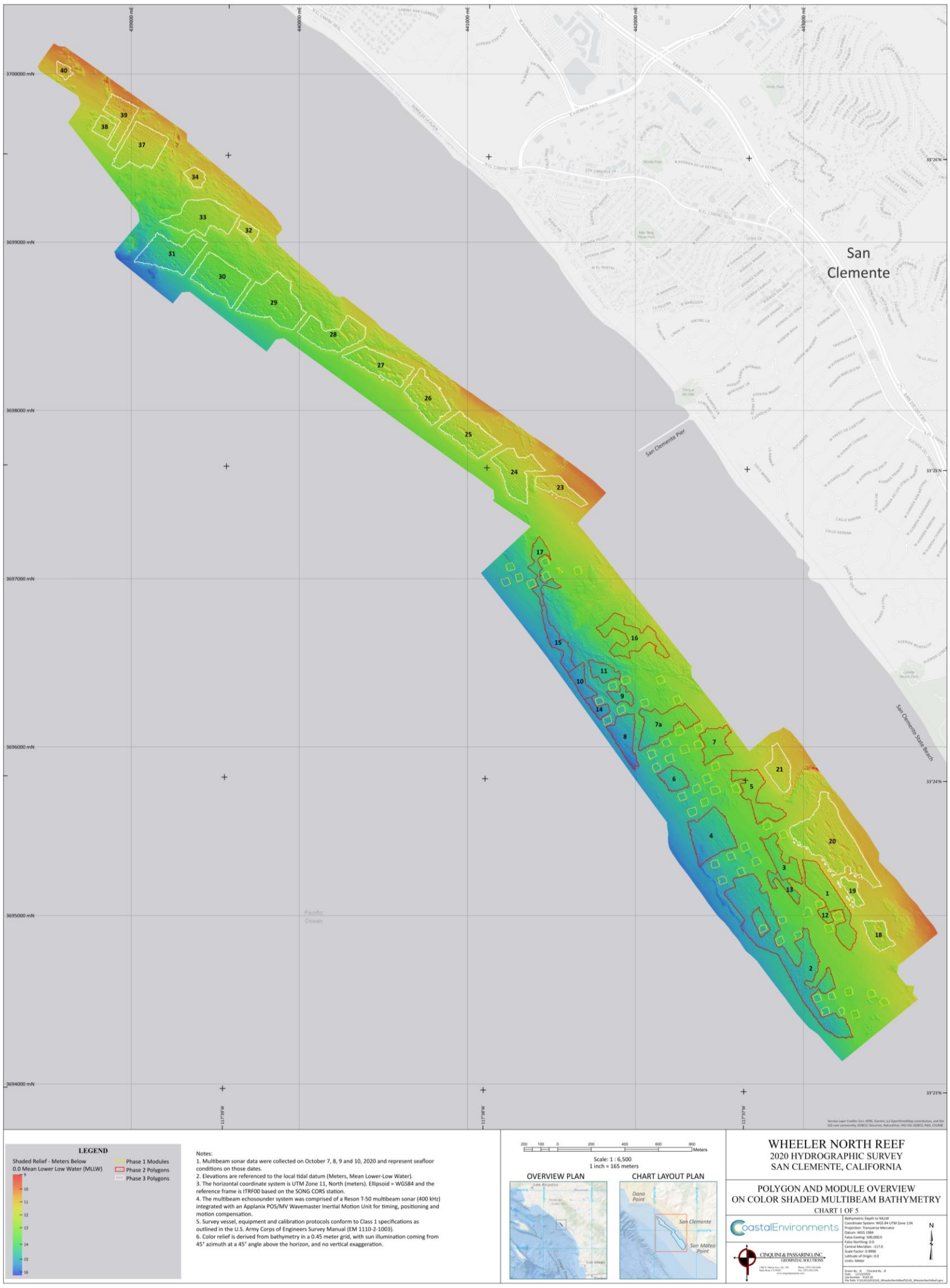

Figure G-1. Polygon and module overview on color-shaded multibeam bathymetry.

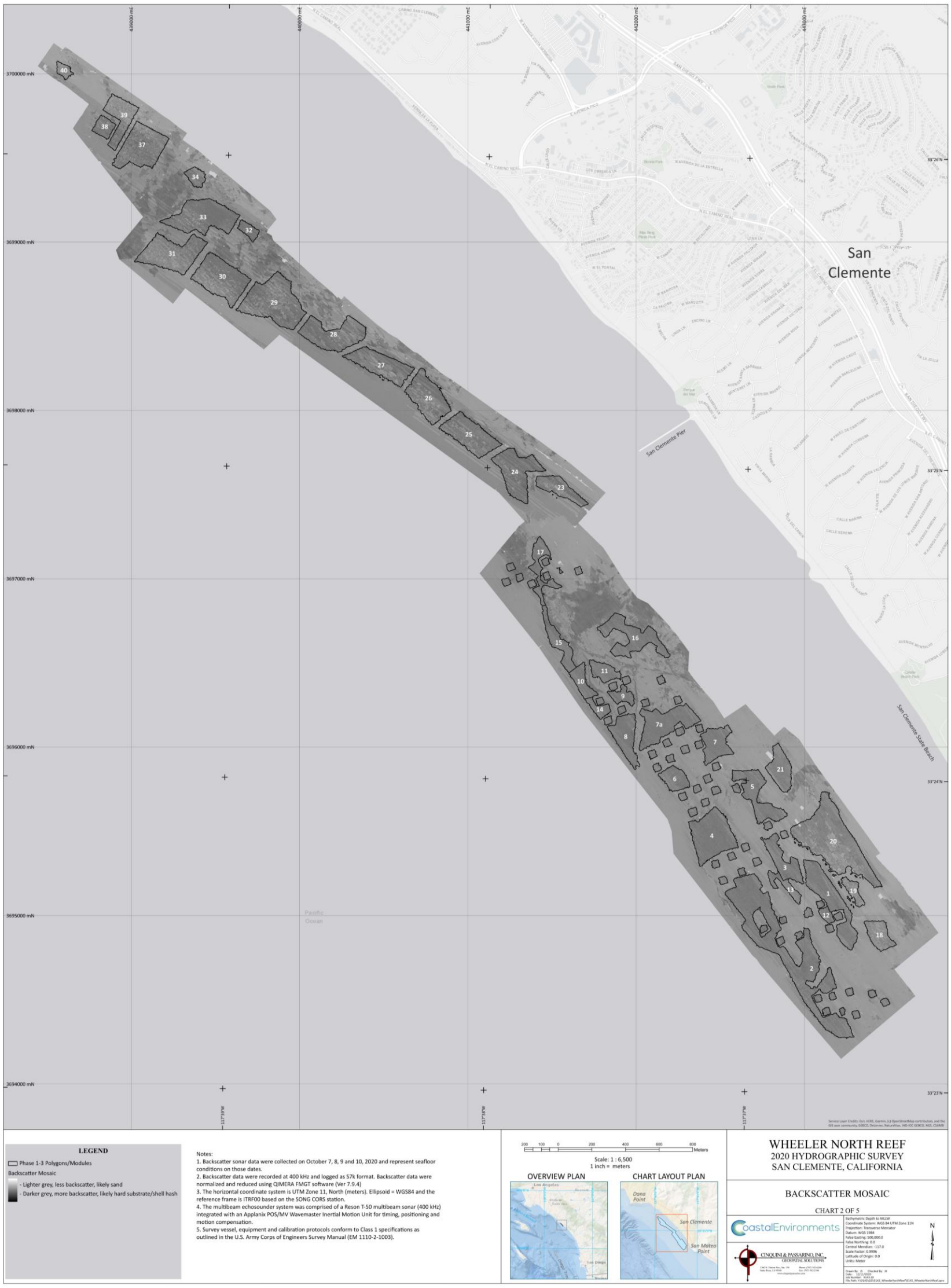

Figure G-2. Backscatter mosaic.

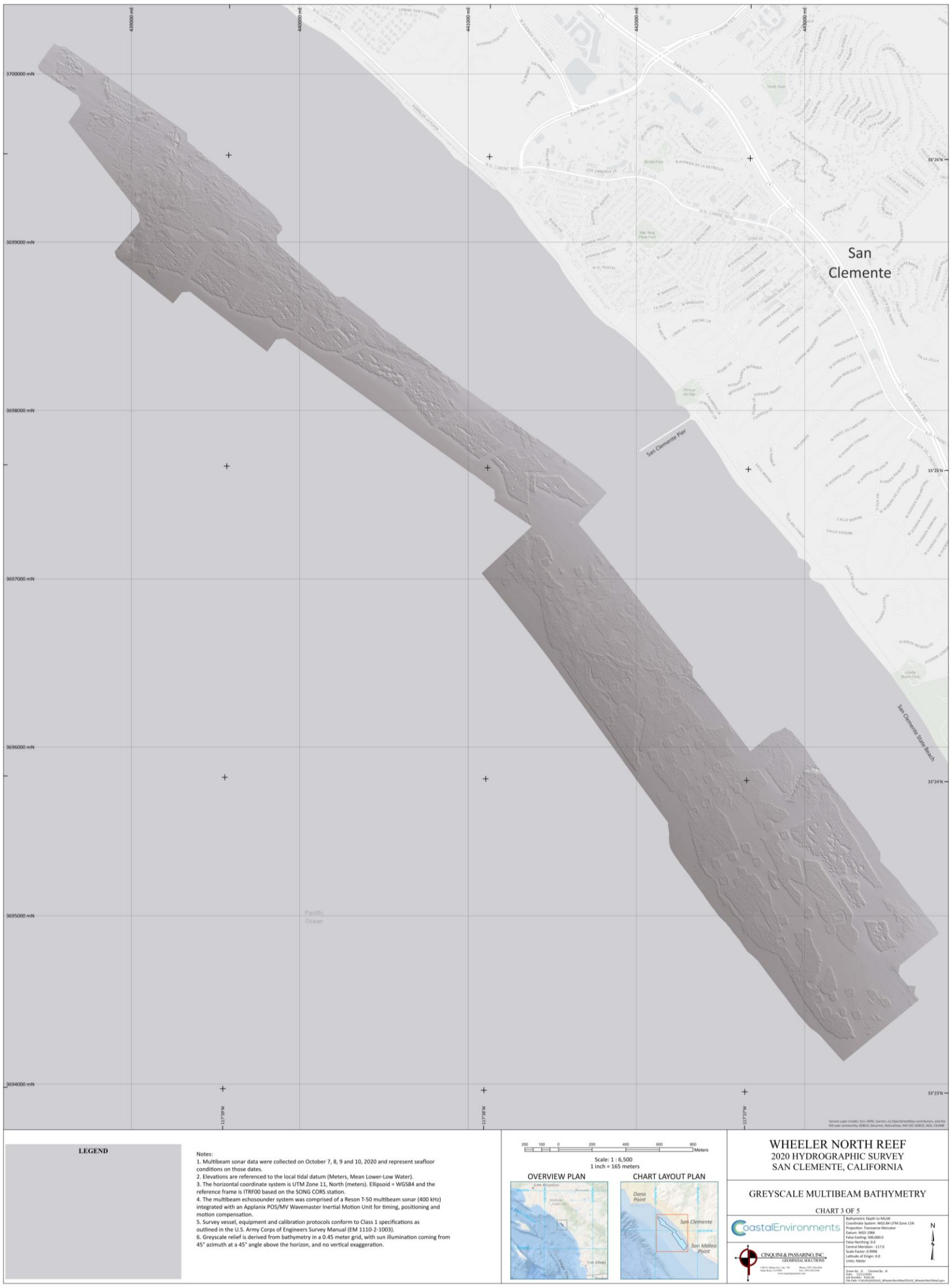

Figure G-3. Grayscale multibeam map.

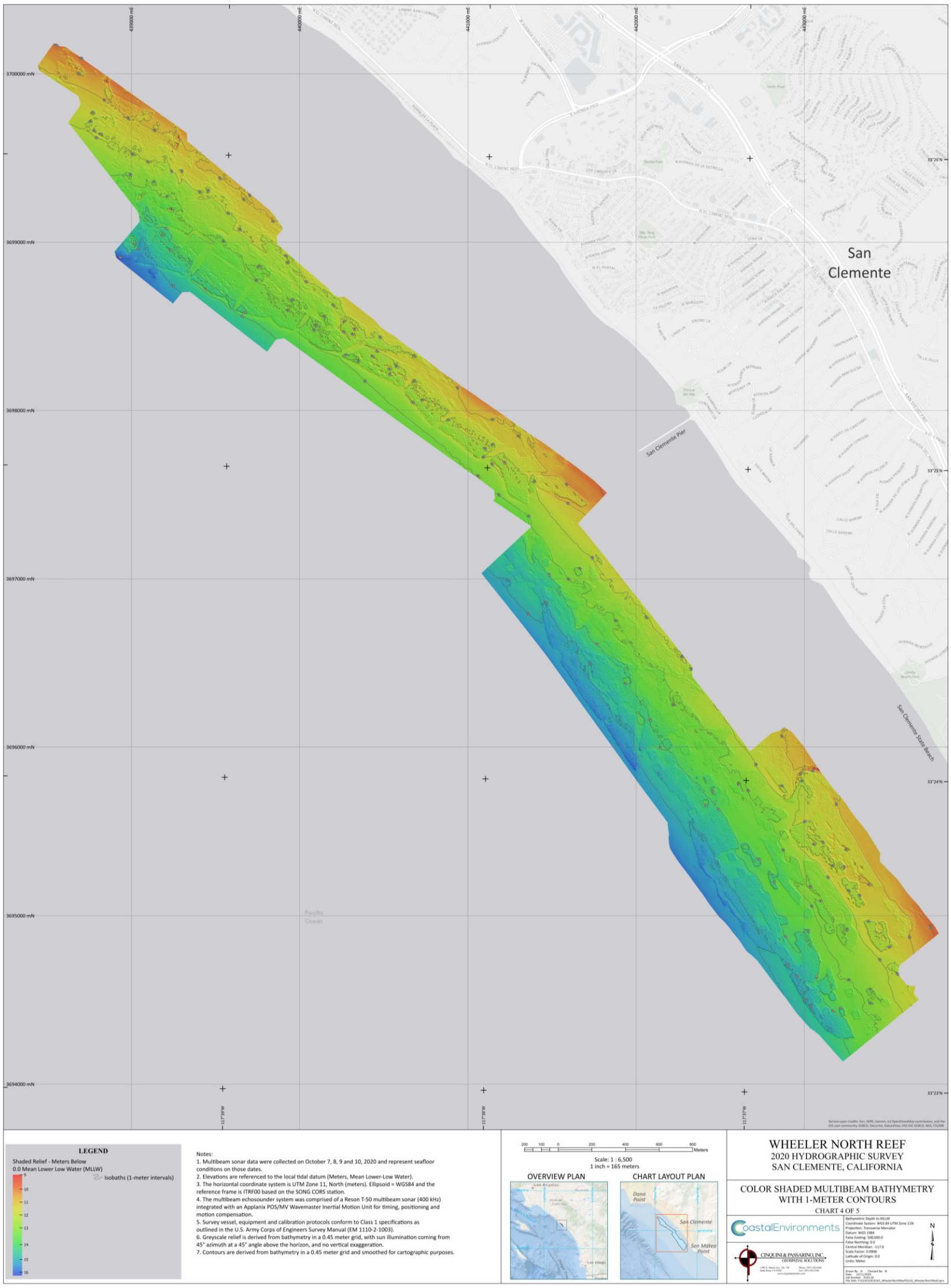

Figure G-4. Color-shaded multibeam bathymetry with 1-meter contours.

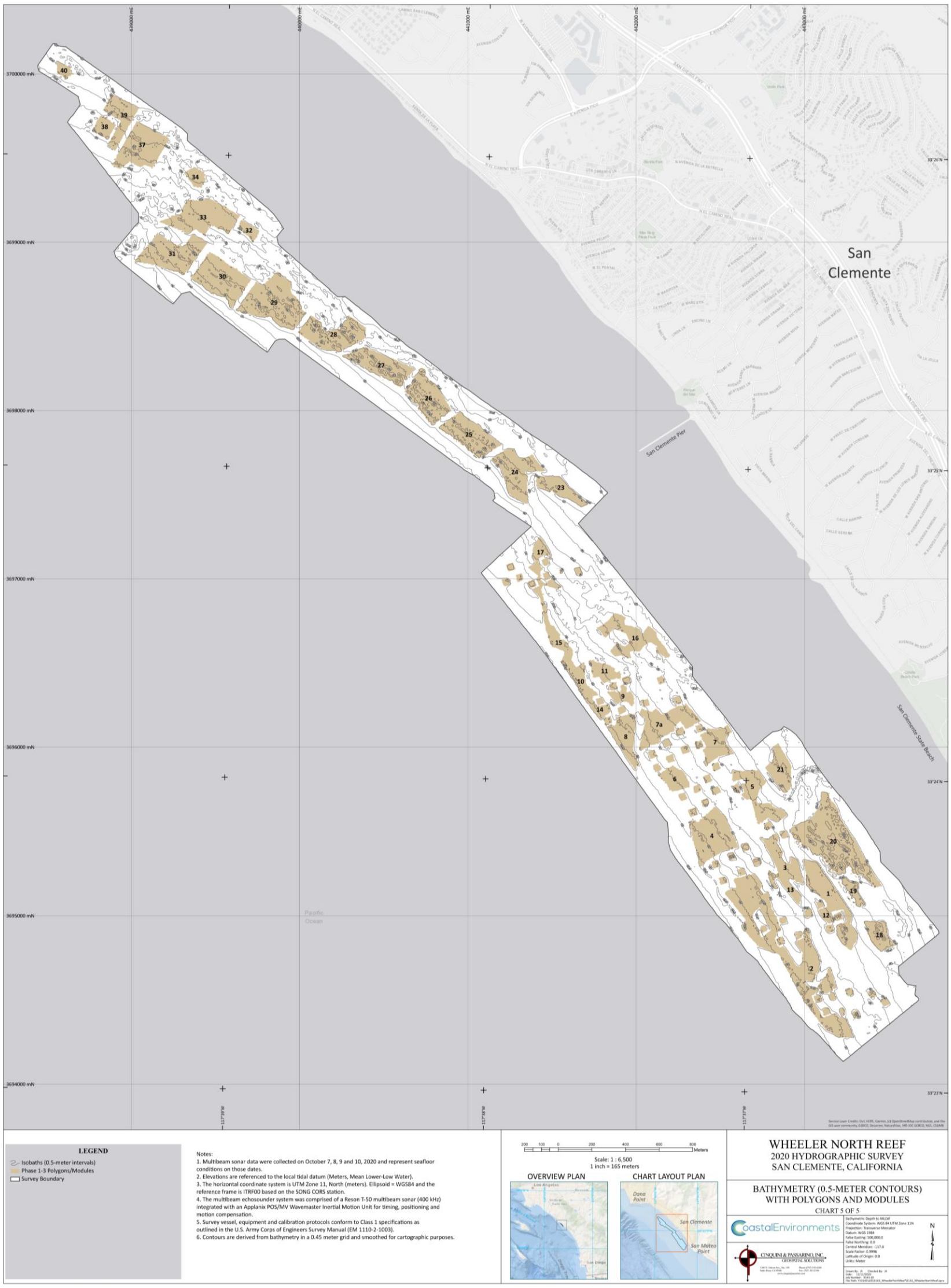

Figure G-5. Polygon and module overview on bathymetry (0.5-meter contours).